

# Functional analysis of the lipid phosphatase, Inpp4b, in osteoblast physiology

By William Liu

Master of Science

Faculty of Medicine

Division of Experimental Medicine

McGill University

Montreal, Quebec, Canada

August 2017

A thesis submitted to McGill University in partial fulfillment of the requirements of the degree of Master of Science

© William Liu 2017 All rights reserved

# ABSTRACT

Bone homeostasis requires a strict balance between bone formation and bone resorption, mediated by osteoblasts and osteoclasts, respectively. Perturbation of these activities can give rise to bone disorders such as osteoporosis and osteopetrosis. Osteopetrosis is an inheritable bone disorder characterized by dense, brittle bones prone to fracture as a result of defects in the osteoclast.

Our laboratory characterized the *Ostm1* gene, which is responsible for the most severe form of osteopetrosis in both mice and humans. Through expression profiles of these *Ostm1*-deficient osteopetrotic mice, we isolated and characterized the lipid phosphatase, *Inpp4b*, as a negative regulator of osteoclastogenesis. Expressed in osteoblasts and osteoclasts, systemic *Inpp4b* loss-of-function in mice resulted in increased osteoclast differentiation and function, leading to an osteoporotic phenotype. Importantly, these mice exhibited an increased mineral apposition rate *in vivo* as well as increased mineral nodule formation *ex vivo*, demonstrating an osteoblast-specific role for *Inpp4b*.

These findings prompted us to investigate the role of this gene in osteoblasts using conditional knock-out and transgenic mouse models. To this end, we used a combination of *ex vivo* and *in vivo* analyses to determine the function of *Inpp4b* in the mature osteoblast using a human osteocalcin (hOcn) promoter. *Inpp4b*<sup>lox/lox</sup>;hOcn-Cre mice exhibited defects in mineral nodule formation and gene expression kinetics *ex vivo*. Histomorphometry of these mice revealed an increase in osteoblast population and

activity at 8 weeks of age, with no observable effects in osteoclast differentiation. Despite this, bone mass remains comparable to control mice. Interestingly, hOcn-*Inpp4b*-hGH transgenic mice displayed bone mass reduction, concomitant with reduced osteoblastic activity and increased capacity for inducing osteoclast differentiation.

Taken together, our results have demonstrated that *Inpp4b* exerts a role in the mature osteoblast, independent of osteoclasts, and that *Inpp4b* osteoblast-specific function is critical for bone homeostasis.

# RÉSUMÉ

L'homéostasie osseuse repose sur un strict équilibre entre la formation de l'os par l'ostéoblaste et sa résorption par l'ostéoclaste. Des pathologies osseuses comme l'ostéoporose et l'ostéopétrose découlent d'un déséquilibre entre la résorption et la formation osseuses. L'ostéopétrose réfère à un groupe d'anomalies osseuses rares et héréditaires, caractérisées par une augmentation de la densité osseuse due à un défaut de développement ou de fonction des ostéoclastes.

Notre laboratoire a caractérisé le gène *Ostm1*, responsable de la forme la plus sévère de l'ostéopétrose chez l'Homme et les souris. Lors de nos études génétiques chez les souris ostéopétrotiques déficientes en *Ostm1*, nous avons caractérisé *Inpp4b* comme un régulateur négatif de l'ostéoclastogénèse. *Inpp4b* est exprimé dans les ostéoblastes et les ostéoclastes. L'ablation systémique de ce gène chez la souris résulte en une augmentation du nombre d'ostéoclastes et en un phénotype ostéoporotique. Le nombre des ostéoblastes ainsi que leur capacité à minéraliser a été aussi augmenté chez ces souris suggérant un rôle spécifique d'*Inpp4b* dans les ostéoblastes.

Afin de caractériser le rôle d'*Inpp4b* dans les ostéoblastes nous avons utilisé des souris transgéniques où *Inpp4b* a été spécifiquement invalidé ou surexprimé dans ces cellules sous le contrôle du promoteur du gène humain ostéocalcine (hOcn). Les souris *Inpp4b*<sup>lox/lox</sup>;hOcn-Cre présentent un défaut de minéralisation et une perturbation de l'expression des gènes associés à la différenciation des ostéoblastes. L'analyse

histomorphométrique de ces souris à l'âge de 8 semaines révèle une augmentation du nombre et de l'activité des ostéoblastes. Cependant, la différenciation des ostéoclastes ainsi que la masse osseuse totale ne semblent pas être affectées. De façon intéressante, les souris transgéniques hOcn-*Inpp4b*-hGH montrent une réduction de la masse osseuse due à une réduction de l'activité ostéoblastique et une augmentation de la différenciation ostéoclastique.

L'ensemble de ces résultats montre que *Inpp4b* joue un rôle important dans l'ostéoblaste mature, indépendamment de sa fonction ostéoclastique, et que la fonction spécifique d'*Inpp4b* dans les ostéoblastes est cruciale pour l'homéostasie osseuse.

# ACKNOWLEDGEMENTS

First and foremost, I would like to acknowledge and thank my supervisor, Dr. Jean Vacher, for welcoming me into his lab and giving me the chance to learn more than I could have ever expected. Through challenging discussions and lab meetings, Dr. Vacher has been an endless source of encouragement and support. More importantly, his excellent guidance, patience, and willingness to listen have nurtured my academic growth, especially when I was feeling overwhelmed or stressed. I am also extremely grateful for the financial support provided by Dr. Vacher which allowed me to focus on my degree as well as to participate in, and travel to, conferences. I feel lucky to have had the chance to learn from you and all the other fantastic members of the lab.

To all past and current Vacher lab members: THANK YOU. From scientific discussions to cake parties, your enthusiasm for science has helped push me to become a better scientist and your friendship has made this experience that much more fun. Hailey, Michael, Eva, Anna, Lucy, Vince, Emily, and Adele: thank you for your kind and thoughtful discussions, advice, and technical assistance in experiments. I'm incredibly fortunate to have had such wonderful labmates to share the bench with! Marie and Cameron: thank you for helping keep me on the graduate school track, but also for reminding me of life beyond the walls of the IRCM. It's been a blast working with you and I hope to share the karaoke stage with you soon! Monica: thank you for all that you do. It has been absolute pleasure shadowing you, taste-testing your baked goods, and learning lab dance moves (though I don't think I will ever master them). Most of all, thank you for showing me that

science IS (and should be) fun! Lina: last, but certainly not least, thank you for everything. From day one, you have been an amazing mentor who somehow never lost your patience with me. I could go on and on about all the ways you've helped shape my scientific learning and I hope every grad student is as fortunate as I am in having worked with someone like you!

I would like to acknowledge Dr. Geoffrey Hendy for sharing the hOcn mice used in this thesis. Thanks also go to the labs of Dr. Marie Trudel, Dr. William Tsang, and Dr. Mathieu Ferron for their thoughtful discussions and technical assistance throughout the project. Thank you also to Dr. Yongjun Xiao and the Centre for Bone and Periodontal Research for performing micro CT scans. Additionally, I want to thank members of the advisory committee: Dr. Javier Di Noia, Dr. Monzur Murshed, and Dr. Lisbet Haglund for their input and suggestions that have helped guide the project, as well as Dr. Mari Kaartinen for reviewing this thesis.

Finally, I would like to thank my incredibly supportive friends and family. To my mom, dad, and sister Rebecca: I could not have made it through this program without your constant and unconditional support. I owe such a large portion of this accomplishment to you. To my friends: thank you for supporting me even if you didn't completely understand what I was doing in grad school/thought I was committing heinous acts against mice for no reason. You have all had a helping hand in getting me through graduate school!

# CONTRIBUTION OF AUTHORS

Dr. Jean Vacher provided substantial contribution to all aspects of the thesis, including, but not limited to, conception of project idea, supervision, and review of results and ultimately thesis.

William Liu designed and performed experiments, collected and analyzed data, and wrote the thesis.

Monica Pata and Dr. Lina Saad provided training, technical assistance, assisted in analysis of results, and edited the French translation of the abstract.

Dr. Yongjun Xiao performed micro CT experiments at the McGill Centre for Bone and Periodontal Research.

# TABLE OF CONTENTS

<b><u>Section</u></b>	<b><u>Page</u></b>
ABSTRACT .....	i
RÉSUMÉ.....	iii
ACKNOWLEDGEMENTS.....	v
CONTRIBUTION OF AUTHORS.....	vii
TABLE OF CONTENTS .....	viii
LIST OF FIGURES .....	xii
LIST OF TABLES.....	xiv
ABBREVIATIONS .....	xv
CHAPTER 1: LITERATURE REVIEW .....	1
1.1 Bone.....	2
1.1.1 Bone development.....	3
1.1.2 Bone structure.....	5
1.2 Bone homeostasis .....	7
1.2.1 Osteoclast and its differentiation.....	7
1.2.2 Osteoblast and its differentiation .....	9
1.2.2.1 Osteocalcin (OCN).....	13
1.2.2.2 Function of osteoblasts.....	14
1.2.3 Osteocytes.....	16
1.3 Bone modelling and remodelling.....	17
1.4 Molecular pathways involved in osteoblastogenesis and bone homeostasis.....	19
1.4.1 TGF $\beta$ /BMP signalling in osteoblasts .....	19
1.4.2 Wnt/ $\beta$ -catenin signalling in osteoblasts .....	21
1.4.3 NFAT signalling in osteoblasts and osteoblasts .....	23
1.4.4 PI3K/AKT signalling in bone.....	24
1.5 Bone disorders .....	25
1.5.1 Paget's disease of the bone.....	25

1.5.2 Osteosarcoma .....	26
1.5.3 Osteoporosis.....	27
1.5.4 Osteopetrosis.....	28
1.5.5 Grey-lethal ( <i>gl/gl</i> ) murine model of ARO .....	30
1.6 <i>Inpp4b</i> and the PI3K/AKT signalling pathway .....	31
1.6.1 Characterization of <i>Inpp4b</i> .....	33
1.6.1.1 <i>Inpp4b</i> gene expression .....	34
1.6.1.2 INPP4B protein.....	34
1.6.1.3 INPP4B binding affinity .....	35
1.6.1.4 INPP4B localization .....	36
1.6.2 PI3K/AKT signalling in osteoblasts .....	36
1.7 Validation of <i>Inpp4b</i> defect in bone homeostasis.....	38
1.7.1 <i>Inpp4b</i> as a negative regulator of osteoclastogenesis.....	38
1.8 Role of <i>Inpp4b</i> .....	39
1.8.1 <i>Inpp4b</i> <sup>-/-</sup> mice are osteoporotic.....	41
1.8.2 <i>Inpp4b</i> <sup>-/-</sup> mice exhibit defects in osteoblastogenesis .....	43
CHAPTER 2: HYPOTHESIS AND APPROACH.....	44
CHAPTER 3: MATERIALS AND METHODS.....	46
3.1 Animals.....	47
3.1.1 Generation of conditional knock-out (cKO) mice.....	47
3.1.2 Generation of transgenic (TR) mice.....	47
3.1.3 Genotyping .....	48
3.1.4 Breeding .....	49
3.2 Cell culture.....	50
3.2.1 Primary cell culture (osteoblast).....	51
3.2.2 Primary cell culture (osteoclast) .....	51
3.2.3 Co-culture .....	52
3.3 Molecular analyses .....	52
3.3.1 DNA extraction .....	52
3.3.2 <i>Inpp4b</i> deletion.....	53
3.3.3 RNA isolation.....	53

3.3.4 Reverse transcription PCR .....	54
3.3.5 qPCR.....	54
3.3.6 Recombination efficiency .....	56
3.3.7 Southern blot for transgene integrity and copy number.....	57
3.3.8 Radioactive probe labelling and membrane hybridization .....	57
3.3.9 Osteoblast mineralization activity <i>ex vivo</i> .....	58
3.3.10 Osteoclast staining <i>ex vivo</i> .....	59
3.4 Biochemical analyses .....	60
3.4.1 Antibodies and reagents.....	60
3.4.2 Protein extraction.....	60
3.4.3 SDS-PAGE .....	60
3.4.4 Western blot.....	61
3.4.5 Enzyme-linked immunosorbent assay (ELISA) .....	61
3.5 Structural analyses .....	62
3.5.1 Histology.....	62
3.5.2 Histomorphometry .....	63
3.6 Statistical analyses .....	63
CHAPTER 4: RESULTS.....	64
4.1 Conditional knock-out (cKO) of <i>Inpp4b</i> .....	65
4.1.1 Specific deletion of <i>Inpp4b</i> in mature osteoblasts .....	65
4.1.2 Recombination specificity – DNA analyses .....	67
4.1.3 Recombination efficiency – RNA analyses.....	68
4.1.4 <i>Inpp4b</i> protein expression during osteoblast differentiation.....	70
4.1.5 Osteoblast-specific gene expression in <i>Inpp4b</i> cKO OB .....	71
4.1.6 <i>Ex vivo</i> mineral nodule formation in <i>Inpp4b</i> cKO OB .....	72
4.1.7 Autophagy in <i>Inpp4b</i> cKO OB <i>ex vivo</i> .....	74
4.1.8 <i>In vivo</i> mineral apposition rate of <i>Inpp4b</i> cKO OB mice.....	75
4.1.9 Evaluation of <i>Inpp4b</i> cKO OB capacity to modulate osteoclastogenesis .....	77
4.1.10 Osteoclast population in mice with <i>Inpp4b</i> cKO in OB.....	79
4.1.11 Characterization of OPG/RANKL ratio in <i>Inpp4b</i> cKO OB mice.....	81
4.2 Osteoblast-specific expression of <i>Inpp4b</i> in transgenic (TR) mice.....	82

4.2.1 Targeted overexpression of <i>Inpp4b</i> in mature osteoblasts .....	82
4.2.2 Generation of transgenic <i>Inpp4b</i> mice .....	82
4.2.3 Determination of copy number .....	83
4.2.4 Specific transgene expression .....	83
4.2.5 Quantitative transgene expression .....	83
4.2.6 <i>Inpp4b</i> protein expression during osteoblast differentiation .....	84
4.2.7 Osteoblast-specific gene expression in <i>Inpp4b</i> TR OB .....	86
4.2.8 <i>Ex vivo</i> mineral nodule formation in <i>Inpp4b</i> TR OB .....	87
4.2.9 <i>In vivo</i> mineral apposition rate of <i>Inpp4b</i> TR OB mice .....	89
4.2.10 Evaluation of <i>Inpp4b</i> TR OB capacity to modulate osteoclastogenesis .....	91
4.2.11 Osteoclast population in <i>Inpp4b</i> TR OB mice .....	93
4.2.12 Characterization of OPG/RANKL ratio in <i>Inpp4b</i> TR OB mice .....	94
CHAPTER 5: DISCUSSION .....	96
5.1 <i>Inpp4b</i> modulates osteoblast mineral formation <i>ex vivo</i> .....	100
5.2 Overexpression of <i>Inpp4b</i> results in bone mass reduction <i>in vivo</i> .....	103
5.3 <i>Inpp4b</i> modulates osteoblast-osteoclast crosstalk .....	105
CHAPTER 6: CONCLUSIONS .....	108
CHAPTER 7: PERSPECTIVES .....	111
APPENDIX 1 .....	117
BIBLIOGRAPHY .....	118

# LIST OF FIGURES

<b><u>Figure</u></b>	<b><u>Page</u></b>
Figure 1.1: Illustration of intramembranous ossification .....	4
Figure 1.2: Illustration of endochondral ossification.....	5
Figure 1.3: Schematic representation of an adult femur long bone .....	6
Figure 1.4: Illustration of osteoclastogenesis.....	9
Figure 1.5: Illustration of osteoblastogenesis .....	12
Figure 1.6: Stages of bone remodelling .....	18
Figure 1.7: Canonical Wnt/ $\beta$ -catenin signalling in osteoblasts.....	22
Figure 1.8: NFATc1 signalling in osteoblasts .....	24
Figure 1.9: PI3K signalling pathway .....	33
Figure 1.10: INPP4B protein structure and function .....	35
Figure 1.11: Summary of previously reported <i>Inpp4b</i> analyses. ....	42
Figure 3.1: Schematic representation of the <i>Inpp4b</i> transgene.....	48
Figure 3.2: Mating scheme to represent generation of mice .....	50
Figure 4.1: PCR assays to determine the specific deletion of <i>Inpp4b</i> in the mature osteoblast.....	67
Figure 4.2: Specificity and efficiency of gene expression in <i>Inpp4b</i> cKO OB.....	69
Figure 4.3: Expression of Inpp4b protein in <i>Inpp4b</i> cKO OB.....	70
Figure 4.4: qPCR gene expression profiles in <i>Inpp4b</i> cKO osteoblasts and controls.....	72
Figure 4.5: Mineralization assay for osteoblasts .....	73
Figure 4.6: qPCR analysis of <i>Atg5</i> and <i>Atg7</i> gene expression .....	75
Figure 4.7: <i>in vivo</i> bone analyses of <i>Inpp4b</i> cKO OB mice at 8 weeks and 4 months of age .....	76-77
Figure 4.8: Quantification of TRAP-positive osteoclasts in co-culture .....	78
Figure 4.9: Characterization of osteoclast population in <i>Inpp4b</i> cKO OB mice .....	79-80
Figure 4.10: Quantification of OPG/RANKL ratio in osteoblast cell culture media and sera.....	81

Figure 4.11: Linearized <i>Inpp4b</i> transgene construct .....	<b>82</b>
Figure 4.12: Characterization of <i>Inpp4b</i> TR OB mice .....	<b>85-86</b>
Figure 4.13: qPCR gene expression profiles in <i>Inpp4b</i> TR OB and controls.....	<b>87</b>
Figure 4.14: Mineralization assay for osteoblasts .....	<b>88</b>
Figure 4.15: <i>in vivo</i> bone analyses of <i>Inpp4b</i> TR OB mice at 8 weeks and 4 months of age .....	<b>89-90</b>
Figure 4.16: Quantification of TRAP-positive osteoclasts in co-culture.....	<b>92</b>
Figure 4.17: Characterization of osteoclast population in <i>Inpp4b</i> TR OB mice.....	<b>93-94</b>
Figure 4.18: Quantification of OPG/RANKL ratio in cell culture media and sera of the TR362 line .....	<b>95</b>
Figure 5.1: Potential mechanism of <i>Inpp4b</i> in <i>Akt</i> -mediated cell survival.....	<b>114</b>

# LIST OF TABLES

<b><u>Table</u></b>	<b><u>Page</u></b>
Table 1: List of genotyping primers.....	49
Table 2: List of RT-PCR/qPCR primers.....	55-56

# ABBREVIATIONS

$\alpha_v\beta_3$ : alpha-v beta-3 integrins

aa: amino acid

Acp5: tartrate-resistant acid phosphatase 5

ADO: autosomal dominant osteopetrosis

AEGC: articular epiphyseal growth plate

AKT: protein kinase B

ALP: alkaline phosphatase

ARO: autosomal recessive osteopetrosis

ATG5: autophagy protein 5

BM: bone marrow

BMP: bone morphogenetic protein

bp: base pairs

BSP: bone sialoprotein

CCL8: chemokine ligand 8

cDNA: complementary DNA

cKO: conditional knock-out

Col1 $\alpha$ 1: collagen type I alpha I

CTSK: cathepsin K

DNA: deoxyribonucleic acid

DVL: dishevelled

ER: endoplasmic reticulum

ESC: embryonic stem cell

Frt: flippase recognition target

FZD: frizzled

GSK3 $\beta$ : glycogen synthase kinase 3 beta

hOcn: human osteocalcin

HSC: hematopoietic stem cell

IAO: intermediate autosomal osteopetrosis

INPP4B $\alpha$ : inositol polyphosphate-4-phosphatase, type II alpha

kDa: kilodalton

loxP: locus of X-over P1

MCSF: macrophage-colony stimulating factor

mRNA: messenger RNA

MSC: mesenchymal stem cell

mTOR: mammalian target of rapamycin

NFATc1: nuclear factor of activated T-cells, cytoplasmic 1

OB: osteoblast

OCL: osteoclast

OCN: osteocalcin

OPG: osteoprotegerin

OPN: osteopontin

OSTM1: osteopetrosis associated transmembrane protein 1

OSX: osterix

NHR2: Nerve homology 2

PCR: polymerase chain reaction

PI3K: phosphoinositide 3 kinase

PKC: protein kinase C

PTEN: phosphatase and tensin homolog

PTH: parathyroid hormone

PU.1: transcription factor PU.1

qPCR: quantitative polymerase chain reaction

RANK: receptor activator of nuclear factor kappa-B

RANKL: receptor activator of nuclear factor kappa-B ligand

RNA: ribonucleic acid

RT-PCR: reverse transcription polymerase chain reaction

RUNX2: Runt-related transcription factor 2

SHIP: SH2 domain-containing inositol 5'-phosphatase

SMAD: transcription factor SMAD

TGF $\beta$ : transforming growth factor-beta

TR: transgenic

TRAP: tartrate-resistant acid phosphatase

# CHAPTER 1: LITERATURE REVIEW

## 1.1 Bone

The human skeletal system is composed of cartilage and bone, both of which are highly specialized forms of connective tissue and critical for several important functions. On the one hand, cartilage is the thin and avascular skeletal component that confers flexibility (Fox *et al.*, 2009), while bone is a highly mineralized tissue that serves a number of essential, physiological roles (Raubenheimer *et al.*, 2017). More specifically, the skeletal system must provide structural support for the entire body, facilitate movement as sites of attachment for muscles, maintain ionic and mineral homeostasis, regulate production of various cytokines and signalling factors, and serve as a site of hematopoiesis (Clarke, 2008). To achieve these functions, bone homeostasis must be tightly regulated by the concerted actions of the bone-forming cells, osteoblasts, and the bone-resorbing cells, osteoclasts. This balance in activities is also known as bone remodelling and is a constant and lifelong process characterized by the removal of mature bone and deposition of newly-formed matrix. Thus, cells of the skeletal system must constantly communicate with each other in a highly-coordinated manner via the interaction of different factors. Any imbalance in the activities and/or communication of either, or both, of these functions can lead to different bone pathologies, including, but not limited to, osteopetrosis and osteoporosis. Furthering our understanding of bone homeostasis and the effectors that can modulate the activities of bone cells can therefore provide novel targets for therapeutic intervention.

### **1.1.1 Bone development**

Bone development begins early in life, originating from three different lineages: somites, which generate the axial skeleton, the lateral plate mesoderm, which generates the appendicular skeleton, and the neural crest cells, which generate the craniofacial bones and cartilage. Osteogenesis, or bone formation, is accomplished through two different processes, known as intramembranous ossification and endochondral ossification, depending on the site of development. Both processes rely on centres of ossification for proper growth. Primary ossification centres are the first areas to begin ossifying and occur in the diaphysis of long bones early in prenatal development. Secondary ossification centres appear later, usually during postnatal development, and can be normally found in the epiphyses.

Intramembranous ossification, as illustrated in Figure 1.1, takes place mainly for the flat bones of the head, including the calvarium. It is initiated when a group of mesenchymal stem cells directly differentiate into osteoblasts that first secrete unmineralized extracellular matrix, called osteoid, which can mineralize. This serves as the ossification centre. As mineralization takes place, the early osteoblasts become trapped within the matrix, thereby becoming osteocytes, while the surrounding osteoprogenitors differentiate into new osteoblasts. Blood vessels will invade the ossification centre and mineralized osteoid surrounding the capillaries becomes trabecular bone, while osteoid on the surface develops into the periosteum which will eventually produce protective compact, or cortical, bone. The inner trabecular, or spongy, bone will house the bone marrow (Gilbert, 2000).

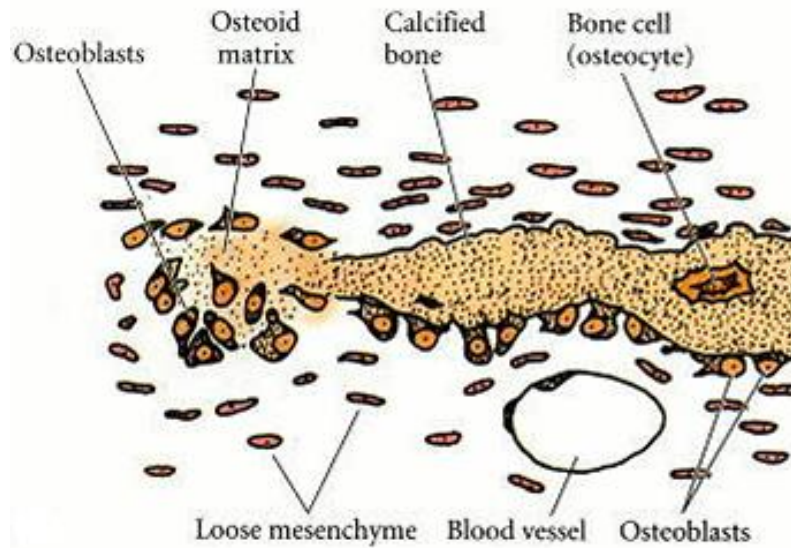


Figure 1.1: Illustration of intramembranous ossification.

A pool of osteoprogenitor cells differentiates into osteoblasts to secrete osteoid, which becomes calcified over time. Trabecular bone is formed around the blood vessels, which condense to become the red bone marrow. Compact bone is formed from the periosteum superior to trabecular bone. (Reprinted from *Developmental Biology*, 6<sup>th</sup> edition, Gilbert, *Osteogenesis: The development of bones*, Copyright (2000), with permission from Oxford University Press)

Endochondral ossification, as illustrated in Figure 1.2, however, takes place in the long bones of the body and relies on a cartilage template that must first be secreted by chondrocytes. A group of chondrocytes will secrete cartilaginous extracellular matrix and become known as the proliferative zone. As proliferation is occurring, morphological changes occur whereby mature chondrocytes increase their volume dramatically, thus becoming the hypertrophic zone. This proliferation and growth is responsible for longitudinal growth of the developing bone. The cartilage matrix is later mineralized (Teti, 2011) and replaced with bone, which is accomplished by the transport of osteogenic cells that will become osteoblasts through the process of vascularization. This process also converts the initial perichondrium into the periosteum, where osteoblasts will form the

compact bone and thus serve as the primary ossification centre. In the meantime, chondrocytes die by apoptosis, leaving a space which will become the site of bone marrow. Chondrocytes and cartilage continue to grow at the ends of the bones and exist as articular cartilage at the surface of joints and between the diaphysis and epiphyses. After birth, this process of ossification occurs at the epiphyses and becomes the secondary ossification centre (Mackie *et al.*, 2008).

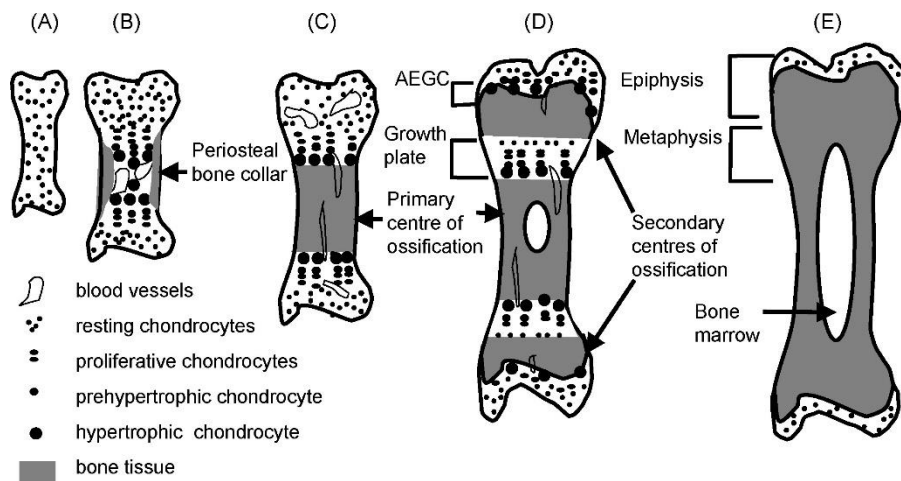


Figure 1.2: Illustration of endochondral ossification.

This process begins first with a cartilage template produced by chondrocytes. Blood vessels eventually invade, bringing osteoblast precursors with them. This converts perichondrium to periosteum and the osteoblasts form a primary ossification centre around the diaphysis. After birth, a second ossification centre is created near the epiphyseal regions. (Reprinted from The International Journal of Biochemistry & Cell Biology, Volume 40, Mackie *et al.*, Endochondral ossification: How cartilage is converted into bone in the developing skeleton, Page 47, Copyright (2007), with permission from Elsevier)

### 1.1.2 Bone structure

Adult long bone is characterized by an organic phase composed of collagen and non-collagenous proteins and an inorganic phase composed of hydroxyapatite crystals. Type I collagen self-assembles into fibrils to provide tensile strength while non-collagenous

proteins, like osteopontin (OPN), can regulate mineralization, cell adhesion, and signalling (Denhardt & Noda, 1998). Hydroxyapatite crystals are comprised mainly of calcium and phosphate, and form the inorganic phase, which confers rigidity to the bone (Boskey, 2013).

Together, these two phases constitute bone, which results in a structure tightly-regulated by the expression of different genes and signalling factors. As illustrated in Figure 1.3, the rounded ends of the adult long bone are called the epiphyses, while the shaft is referred to as the diaphysis. Separating the epiphyses and diaphysis is the metaphysis, which contains the growth plate and is the site of longitudinal growth during childhood. The growth plate arrests its growth after adolescence and becomes the epiphyseal line.

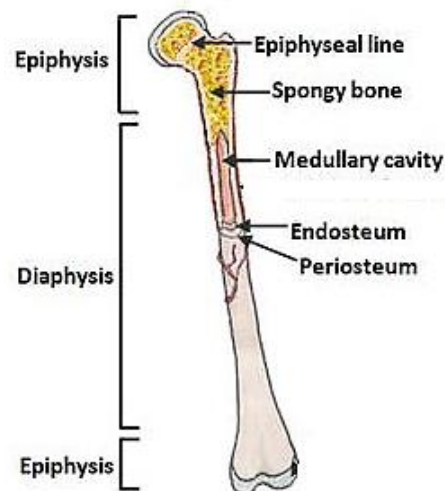


Figure 1.3: Schematic representation of an adult femur long bone.

(Reprinted from SEER Training Modules, Anatomy and Physiology. U. S. National Institutes of Health, National Cancer Institute. 1 Sept 2017 <https://training.seer.cancer.gov/anatomy/skeletal/classification.html>, from SEER as public domain)

## 1.2 Bone homeostasis

### 1.2.1 Osteoclast and its differentiation

Osteoclasts are large and multinucleated cells responsible for the resorption of bone matrix. This requires fusion of mononuclear osteoclasts to become mature osteoclasts. They must produce a ruffled border, sealing zone, and vacuolar proton pump to facilitate attachment to bone matrix, as well as for the secretion of acids, protons, and enzymes that will degrade the bone. This will result in the acidification, and subsequent degradation, of the bone matrix under the ruffled border of the osteoclast. The liberated matrix will then be endocytosed by the osteoclast and released (Teitelbaum, 2000).

Mature osteoclasts originate from hematopoietic stem cells, which will become committed to the monocyte/macrophage lineage. Key to this process is the expression of certain transcription factors and cytokines (Figure 1.4). PU.1 is the master regulator of osteoclastogenesis and is responsible for stimulating expression of several osteoclast-specific genes important for their proliferation, survival, and differentiation. For example, PU.1 will activate expression of both macrophage-colony stimulating factor (M-CSF) and receptor activator of nuclear factor kappa-B ligand (RANKL) receptors, which are important for the survival and differentiation of osteoclasts, respectively. *PU.1*<sup>-/-</sup> mice present with osteopetrosis, similar to *op/op* mice (McKercher *et al.*, 1996). The interaction of M-CSF with its receptor, colony stimulating factor-1, on monocytic cells also promotes their commitment to the osteoclast lineage, while the RANKL/RANK/osteoprotegerin (OPG) signalling axis induces the differentiation of pre-osteoclasts to mature osteoclasts. This is because the binding of RANKL to its receptor, RANK, initiates the nuclear factor

of activated T-cells, cytoplasmic 1 (NFATc1) signalling cascade. NFATc1 is a transcription factor that induces the activation of several osteoclast target genes. Interestingly, NFATc1 has also been shown to promote osteoblastogenesis.

In the presence of MCSF and melanogenesis associated transcription factor (MITF), these monocytic precursors proliferate and differentiate into pre-osteoclasts. MCSF is critical for the proper differentiation of osteoclasts; the *op/op* mouse model encodes a spontaneous mutation of *Mscf*, producing non-functional MCSF, deficits in osteoclastogenesis, and osteopetrosis (Schönlau *et al.*, 2003). MCSF is responsible for activating downstream signalling pathways, including mitogen-activated protein kinase (MAPK) and phosphoinositide 3 kinase (PI3K)/AKT to induce cell cycle progression. In the presence of RANKL, these mononuclear osteoclasts, which express the RANKL receptor, fuse and polarize to become a mature osteoclast (Boyle *et al.*, 2003; Miyamoto & Suda, 2003). At this point, there is an increase in fusion and maturation genes, such as *Ap1* transcription factors, *Nfkb*, tumour necrosis factor receptor associated factor 6 (*Traf6*), etc. RANKL is essential for the maturation of osteoclasts and mouse models lacking RANKL or RANK, result in severe forms of osteopetrosis (Dougall *et al.*, 1999; Lo lacono *et al.*, 2012). Importantly, osteoclastogenesis relies on osteoblasts, which produce and secrete RANKL, as well as its antagonist, OPG. Following fusion, these multinucleated cells produce c-*Src* and  $\alpha_v\beta_3$  integrins, which allow for their attachment to bone matrix (Miyazaki *et al.*, 2004; Saltel *et al.*, 2004). Finally, these osteoclasts undergo polarization and produce proteases and channels, such as CLCN7 and cathepsin K

(CTSK), that will facilitate bone resorption. The process is outlined in Figure 1.4 (Teitelbaum & Ross, 2003).

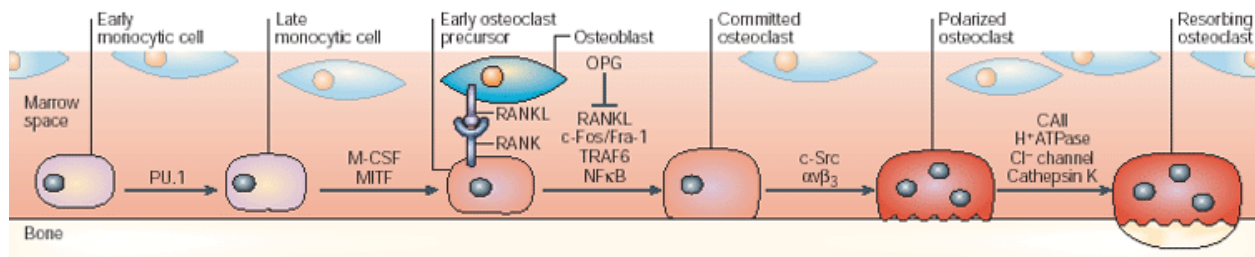


Figure 1.4: Illustration of osteoclastogenesis.

Activation of PU.1, coupled with MCSF interaction, commits a HSC to the osteoclast lineage. RANKL/RANK signalling will trigger the maturation and fusion of osteoclasts, which eventually must attach to the bone matrix, polarize, and secrete proteases and protons in a resorption pit. c-Src and  $\alpha_v\beta_3$  are involved in cytoskeletal attachment and rearrangement; ATP6I, CLCN7, and CAII are ionic pumps that allow for H<sup>+</sup> secretion for acidification of the resorption pit; CTSK is a protease involved in collagen breakdown. (Reprinted from Nature Review Genetics, Volume 4, Teitelbaum & Ross, Genetic regulation of osteoclast development and function, Page 639, Copyright (2003), with permission from Nature Publishing Group)

### 1.2.2 Osteoblast and its differentiation

Unlike osteoclasts, osteoblasts are not terminally differentiated. Moreover, they are mononuclear and cuboidal cells with a large endoplasmic reticulum (ER). The large ER suggests high levels of protein synthesis, which is necessary as these cells are responsible for producing extracellular bone matrix proteins, including type I collagen. Osteoblasts secrete alkaline phosphatase (ALP), which helps to liberate inorganic phosphate (P<sub>i</sub>) from pyrophosphate (PP<sub>i</sub>) and therefore promote mineralization (Arnett, 2007) of the initially unmineralized matrix, termed osteoid. Importantly, this P<sub>i</sub>/PP<sub>i</sub> ratio is crucial in regulating mineralization. A product of different metabolic reactions mediated by proteins such as NPP1 and ANKH, PP<sub>i</sub> acts as a potent negative regulator of mineral

nucleation by adsorbing to crystal growth sites and preventing further mineral ion deposition (Addison *et al.*, 2007). Thus, the enzymatic activity of alkaline phosphatase, specifically the tissue non-specific form, is critical for maintaining inorganic phosphate levels required for hydroxyapatite formation. Osteoblasts are also known to release matrix vesicles containing calcium and phosphate ions, which contribute to the mineralization of osteoid. Furthermore, these matrix vesicles seed additional crystals and mineralize collagen fibrils (Golub, 2009). Finally, osteoblasts are responsible for secreting cytokines that modulate osteoclastogenesis and thereby couple the activities of osteoblasts and osteoclasts.

Mature osteoblasts originate from the mesenchymal stem cell (MSC) lineage. Under the control of transcription factors, including the “master regulator” of osteoblastogenesis, Runt-related transcription factor 2 (RUNX2), these MSCs become pre-osteoblasts and are committed to the osteoblast lineage (Figure 1.5). From this point on, osteoblast differentiation is broadly characterized by three distinct stages: proliferation, maturation, and mineralization. The proliferation stage exhibits high levels of proteins such as collagen and fibronectin, followed by the maturation phase in which there is high expression of *Alp*. Lastly, the mineralization phase is defined by the increased expression of *Ocn* and *Opn*.

For osteoblastogenesis to occur, MSCs require the concerted and tightly-regulated expression of certain transcription factors, hormones, and cytokines. The initial commitment from a stem cell to the pre-osteoblast is dependent on RUNX2 and the

regulators, osterix (OSX) and  $\beta$ -catenin. *Runx2* is known to be highly expressed at the early stage of osteoblastogenesis to promote the commitment to pre-osteoblasts. It has also been found to inhibit the maturation of osteoblasts, therefore suggesting it is critical for the early steps of differentiation, but then maintains the pre-osteoblast pool by inhibiting the later stages. Accordingly, *Runx2*<sup>-/-</sup> mice fail to demonstrate ossification, and instead these animals possess a cartilaginous skeleton due to increased adipogenesis and chondrogenesis (Komori *et al.*, 1997; Otto *et al.*, 1997). Conversely, mice overexpressing *Runx2* using a 2.3 kb *Col1a1* promoter display decreased mature osteoblasts (Liu *et al.*, 2001). Interestingly, *Osx*<sup>-/-</sup> mice also lack evidence for ossification, although they do express *Runx2*, while the *Runx2*<sup>-/-</sup> mice do not express *Osx*. This suggests that *Runx2* is upstream of *Osx* (Nakashima *et al.*, 2002). Lastly,  $\beta$ -catenin has also been implicated in the process of osteoblast commitment as  $\beta$ -catenin knock-out MSCs differentiate into chondrocytes instead (Day *et al.*, 2005). Additionally, these knock-out MSCs still express *Runx2*, but not *Osx*, thereby demonstrating again that *Runx2* is upstream and the overall master regulator that is responsible for coordinating the differentiation of a MSC into a pre-osteoblast in conjunction with *Osx* and  $\beta$ -catenin (Komori, 2006). Previous evidence has also demonstrated the potential for cytokines and hormones, such as bone morphogenetic proteins (BMPs), parathyroid hormone (PTH), and vitamin D, in modulating osteoblastogenesis. For example, BMPs, which are upstream of *Runx2* and activate SMADs to stimulate target gene transcription, are thought to cooperate with *Runx2* to accomplish their pro-osteoblastic function. Similarly, another upstream effector of *Runx2*, PTH, is thought to stimulate osteoblastogenesis via

transforming growth factor- $\beta$  (TGF $\beta$ ), while vitamin D has been shown to interact with Runx2 to promote osteoblast differentiation (Rutkovskiy *et al.*, 2016).

After this initial commitment into the pre-osteoblast stage, the pre-osteoblasts will proliferate and become mature osteoblasts. This transition is characterized by the decreased expression of the early markers, like *Runx2*, and the increased expression of *Alp* and type I collagen (*Col1*). Finally, these mature osteoblasts will mineralize the osteoid, which is concomitant with elevated expression of bone matrix proteins such as osteopontin (OPN), which contribute to proper mineralization of bone tissue, as well as OCN. The process is outlined in Figure 1.5 (Miron & Zhang, 2012).

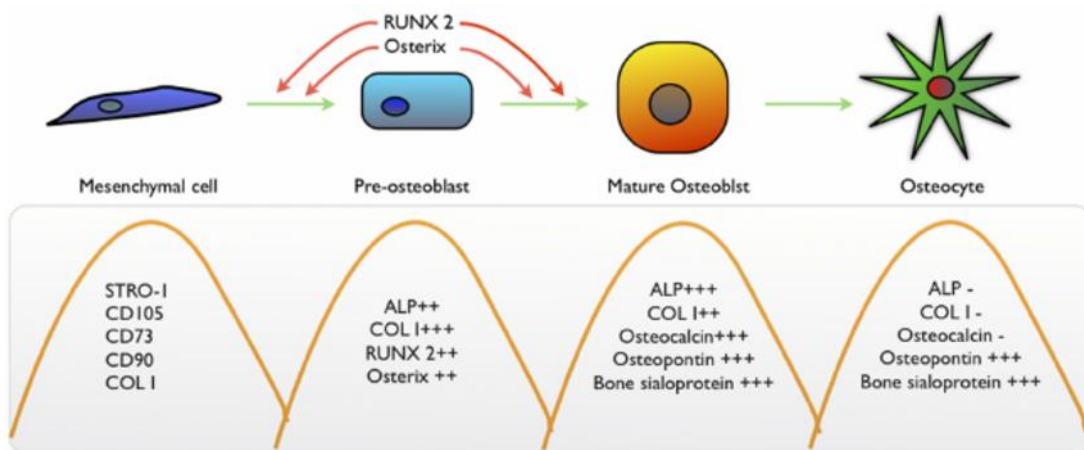


Figure 1.5: Illustration of osteoblastogenesis.

Interaction of Runx2, Osx, and  $\beta$ -catenin commits a MSC to the osteoprogenitor. Expression of *Alp* and *Col1* increase and the osteoprogenitor becomes a pre-osteoblast. Over time, markers like *Ocn* and *Opn* increase until the mature osteoblast stage. Osteoblasts will secrete type I collagen and non-collagenous proteins, which will become mineralized. Afterwards, a mature osteoblast can undergo one of three fates: terminal differentiation into an osteocyte, cell death via apoptosis, or quiescence as a lining cell. (Reprinted from Journal of Dental Research, Volume 91, Miron & Zhang, Osteoinduction: a review of old concepts with new standards, Page 740, Copyright (2012), with permission from SAGE Publications)

### 1.2.2.1 Osteocalcin (OCN)

OCN is a  $\gamma$ -carboxylated protein produced by mature osteoblasts to regulate glucose homeostasis. One of very few osteoblast-specific genes, *Ocn*, has been utilized extensively to study bone physiology (Harada & Rodan, 2003).

OCN exists in two forms: carboxylated on its three glutamate residues or undercarboxylated. Although its carboxylated form (Gla) has been shown to have high affinity for hydroxyapatite minerals (Hauschka *et al.*, 1989), loss- and gain-of-function experiments have failed to show an essential role for this protein in bone mineralization (Ducy *et al.*, 1996; Murshed *et al.*, 2004). Interestingly, studies involving *Ocn* knock-out mice demonstrated its ability to control glucose metabolism through its activity on the pancreas, in addition to insulin synthesis and secretion (Lee *et al.*, 2007). In particular, these *Ocn*-deficient mice exhibited decreased insulin secretion, insulin sensitivity, and glucose tolerance, coupled with decreased islet cell number,  $\beta$ -cell area and mass, and insulin content in the pancreas. Moreover, it was found that the majority of osteocalcin secreted by osteoblasts is bound to the bone extracellular matrix, while its undercarboxylated form (Glu) is secreted into the serum to promote insulin secretion via pancreatic  $\beta$ -cells (Ferron & Lacombe, 2014). To generate the Glu form, osteocalcin can be decarboxylated by the acidic pH generated as a result of osteoclastic bone resorption. Decarboxylation will decrease its binding affinity to the extracellular matrix, thereby releasing the undercarboxylated form into the bloodstream (Lacombe *et al.*, 2013) where it can exert its functions to regulate metabolism.

The carboxylation status of OCN can also be regulated by members of the vitamin K cycle (Lacombe & Ferron, 2015). This inactive, or Gla, form shows high affinity for hydroxyapatite crystals, though its exact function is independent of the mineralization process (Ducy *et al.*, 1996). However, once active, the Glu form of OCN exerts a role on the pancreas via interaction with the G protein-coupled receptor, GPRC6A. *Gpcr6a*<sup>-/-</sup> mice phenocopy the metabolic abnormalities of the *Ocn*<sup>-/-</sup> mice and the capacity for OCN to promote insulin secretion was abrogated in *Gpcr6a*<sup>-/-</sup> knock-out mice (Wei *et al.*, 2014).

Despite no significant role in biomineralization, OCN is produced exclusively by the mature osteoblast. Studies have therefore capitalized on this property of OCN to target specific gene disruption or overexpression in the mature osteoblast only (Kanazawa *et al.*, 2015; Kesterson *et al.*, 1993; Liu *et al.*, 2007).

### **1.2.2.2 Function of osteoblasts**

Osteoblasts serve two important functions: 1) being responsible for secreting and mineralizing the extracellular bone matrix and 2) regulating osteoclastogenesis by the secretion of different signalling factors.

Mineralization is a function of the mature osteoblast, via two steps. First, osteoblasts must elaborate a collagen-rich template via secretion of type I collagen, proteoglycans, and many non-collagenous proteins such as OCN, OPN, and BSP (Ducy *et al.*, 1997; Glass *et al.*, 2005). These components make up the osteoid, or organic part of the matrix. Next, the osteoid will be mineralized by the deposition of calcium ions, which are

transported in “matrix vesicles” secreted by the osteoblast (Yoshiko *et al.*, 2007). These “matrix vesicles” have been shown to derive from double-membraned autophagosome-like structures that release needle-like structures resembling crystals into extracellular medium, thereby implicating autophagy in the process of mineralization. For example, autophagy-related proteins such as ATG5 and ATG7 facilitate the conjugation of LC3-I to phosphatidylethanolamine to form LC3-II, which is associated with double-membraned autophagic vesicles (Bestebroer *et al.*, 2013). Moreover, knock-out of *Atg5* in osteoblasts under the control of the *Col1a1* promoter revealed a significant decrease in mineralization *ex vivo* (Nollet *et al.*, 2014). During this time, osteoblasts secrete enzymes that degrade the proteoglycans, thereby releasing the trapped calcium ions that can travel across the vesicular membrane. At the same time, osteoblasts secrete ALP, which liberates phosphate ions inside the membrane. Calcium and phosphate ions nucleate in the matrix, resulting in the hydroxyapatite crystals. Eventually, the vesicle will burst and release the hydroxyapatite crystals, which can grow and propagate (Florencio-Silva *et al.*, 2015). Following mineralization, it is estimated that approximately 5% of osteoblasts become the quiescent bone-lining cells, 30% become osteocytes, and the remaining cells die by apoptosis (Weinstein & Manolagas, 2000).

The second main function of the osteoblast is to communicate with osteoclast precursors and modulate their subsequent differentiation. Osteoblasts accomplish this by producing MCSF, RANKL, and OPG, which are critical players in osteoclastogenesis. MCSF is the main proliferation and survival cytokine necessary for pre-osteoclasts to undergo osteoclastogenesis while the RANKL/RANK/OPG system has been extensively studied

to show that the interactions of RANKL with the pro-osteoclastic RANK and the decoy receptor, OPG, can alter osteoclastogenesis (Udagawa *et al.*, 1999). As such, osteoblasts serve an important, and necessary, role not only in building bone, but in fine-tuning proper bone mass by the modulation of osteoclastogenesis.

### **1.2.3 Osteocytes**

Osteocytes are the major cellular component of bone and are found embedded within the extracellular matrix. These cells arise from a subpopulation of osteoblasts that have undergone a series of subtle morphological changes, including the adoption of a dendritic appearance, reduction in ER and Golgi apparatus, and an increase in nucleus-to-cytoplasm ratio (Florencio-Silva *et al.*, 2015). Importantly, osteocytes acquire an elaborate network of cytoplasmic processes that are used to communicate via gap junctions and intracellular signalling. They also provide a means of communicating with osteoblasts and osteoclasts on the bone surface to regulate their activities and functions (Palumbo *et al.*, 1990).

The presence of these intercellular processes facilitates intercellular communication between bone cells to allow for proper bone maintenance. Firstly, osteocytes serve an important role as mechanosensitive cells that can detect microstructural damage and transduce signals via biochemical reactions (Zaman *et al.*, 1999). Increasing evidence has demonstrated their ability in directly or indirectly affecting the activities of osteoblasts and osteoclasts to repair bone (Mason *et al.*, 1997). In particular, it was shown that shear-stress of the osteocyte by mechanical strain induces the production of several signalling

molecules such as nitric oxide and prostaglandins (McAllister & Frangos, 1999; Rawlinson *et al.*, 1995) that can influence osteoblastic and osteoclastic functions. Beyond the response to mechanical stress, osteocytes may also play a role in recruiting and regulating the activities of osteoclasts in local sites of bone remodelling through the secretion of RANKL and OPG (Tatsumi *et al.*, 2007). However, the exact mechanisms that control this entire process are not completely understood and require further studies. In addition, osteocytes may affect bone homeostasis via production of sclerostin (SOST). SOST is known to influence bone remodelling by antagonizing Wnt signalling. Specifically, SOST binds to the co-receptors, LRP5/6, which are important in the activation of the Wnt signalling pathway. SOST loss-of-function studies revealed a hyperactivation of the Wnt signalling pathway thereby resulting in bone overgrowth and sclerosteosis (Semënov *et al.*, 2005).

Finally, osteocytes have also been shown to serve a function in maintaining proper ionic concentrations. This is thought to be a consequence of a large surface area associated with the osteocytic network, along with the presence of certain receptors that affect ion homeostasis (Pajevic, 2009).

### **1.3 Bone modelling and remodelling**

Bone modelling is the process during which bones grow and are shaped to respond to mechanical loading. In this case, the processes of bone formation and resorption are uncoupled and occur at different sites. Therefore, the balance is shifted in favour of the bone-building osteoblast. This is especially important during development and slows

down in adulthood. In contrast, bone remodelling is a process that constantly occurs throughout life and couples the activities of osteoblasts and osteoclasts, thereby maintaining bone homeostasis (Figure 1.6). Remodelling is particularly important as it occurs primarily in response to microfractures of the bone. Broadly, remodelling is initiated when osteocytes, the mechanosensitive cells, are triggered by mechanical stress or signals during their resting phase. In response, an activation phase takes place, whereby osteoclasts are recruited to the site of damage/signalling on the bone. They then resorb the bone as a part of the resorption phase, which is followed by a reversal phase wherein these osteoclasts undergo cell death via apoptosis while osteoblasts are recruited to this site. Next, the recruited osteoblasts build new bone that is mineralized soon after (Kapinas & Delany, 2011; Langdahl *et al.*, 2016).

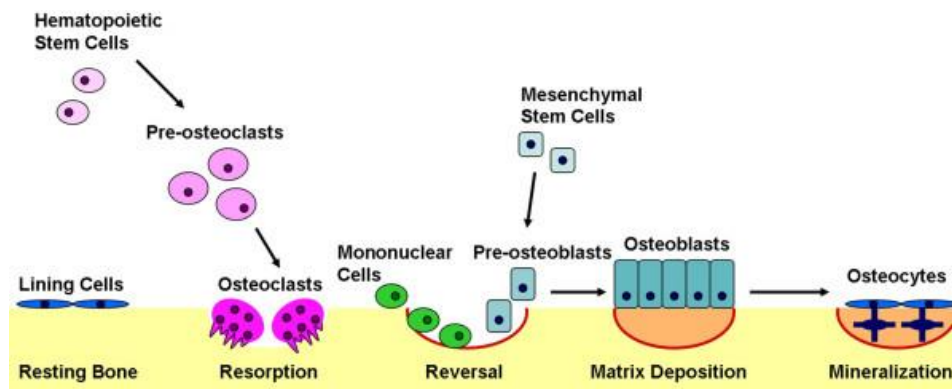


Figure 1.6: Stages of bone remodelling.

(Reprinted from Arthritis Research & Therapy, Volume 13, Kapinas & Delany, MicroRNA biogenesis and regulation of bone remodeling, Page 5, Copyright (2011), with permission from BioMed Central as open access)

## **1.4 Molecular pathways involved in osteoblastogenesis and bone homeostasis**

A number of signalling pathways have been implicated in osteoblast proliferation and differentiation. These pathways, therefore, exhibit bone-specific effects that can regulate overall bone mass that is otherwise maintained by bone remodelling. Among them, the TGF $\beta$ /BMP and Wnt/ $\beta$ -catenin pathways have been characterized in the overall coordination of osteoblast proliferation and differentiation. Moreover, the NFATc1 signalling pathway has also been shown to be a key player not only in osteoclastogenesis, but in osteoblastogenesis as well.

### **1.4.1 TGF $\beta$ /BMP signalling in osteoblasts**

BMPs form a subgroup of growth factors in the TGF $\beta$  superfamily. In brief, BMPs, through ligand-receptor interactions, activate intracellular SMAD or MAPK signalling pathways. These pathways play an important role in skeletal development, as well as in postnatal bone homeostasis.

The TGF $\beta$  isoforms (TGF $\beta$ 1, TGF $\beta$ 2, and TGF $\beta$ 3) have been shown to regulate bone mass in several studies. TGF $\beta$ 1 has been associated with many important functions in the osteoblast, including recruitment, proliferation, and early differentiation (Pfeilschifter *et al.*, 1990). TGF $\beta$ 1-knockout mice present with a reduction in bone mass and mineralization (Gordon & Blobe, 2008). The molecular basis of these findings come from the fact that many osteoblast-specific genes, such as *Alp*, *Opn*, *Ocn*, etc., have an AP-1 binding site, which is important for TGF $\beta$  binding (Banerjee *et al.*, 1996; Chung *et al.*, 1996). Moreover, double knock-out mice for TGF $\beta$ 2 and TGF $\beta$ 3 exhibit bone defects at

the level of the ribs (Dünker & Krieglstein, 2002). Mutations in the receptors for TGF $\beta$  also play a role in proper bone formation (Iwata *et al.*, 2010; Matsunobu *et al.*, 2009). As a part of the canonical signalling pathway, the activation of TGF $\beta$  receptor types I and II (TGF $\beta$ RI and II) mediates the activity of R-SMADs, specifically SMAD2 and SMAD3, which must complex with SMAD4 to translocate to the nucleus and activate target gene transcription of early osteoblast genes, such as Runx2 (Chen *et al.*, 2012). Mutations of SMAD2/3 regulators (Sapkota *et al.*, 2006) or activations of their inhibitors (Kavsak *et al.*, 2000), therefore, play a major role in bone homeostasis. The non-canonical TGF $\beta$  signalling pathway, which involves the p38 MAPK has also been demonstrated to exert effects on osteoblast differentiation. This pathway involves the activation of TGF $\beta$  activation kinase-1 (TAK1), which is important for the overall activation of MKK/p38 MAPK-dependent activation of Runx2 (Matsunobu *et al.*, 2009).

BMPs have also been shown to modulate bone through canonical and non-canonical pathways. Addition of BMP2, for example, increased OCN expression, as well as overall bone formation (Huang *et al.*, 2010; Noël *et al.*, 2004). In general, however, BMPs activate SMADs 1, 5, and 8, which must complex with SMAD4 to translocate to the nucleus (Figure 1.7). Non-canonical signalling by BMPs also requires the TAK1/MKK/p38 MAPK axis, which is important for *Runx2* transcription.

Interestingly, the TGF $\beta$ /BMP signalling pathway has been shown to interact with another important signalling pathway for osteoblastogenesis, Wnt/ $\beta$ -catenin. The two pathways appear to coordinate the overall differentiation of osteoblasts through complex effectors

and therefore require further studies to fully elucidate this interaction (Zhang *et al.*, 2009; Zhou, 2011).

#### **1.4.2 Wnt/ $\beta$ -catenin signalling in osteoblasts**

The canonical Wnt/ $\beta$ -catenin signalling pathway has been previously implicated in osteoblastogenesis as an important factor that promotes osteoblast differentiation from the MSC while simultaneously inhibiting chondrogenesis (Figure 1.7). This pathway involves the inhibition of the APC/Axin/GSK3 $\beta$ /CK1 complex, thereby allowing  $\beta$ -catenin to translocate to the nucleus and activate its target genes in osteoblastogenesis (Choi *et al.*, 2009).

The nuclear translocation of  $\beta$ -catenin relies on Wnt binding to the Frizzled (FZD)/LRP5/6 receptor complex. This interaction allows for the activation of dishevelled (DVL), which can in turn inactivate the APC/Axin/GSK3 $\beta$ /CK1 complex. In the absence of Wnt, this complex will phosphorylate  $\beta$ -catenin, through the actions of GSK3 $\beta$ , which promotes its degradation in the cytoplasm. However, the presence of Wnts, such as Wnt1 and Wnt3a, coupled with the activation of DVL, will inhibit this degradation complex by the phosphorylation and subsequent inhibition of GSK3 $\beta$  by DVL, thereby allowing unphosphorylated  $\beta$ -catenin to accumulate and then translocate to the nucleus of the cell where it can associate with LEF/TCF1 class of genes important for bone formation. Antagonists that interfere with the activation of the canonical Wnt signalling, such as secreted frizzled-related proteins and sclerostin (SOST) represent novel strategies in regulating bone homeostasis. Interestingly, SOST has been shown to bind the LRP5/6

receptor, thereby preventing the activation of  $\beta$ -catenin (Semenov *et al.*, 2005). Furthermore,  $SOST^{-/-}$  mice exhibit a high bone mass (Loots *et al.*, 2005), while transgenic mice overexpressing SOST display low bone mass (Winkler *et al.*, 2003).

A non-canonical pathway for Wnt/ $\beta$ -catenin also exists and in recent years, it has been determined to play a role in osteoblast differentiation and bone formation through a PKC-dependent mechanism. This non-canonical pathway has been highlighted in studies involving either  $PKC\delta^{-/-}$  or  $Wnt7b$  mutant mice, in which there was a bone formation deficit in embryonic development, as well as in bone nodule formation *in vitro* (Tu *et al.*, 2007).

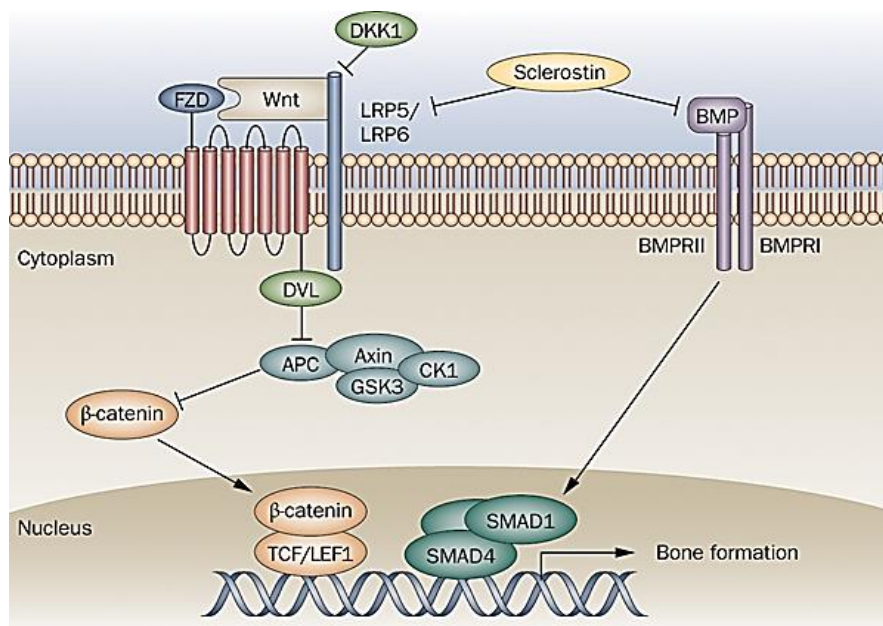


Figure 1.7: Canonical Wnt/ $\beta$ -catenin signalling in osteoblasts.

Interaction of WNT with FZD and LRP5/6 activates DVL. This prevents the GSK3 $\beta$  complex from phosphorylating  $\beta$ -catenin, thereby allowing for its nuclear translocation where it will stimulate the TCF/LEF1 transcription factors. In a separate pathway, BMP signalling can activate transcription of osteoblast genes through SMAD1/5/8 complexes with SMAD4. DKK1 and sclerostin, produced by osteocytes, can inhibit these pathways. (Reprinted from Nature Reviews Rheumatology, Volume 5, Choi *et al.*, Promising bone-related therapeutic targets for rheumatoid arthritis, Page 545, Copyright (2009), with permission from Nature Publishing Group)

### 1.4.3 NFAT signalling in osteoclasts and osteoblasts

NFATc1 signalling is considered the main signalling pathway for osteoclastogenesis. Upon binding of RANKL to RANK on the pre-osteoclast surface, there is the activation of a signalling cascade involving the second messenger, TRAF6. This interaction, in turn, recruits MAPKs and NF $\kappa$ B, which activate the transcription factor NFATc1, amongst others. NFATc1 promotes the maturation of osteoclasts by expression of late genes, such as tartrate-resistant acid phosphatase (TRAP) and CTSK. NFATc1 can also be activated by calcium oscillations wherein the RANKL/RANK interaction activates PLC $\gamma$ , triggering the release of intracellular Ca<sup>2+</sup> by inositol-1,3,4-trisphosphate (IP3) generation. Ca<sup>2+</sup> binds to the phosphatase, calcineurin, which can dephosphorylate NFATc1, thus allowing NFATc1 to translocate to the nucleus of the cell. Again, this will promote the maturation of osteoclasts.

While this pathway has been well-characterized in the context of osteoclastogenesis, there is also evidence demonstrating that it is involved in osteoblast proliferation and differentiation as well (Figure 1.8). Targeted therapies for calcineurin inhibition, such as cyclosporine, result in bone loss (Sprague, 2000), suggesting a possible role for calcineurin, and thus NFATc1, in osteoblasts. A constitutively-active form of nuclear NFATc1 in osteoblasts resulted in mice with high bone mass due to an increase in osteoblast number and activity, concomitant with increased Wnt effectors (Winslow *et al.*, 2006). There was also an increase in osteoclastogenesis that was coupled with increased expression of chemoattractants such as CCL8.

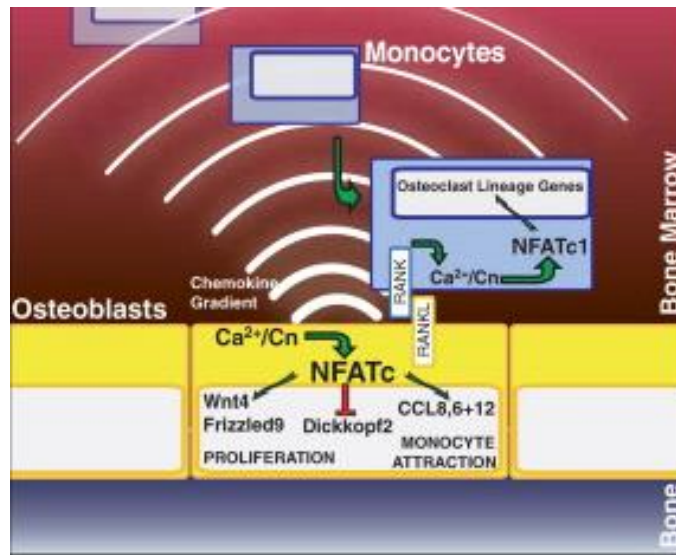


Figure 1.8: NFATc1 signalling in osteoblasts.

Increased  $\text{Ca}^{2+}$  signalling activates the calcineurin phosphatase, which will activate NFATc1 nuclear translocation. Increased nuclear NFATc1 will promote osteoblast proliferation through Wnt signalling. NFATc1 will also activate transcription of monocyte cytokines that will recruit osteoclast precursors. (Reprinted from *Developmental Cell*, Volume 10, Winslow *et al.*, Calcineurin/NFAT Signaling in Osteoblasts Regulates Bone Mass, Page 778, Copyright (2006), with permission from Elsevier)

#### 1.4.4 PI3K/AKT signalling in bone

The PI3K/protein kinase B (AKT) pathway is an emerging field of study in our understanding of bone biology. In general, the PI3K/AKT pathway is responsible for cell survival, growth, and proliferation in many cells. However, over the years, mounting evidence has illustrated that some molecular players may exert effects specifically within the osteoblast.

## **1.5 Bone disorders**

Given the variety of functions performed by bone, a dysregulation in bone formation and/or resorption by any combination of the aforementioned pathways can result in various bone diseases, including, but not limited to, Paget's disease, osteosarcoma, osteoporosis, and osteopetrosis.

### **1.5.1 Paget's disease of the bone**

Considered one of the most prevalent bone remodelling disorders, Paget's disease of the bone (PD) is characterized by excessive breakdown and formation of bone tissue, resulting in weakened bones. Although the majority of individuals afflicted with PD are asymptomatic, some may experience significant bone pain and skeletal deformity, increasing the likelihood of developing fractures, arthritis, and bone cancer. PD is particularly prevalent in elder populations (typically over the age of 50), affects both males and females, and is highly localized to one or a few affected bones (Roodman & Windle, 2005).

In PD, the osteoclast is the main cell affected. Compared to normal osteoclasts, pagetic osteoclasts are increased in size and number, contain more nuclei, and have been found to be hypersensitive in response to osteoclastogenic factors (Neale *et al.*, 2000). As a result, pagetic bones are subjected to excessive resorption at localized sites. Due to the coupling between resorption and formation, there is an increased number of hyperactive osteoblasts that rapidly deposit new bone at the site of osteolytic lesion; however, these osteoblasts deposit bone in a disorganized fashion, thereby predisposing PD patients to

bowing and/or fractures of the bone (Roodman & Windle, 2005). Ultimately, the development of PD can lead to other medical conditions, including osteoarthritis and bone tumours. Given its high prevalence, determining the cause of PD is under intense investigation as it has both genetic and non-genetic factors. For example, the *SQSTM1* gene is most commonly implicated in the pathogenesis of PD as it is known to play a role in osteoclastogenesis. More specifically, mutations in this gene have resulted in hypersensitive osteoclasts, leading to the increased bone resorption characteristic of pagetic bones (Laurin *et al.*, 2002).

### **1.5.2 Osteosarcoma**

Osteosarcoma represents the most common primary bone malignancy in children and young adults. Owing to its large, heterogeneous genetic profile, osteosarcoma involves a number of genetic events that together contribute to its pathogenesis. With age, the frequency of sites of osteosarcoma in individuals shifts from the metaphysis of lower long bones in children and adolescents to the axial and craniofacial bones of people over 60 (Durfee *et al.*, 2016; Mirabello *et al.*, 2009).

Osteosarcoma can arise from spontaneous mutations that result in the loss of tumour suppressor genes. The most well-studied instances of osteosarcoma include the loss-of-function of the *TP53* and *RB1* genes, which encode for the p53 and pRb proteins, respectively. The p53 protein is a master transcription factor responsible for DNA repair, thus mutations in this gene can lead to several malignancies, of which approximately 30% result in osteosarcoma (Bougeard *et al.*, 2015). In the case of *RB1*, loss of the pRb

protein results in unregulated cell cycle progression, leading to increased risk for retinoblastoma, melanoma, and osteosarcoma (Wong *et al.*, 1997). Mutations in major signalling pathways can also promote metastasis in the bone. For example, alteration of the insulin-like growth factor receptor pathway has been shown to activate the PI3K/Akt/mTOR and MAPK/ERK cascades. These cascades promote proliferation, migration, and survival (Kappel *et al.*, 1994; Lamplot *et al.*, 2013) which are associated with osteosarcoma metastasis. To date, genome-wide association studies continue to identify novel loci contributing to the pathophysiology of osteosarcoma, thereby uncovering novel susceptibility loci and therapeutic targets.

### **1.5.3 Osteoporosis**

Osteoporosis is a metabolic bone disorder characterized by low bone mass. This translates to increased fragility and risk of fracture, and is therefore considered a “silent thief”, according to Osteoporosis Canada, particularly for postmenopausal women. In fact, current estimates suggest that one third of women and one fifth of men will develop osteoporosis in their lifetime. Worldwide, this has led to approximately 200 million women affected by osteoporosis, and about 9 million fractures annually, making fractures more common than heart attack, stroke, and breast cancer combined. Evidently, osteoporosis can have huge implications on personal and economic health and only highlights the need to further our understanding of potential preventative strategies.

Both genetic and environmental factors contribute to the development of osteoporosis. Broadly speaking, it occurs when there’s an imbalance in bone formation and resorption,

such that resorption is favoured. As a polygenic disease, the combination of common polymorphic alleles, pre-existing medical conditions, nutrition, and exercise all contribute to this dysregulation. In addition, hormonal imbalances, especially in women, can drastically increase the likelihood of developing osteoporosis. Studies have shown that estrogen is a key player in osteoclastogenesis. More specifically, estrogen-deficiency leads to the recruitment and hyperactivation of osteoclasts via proinflammatory cytokines like interleukin-1 (IL1), interleukin-6 (IL6), and tumor necrosis factor alpha (TNF $\alpha$ ). To date, hormone therapy for estrogen is available, albeit with the increased potential of developing cancer (Gambacciani & Levancini, 2014). Similarly, bisphosphonates are widely used to treat postmenopausal osteoporosis as they can inhibit osteoclast activity and restore the bone. However, there are different adverse side-effects associated with their use (Kennel & Drake, 2009). Thus, the identification of novel genetic determinants of osteoporosis may provide effective interventions of this crippling disease.

#### **1.5.4 Osteopetrosis**

Osteopetrosis is a family of rare bone disorders first characterized by Dr. Albers-Schönberg in 1904 as “marble bone disease” due to its appearance on X-ray radiographs. Patients suffering from osteopetrosis develop hardened and dense bones due to defects in the differentiation or activity of osteoclasts, which results in decreased bone resorption and therefore increased likelihood of developing fractures. Based on inheritance, clinical presentation, and severity, there are three categories of osteopetrosis: autosomal dominant (benign), intermediate autosomal, and autosomal recessive (malignant). This variation in disease phenotype also gives rise to other symptoms beyond the skeleton,

including in the immune and nervous systems. Causative genes have been identified in humans, which account for approximately 70% of all cases of osteopetrosis (Zornitza & Savarirayan, 2007). Furthermore, mouse models of osteopetrosis provide an opportunity to better characterize the molecular pathways involved and thus help to identify new avenues for prevention and intervention.

Autosomal dominant osteopetrosis (ADO), also termed “Albers-Schönberg disease” after its founder, is the mildest form of the disease. It is expected to occur in approximately 1:20,000 individuals (Bollerslev & Andersen, 1988), with most being diagnosed in adulthood by chance. This is because ADO patients are usually asymptomatic; for those who do present with symptoms, they are mainly restricted to bone defects such as increased incidence of fractures and scoliosis.

Intermediate autosomal osteopetrosis (IAO) represents a rare classification of osteopetrosis, which can be inherited in an autosomal dominant or recessive fashion. Usually, children develop signs and symptoms of IAO, which include bone fragility and anemia; however, for more severe cases, children can also present with neurological deficits resulting from calcification of the brain.

Autosomal recessive osteopetrosis (ARO) is an extremely rare class of osteopetrosis that affects every 1:250,000 births, resulting primarily in premature death during the first decade of life. On top of an increased risk for bone fracture, these patients are severely afflicted by hematological, hematopoietic, and neurological symptoms. Increased bone

mass in the skull can pinch the cranial nerves, leading to vision loss, hearing loss, and paralysis. Moreover, there is a lack of bone marrow cavity due to excessive bone growth, impeding the hematopoietic niche which is essential for blood cells and immune cells (Tolar *et al.*, 2004). Treatment for ARO is particularly difficult because of the heterogeneity of affected systems; to date, the only successful treatment method is bone marrow transplant, though recipients can continue to suffer from bone-related symptoms (Wilson & Vellodi, 2000).

As previously mentioned, genes that affect the differentiation and/or activity of osteoclasts can give rise to ADO, IAO, or ARO when perturbed or mutated. Knowing this, animal models of osteopetrosis can give deeper insight into the interactions affected.

### **1.5.5 Grey-lethal (*gl/gl*) murine model of ARO**

Previous findings in the lab have resulted in the characterization of a murine model of human ARO. A mutation in the *Ostm1* gene was found to be responsible for the “grey-lethal” phenotype (Chalhoub *et al.*, 2003). Grey-lethal mice possess a grey coat colour, instead of agouti, and consistently die between 3 and 4 weeks of age due to a combination of skeletal and extra-skeletal phenotypes. Although these mutant mice displayed increased osteoclastogenesis *in vivo*, these osteoclasts were found to have disrupted cytoskeletal rearrangement and defective ruffled border formation which is essential for resorption to take place (Rajapurohitam *et al.*, 2001). These mice also showed a defective neuronal phenotype and impaired immunological development. Together, this disrupted multi-system phenotype highly mimics the OSTM1 mutation seen in humans

(Maranda *et al.*, 2008). As such, the grey-lethal mouse represents an excellent background to study other potential regulators of bone homeostasis.

One such example in which the *gl/gl* mouse contributed to the identification of a novel bone mass regulator is in the case of inositol polyphosphate-4-phosphatase, type II (*Inpp4b*). Differential display screens from *gl/gl* bone revealed a significant downregulation of the *Inpp4b* transcript. Moreover, INPP4B was found to be associated with bone mineral density (BMD) in humans, and therefore act as a prognostic locus of osteoporosis in postmenopausal women (Ferron *et al.*, 2011). Consequently, our lab became interested in determining the role of this lipid phosphatase in bone homeostasis.

### **1.6 *Inpp4b* and the PI3K/AKT signalling pathway**

The opposing actions of kinases and phosphatases is critical for maintaining lipid homeostasis, which has been implicated in a number of physiological processes, including, but not limited to, differentiation, growth, and apoptosis (Cantley, 2002). Phosphorylation and dephosphorylation of these lipids occurs at the D3, D4, or D5 position. The site of phosphorylation is important for the activation and induction of different signalling pathways (Figure 1.10). Initiation of this pathway requires the interaction of a growth factor with its receptor on a cell membrane. Usually, this interaction occurs between members of the receptor tyrosine kinase and receptor family, which include fibroblast growth factor and insulin-like growth factor (McGonnell *et al.*, 2012). This causes dimerization and activation of the receptor, thereby recruiting phosphoinositide 3-kinase (PI3K). PI3K is one of the most critical components of this intracellular signalling pathway and is responsible for phosphorylating the D3 position of

phosphoinositides to generate phosphatidylinositol 3,4,5-triphosphate (PI(3,4,5)P3) from its substrate, PI(4,5)P2. PI(3,4,5)P3's role in cell growth and proliferation results from the recruitment of AKT and phosphoinositide-dependent kinase-1, PDK1, to the cell membrane. This recruitment allows PDK1 to phosphorylate AKT on the threonine 308 position, thereby activating AKT which will phosphorylate its downstream targets. For example, AKT negatively regulates pro-apoptotic factors, such as BCL2, thereby promoting cell survival (Datta *et al.*, 1997). AKT has also been shown to play a role in regulating the actions of mammalian target of rapamycin (mTOR) (Scott *et al.*, 1998). mTOR and its targets serve critical roles in cell growth, and thus its activation by AKT can lead to extensive growth. Lastly, AKT activation promotes cell cycle progression by the inactivation of p53-inhibitors (Liang *et al.*, 2002). Together, these studies demonstrate that without a proper mechanism of regulating PI(3,4,5)P3 activity, there can be negative consequences such as cancer that arise.

PI(3,4,5)P3 can be deactivated through dephosphorylation by phosphatases such as phosphatase and tensin homolog (*Pten*), SH2 domain-containing inositol 5'-phosphatase (*Ship*), and *Inpp4b*. Overactive PI(3,4,5)P3 can demonstrate pro-oncogenic properties, and therefore its inactivation is important as a means to prevent the tendency towards tumourigenesis. *Pten* and *Ship* dephosphorylate PI(3,4,5)P3 at the D3 and D5 positions to generate PI(4,5)P2 and PI(3,4)P2, respectively. PI(3,4)P2 can also trigger AKT activation (Scheid *et al.*, 2002) and therefore requires further dephosphorylation to inactivate it. This can be accomplished by *Inpp4b* to dephosphorylate the D4 position and generate PI3P. In fact, previous groups have noted that in the absence of *Inpp4b*,

there is increased AKT activation and tendency towards cancer progression, as is the case for prostate cancer (Hodgson *et al.*, 2011).

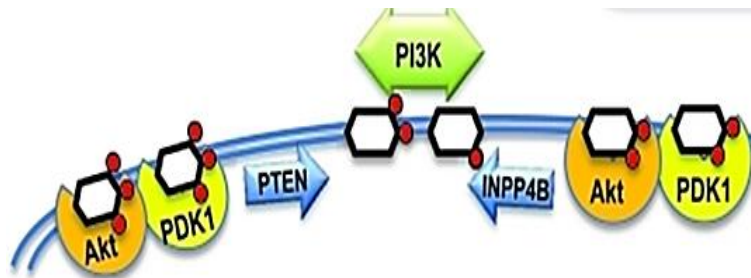


Figure 1.9: PI3K signalling pathway.

Recruitment of AKT and PDK1 is mediated by the presence of PI(3,4,5)P<sub>3</sub>. PTEN and INPP4B are phosphatases that will generate PI(4,5)P<sub>2</sub> and PI3P, respectively, from PI(3,4,5)P<sub>3</sub>. This dephosphorylation is reversible by the actions of PI3K. (Reprinted from *Oncotarget*, Volume 2, Agoulnik *et al.*, INPP4B: the New Kid on the PI3K Block, Page 322, Copyright (2011), with permission from Impact Journals LLC)

The fact that *Inpp4b* mRNA was significantly down regulated in the grey-lethal model prompted in-depth studies to dissect the function of PI3K signalling and lipid phosphatases in bone physiology. This was particularly important given the fact that other phosphatases in this pathway have been shown to have bone-specific roles themselves.

### 1.6.1 Characterization of *Inpp4b*

The *Inpp4b* gene exists as two isoforms, type I (a) or type II (b), each with two variants,  $\alpha$  or  $\beta$ . *Inpp4* isoforms were originally identified in rat brain, share 37% homology, and differ at their C-terminal ends: the  $\alpha$  isoforms have a hydrophilic C-terminal region, while  $\beta$  isoforms have a hydrophobic one (Norris *et al.*, 1997). Murine *Inpp4b* was isolated and characterized in our lab using the rat *Inpp4b* cDNA sequence for alignment and amplification on a C57BL/6J spleen cDNA library to obtain a murine clone. Genetic

mapping studies involving a (GATA)<sub>n</sub> repeat polymorphism allowed us to identify the locus within a 2.2cM genetic interval, which was syntenic to the human *INPP4B*. This region displayed perfect conservation of gene order to the human locus and the more precise physical mapping analysis narrowed the region to a one megabase interval. Subsequent alignment with the murine *Inpp4b* cDNA identified the gene, which is composed of 25 exons and approximately 800kb of genomic DNA (Ferron & Vacher, 2006). Alternative splicing at exon 25 gives rise to the splice variants,  $\alpha$  and  $\beta$ .

#### **1.6.1.1 *Inpp4b* gene expression**

*Inpp4* isoform expression pattern reveals differential gene expression. The  $\beta$  isoforms show more restricted expression in the brain while  $\alpha$  isoforms are more broadly expressed in various tissues (Ferron & Vacher, 2006). As they are both expressed in the spleen and thymus, a more detailed analysis revealed their expression in hematopoietic lineage. Only *Inpp4ba* is detected in these lineages, which include natural killer and mast cell populations.

#### **1.6.1.2 INPP4B protein**

Murine INPP4A and INPP4B proteins encode for 927 and 941 amino acid (aa) proteins, respectively. These proteins have a molecular weight of approximately 105kDa and 106kDa, respectively, and share 45% aa identity between isoforms. Moreover, the murine forms exhibit 96% identity with the human forms (Ferron & Vacher, 2006). INPP4 proteins contain three important domains: a C2 lipid-binding domain, a Nervy homology 2 (NHR2) domain, and a phosphatase domain (Agoulnik *et al.*, 2011) (Figure 1.11A).

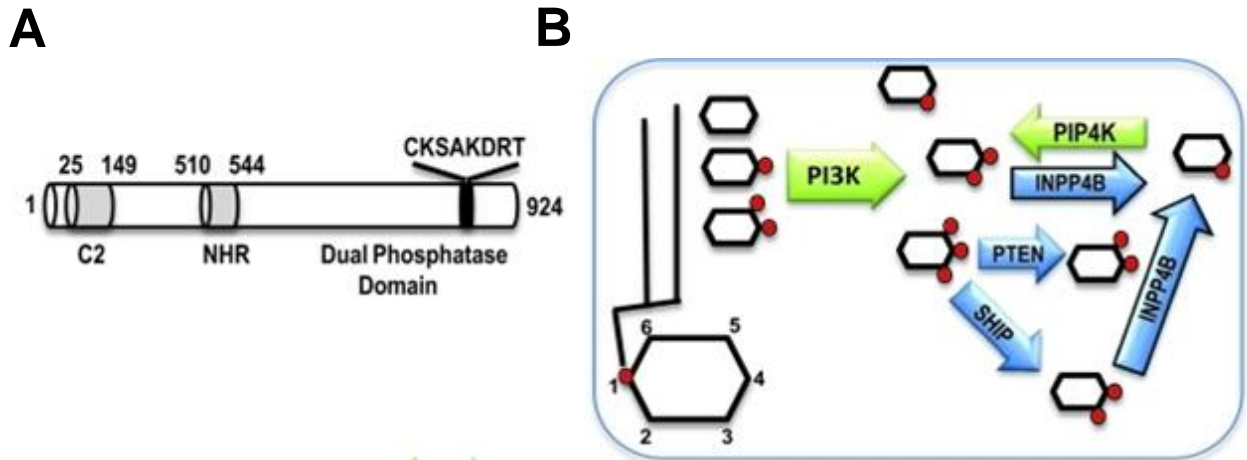


Figure 1.10: INPP4B protein structure and function.

(A) INPP4B protein with three domains: C2 lipid-binding domain, Nervy Homology 2 (NHR2) domain, CX<sub>5</sub>R dual phosphatase domain. (B) PI3K signalling factors and their preferred substrates. (Reprinted from *Oncotarget*, Volume 2, Agoulnik *et al.*, INPP4B: the New Kid on the PI3K Block, Page 322, Copyright (2011), with permission from Impact Journals LLC)

The INPP4B is classified as Mg<sup>2+</sup>-independent and is primarily responsible for dephosphorylating PI(3,4)P<sub>2</sub> to produce PI3P (Figure 1.11B). This activity is mediated by the different domains of the protein. The N-terminal C2 lipid-binding domain binds preferentially PI(3,4,5)P<sub>3</sub> and phosphatidic acid (Ferron & Vacher, 2006). NHR2 domains appear to play a role in protein-protein interactions and oligomerization (Liu *et al.*, 2006). Lastly, the C-terminal phosphatase region contains a CX<sub>5</sub>R motif that demonstrates dual phosphatase activity for both lipids and proteins (Agoulnik *et al.*, 2011)

### 1.6.1.3 INPP4B binding affinity

As previously reported, the major substrate for INPP4B is PI(3,4)P<sub>2</sub>, with lower affinity for Ins(3,4)P<sub>2</sub> and Ins(1,3,4)P<sub>3</sub> (Norris *et al.*, 1995). Once bound, INPP4B will dephosphorylate the D4 phosphate group. Integral to this process is the dual

phosphatase domain of the protein. Consequently, a previously described site-directed mutation of cysteine 845 to alanine rendered the protein unable to exert its function. As C2 domains have also been implicated in the recruitment of lipids and proteins, *in vitro* binding assays with recombinant INPP4B-C demonstrated that the C2 domain preferentially binds phosphatidic acid and PI(3,4,5)P3 (Ferron & Vacher, 2006). Not much is known about the NHR2 domain, though it is thought to be involved in protein-protein interactions.

#### **1.6.1.4 INPP4B localization**

INPP4B is predominantly expressed in the brain, spleen, small intestine, lung, and testis. *Inpp4b* cDNA that was inserted in frame with an EGFP expression vector transfected into COS-7 cells demonstrated that INPP4B $\alpha$  was expressed diffusely in the cytoplasm, while the  $\beta$  isoform was restricted to the Golgi apparatus (Ferron & Vacher, 2006).

#### **1.6.2 PI3K/AKT signalling in osteoblasts**

The PI3K/AKT signalling pathway is important for a number of processes critical for cells, including the osteoblast. To determine a bone-specific role of this pathway, groups have capitalized on transgenic and conditional knock-out mice to ascertain an osteoblastic function.

To this end, a global *Akt1* knock-out resulted in mice that display a reduction in bone mass. This was found to be a consequence from decreased survival signals in

osteoblasts, which are normally regulated by *Akt1*. Moreover, *Akt1*-deficiency suppressed Runx2-dependent proliferation and differentiation (Kawamura *et al.*, 2007).

Beyond the *Akt1* knock-out, phosphatase members of this pathway like *Pten* also play a role in osteoblast physiology. *Pten* dephosphorylates PI(3,4,5)P3 to generate PI(4,5)P2 and therefore plays a role in AKT signalling. Osteoprogenitor-specific knock-out of *Pten* exhibited increased proliferation and survival of the progenitors, consistent with elevated levels of AKT. Interestingly, this also increased osteoblast differentiation, resulting in premature mineralization of the osteoid (Guntur *et al.*, 2011). A late-stage deletion of *Pten* in mature osteoblasts using *Ocn-Cre* produced mice with excessive bone formation due to increased cellular survival mediated by increased AKT levels (Liu *et al.*, 2007).

*Ship* is another phosphatase that dephosphorylates PI(3,4,5)P3 to produce PI(3,4)P2, which can still activate AKT signalling (Ma *et al.*, 2008). A global *Ship*<sup>-/-</sup> knock-out resulted in animals that were severely osteoporotic due to a hyperactivation of osteoclasts. These osteoclasts were also more resistant to apoptosis. Osteoblasts in these mice were unaffected, however, suggesting that the role of *Ship* may be confined to the hematopoietic lineage (Takeshita *et al.*, 2002). This conclusion is further supported by the fact that SHIP has been demonstrated to be critical for maintaining a proper niche microenvironment for hematopoietic stem cells (Hazen *et al.*, 2009).

Given such a dramatic reduction in *Inpp4b* transcript in *gl/gl* bone, along with evidence supporting a role for PI3K/AKT signalling in bone, our lab sought to characterize the role of *Inpp4b* in bone homeostasis.

## 1.7 Validation of *Inpp4b* defect in bone homeostasis

The significant downregulation of *Inpp4b* in *gl/gl* mice prompted us to first validate the specificity of this transcriptional defect, rather than as a secondary effect from osteopetrosis. To this end, there was no observed defect of the *Ship1* phosphatase in *gl/gl* mice nor any change in *Inpp4b* expression in other osteopetrotic mutants. Thus, the downregulation of *Inpp4b* is specific to the defects in the *gl/gl* osteopetrotic mice and not a general effect from either osteopetrosis or dysregulation of phosphoinositide signalling. Moreover, it was concluded that *Inpp4b $\alpha$*  (herein referred to as *Inpp4b*) isoform was affected, and not *Inpp4b $\beta$* . (Ferron *et al.*, 2011).

### 1.7.1 *Inpp4b* as a negative regulator of osteoclastogenesis

In an effort to elucidate the function of *Inpp4b* in the maturation of osteoclasts, our lab previously characterized transfected RAW264.7 cell lines. The RAW264.7 cell line is an easily-transfectable macrophage cell line that requires the exogenous addition of RANKL to study osteoclastogenesis *in vitro* (Cuetara *et al.*, 2006). Stable RAW264.7 clones were therefore transfected with one of three constructs: *Inpp4b*-EGFP, *Inpp4b*(C845A)-EGFP, or control EGFP. The *Inpp4b*(C845A) construct is the phosphatase-inactive form. Mature osteoclasts can be assessed by TRAP staining and it was found that clones expressing native *Inpp4b* exhibited a significant reduction in differentiation kinetics and total number and size of TRAP-positive cells compared to the phosphatase-inactive form. (Ferron *et al.*, 2011). *Inpp4b*-GFP clones also displayed decreased nuclei per cell, as compared to the control and *Inpp4b*(C845A) clones. Furthermore, clones with native *Inpp4b* demonstrated increased apoptosis, as revealed by Annexin V staining (Ferron *et al.*,

2011). Together, these *in vitro* results indicate that *Inpp4b* can negatively regulate osteoclastogenesis and that this is dependent on the phosphatase domain.

The mechanism through which *Inpp4b* was negatively regulating osteoclastogenesis *in vitro* was determined to be dependent on NFATc1 levels. As these clones did not exhibit any significant differences in survival or differentiation signals (AKT, MAPK, or PLC $\gamma$ ), the transcription factors NF $\kappa$ B and NFATc1 were analyzed. Native *Inpp4b* appeared to repress both NF $\kappa$ B and nuclear NFATc1, while the phosphatase-inactive form displayed increased levels of both, suggesting that *Inpp4b* may be involved in the nuclear localization and transport of NFATc1 to activate osteoclast-specific genes.

These findings were supported further by the fact that *Inpp4b*-expressing cells experience reduced Ca<sup>2+</sup> oscillations compared to controls and phosphatase-inactive cells, which can explain the NFATc1 results. Downstream of NFATc1, target genes like *Acp5* and *Ctsk* were affected; native *Inpp4b* expression was inhibitory while phosphatase-inactive *Inpp4b* was stimulatory (Ferron *et al.*, 2011). Thus, we were prompted to study the capacity for *Inpp4b* to modulate bone mass using a combination of *ex vivo* and *in vivo* analyses from *Inpp4b*<sup>-/-</sup> mice.

### **1.8 Role of *Inpp4b***

In order to study the role of *Inpp4b* in bone homeostasis, a full deletion of the gene was generated using a Cre-lox system. This deletion mimicked the spontaneous *weeble* (*wbl*) mutation, which occurs in exon 10 of *Inpp4a*, and is a single nucleotide deletion.

Ultimately, this generates a frameshift that produces a premature stop codon, causing the mRNA to degrade before protein translation can occur (Nystuen *et al.*, 2001). For the purposes of the full knock-out, exon 11 of *Inpp4b* was deleted specifically given its sequence homology to the *weeble* mutation in exon 10 of *Inpp4a*.

*Weeble* mice present with severe neurological deficits, resulting from neuronal loss in the cerebellum and the CA1 field of the hippocampus. This can be explained by the fact that INPP4A regulates PI(3,4,5)P3 levels in the brain, which is an important effector of intracellular Ca<sup>2+</sup> release. Ca<sup>2+</sup> levels are particularly important for neurotransmitter release and as such, the loss of INPP4A gives rise to mice with locomotor defects, coupled with increased incidence of epilepsy and ataxia (Nystuen *et al.*, 2001), phenotypes associated with the cerebellum and hippocampus. The observation that *weeble* mice exhibited defects in intracellular Ca<sup>2+</sup> signalling is an interesting finding that was also seen in our *Inpp4b*-null mice.

In brief, a targeting vector containing two loxP sites, two Frt sites, and a Neomycin (Neo) resistance selection cassette were inserted flanking exon 11 of *Inpp4b* by homologous recombination in mouse embryonic stem cells (ESCs). Positive ES clones were selected for proper integration of the targeting vector, then injected into C57BL/6J blastocysts. These mice were then intercrossed to obtain the *Inpp4b*<sup>lox/lox</sup> mice which were crossed to transgenic CMV-Cre mice to generate the excision of exon 11 and Neo cassette (Ferron *et al.*, 2011).

### 1.8.1 *Inpp4b*<sup>-/-</sup> mice are osteoporotic

*Inpp4b*-null mice were analyzed at 8 weeks and 4 months of age to determine whether there was an impact *in vivo* (Ferron *et al.*, 2011). These mice displayed an osteoporotic phenotype that was explained by decreases in femur trabecular bone density, bone volume fraction, and trabecular number. Furthermore, these mice exhibited increased TRAP-positive cells, bone resorption, trabecular spacing, and erosion surface, demonstrating overall bone loss from increased osteoclast differentiation and activity.

*Ex vivo* osteoclast cultures from these mice exhibited increased osteoclastogenesis, due to an increase in osteoclast number and size, coupled with increased resorption pit areas. Molecular analyses revealed that the absence of *Inpp4b* increases Ca<sup>2+</sup> oscillations, which in turn stimulated the nuclear translocation of NFATc1. NFATc1 target genes were similarly increased (Ferron *et al.*, 2011). Taken together, studies on the *Inpp4b* knock-out mice corroborate *in vitro* results from the RAW264.7 cell lines. Therefore, *Inpp4b* acts as a negative regulator of osteoclastogenesis in an NFATc1-dependent manner (Figure 1.12).

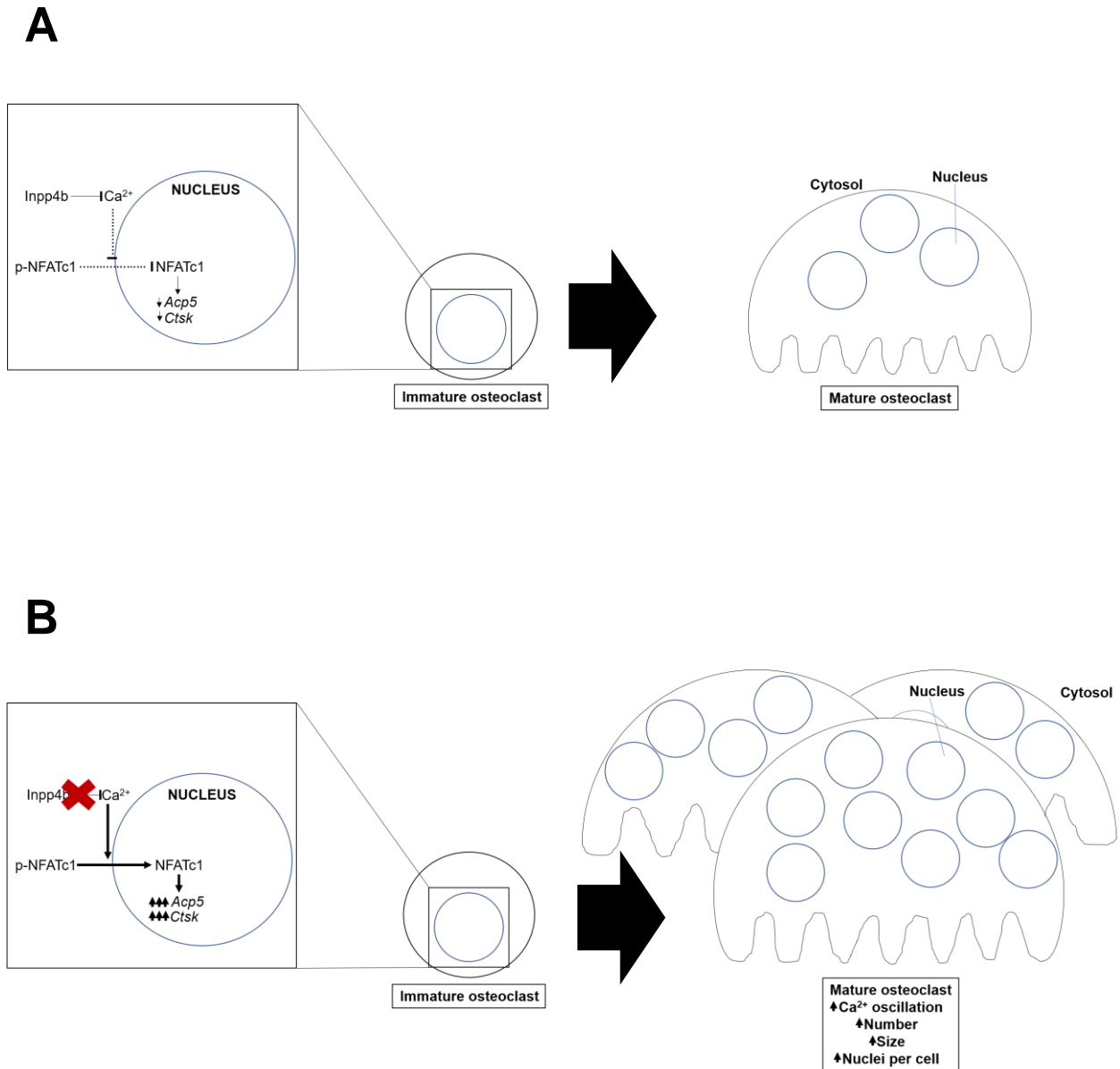


Figure 1.11: Summary of previously reported *Inpp4b* analyses.

(A) Under normal conditions, *Inpp4b* inhibits the nuclear translocation of NFATc1 through modulation of intracellular  $\text{Ca}^{2+}$  levels, thereby negatively regulating osteoclast differentiation kinetics and potential. (B) When *Inpp4b* is abrogated, osteoclastogenesis is enhanced due to an increase in NFATc1 nuclear translocation, which increases expression of its target genes. This results in an overall osteoporotic phenotype.

### **1.8.2 *Inpp4b*<sup>-/-</sup> mice exhibit defects in osteoblastogenesis**

Although our findings have demonstrated a role of *Inpp4b* in osteoclastogenesis, osteoblast-specific defects were also observed in *Inpp4b*-deficient mice. These mice displayed an increase in osteoblast cell population and mineral apposition rate *in vivo*, which was coupled with an increase in mineralization *ex vivo*, despite no change in ALP staining (Ferron *et al.*, 2011). This suggests that *Inpp4b* could modulate osteoblastogenesis as well, though at a later stage of osteoblast differentiation since mineralization is a function of the mature osteoblast.

# CHAPTER 2: HYPOTHESIS AND APPROACH

Our lab has identified a novel role of *Inpp4b* in osteoclastogenesis. More specifically, we have determined that *Inpp4b* functions as a negative regulator of osteoclastogenesis via the NFATc1 signalling pathway. Moreover, we observed alterations in osteoblast population and activity, wherein *Inpp4b*-null mice exhibit increased osteoblastogenesis and mineralization. Since mineralization is a function of the mature osteoblast, the aim of this thesis was to determine whether *Inpp4b* could exert a cell-autonomous role in the mature osteoblast. As such, we hypothesized that *Inpp4b* can modulate osteoblastogenesis, independent of any modulation of osteoclasts. To test this hypothesis, we have generated conditional knock-out and transgenic mouse models wherein *Inpp4b* was specifically deleted or overexpressed in the mature osteoblast only, respectively. Furthermore, we characterized any molecular or structural defects in these mice. The ultimate goal of this project was to contribute to our understanding of osteoblastogenesis in an effort to identify potential therapies for bone mass-associated disorders.

# CHAPTER 3: MATERIALS AND METHODS

### 3.1 Animals

Mice were crossed to obtain the *Inpp4b* conditional knock-out or transgenic mice. In short, these mouse lines were generated with mature osteoblasts either lacking or overexpressing the *Inpp4b* gene. All mice were bred on a C57BL/6J background and maintained in a pathogen-free animal facility, with laboratory chow and water *ad libitum* in a 12-hour light/dark cycle at 22-26°C. Protocols were approved by the institutional animal care committee of the Institut de recherches cliniques de Montréal and in compliance with the Canadian Council on Animal Care.

#### 3.1.1 Generation of conditional knock-out (cKO) mice

*Inpp4b*<sup>lox/lox</sup> mice were previously generated in the lab by insertion of loxP sites that flanked exon 11 of *Inpp4b* (Ferron *et al.*, 2011). This method has been previously used to generate a null mutation for *Inpp4a*. These mice were then crossed to human osteocalcin promoter-expressing Cre (hOcn-Cre) mice, which express the Cre recombinase with high specificity in mature osteoblasts (Riddle *et al.*, 2013). These *Inpp4b*<sup>lox/+</sup>;hOcn-Cre were then intercrossed to obtain *Inpp4b*<sup>lox/lox</sup>;hOcn-Cre, which were used for future crosses. *Inpp4b*<sup>lox/lox</sup> mice served as controls.

#### 3.1.2 Generation of transgenic (TR) mice

The hOcn promoter (3.8 kb) was excised from a pBS vector with EcoRV digestion. The full-length mouse *Inpp4b* cDNA sequence (2.8 kb) was previously isolated from a C57BL/6J spleen cDNA mouse library (Ferron & Vacher, 2006). The *Inpp4b* cDNA was then subsequently isolated and inserted between the hOcn promoter and a human growth

hormone minigene and polyadenylation signal (2.1 kb) with a double KpnI and SpeI digestion (Figure 3.1). The complete linearized transgene was injected by pronuclear microinjection into fertilized oocytes from F1 (C57BL/6J x C3H) x C57BL/6J crosses and then the eggs were re-implanted into a pseudopregnant female mouse. Transgenic *Inpp4b*<sup>TR/+</sup> (hOcn-*Inpp4b*-hGH) founder lines were identified by PCR and then crossed to *Inpp4b*<sup>+/+</sup> to establish four transgenic lines (TR95, TR352, TR363, and TR362), of which the TR95 and TR362 were further characterized. Non-transgenic (*Inpp4b*<sup>+/+</sup>) mice served as controls.

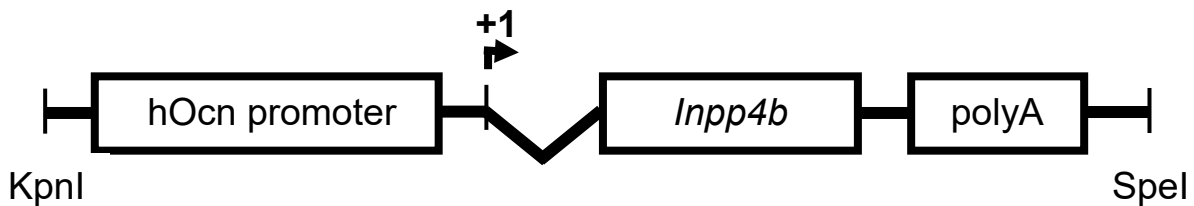


Figure 3.1: Schematic representation of the *Inpp4b* transgene.

### 3.1.3 Genotyping

Tail biopsies were digested at 100°C in lysis buffer (25 mM NaOH, 2 mM EDTA), followed by addition of a neutralization buffer (40 mM Tris-HCl pH 5). Conventional PCR was conducted on the DNA tail tip extracts, followed by visualization on a 1X TBE agarose gel stained with ethidium bromide. DNA extract was added to a PCR reaction buffer containing 10 mM Tris-HCl pH 8.3, 50 mM KCl and 1.5 mM MgCl<sub>2</sub>, 2-12 μM primers (depending on assay, see Table 1) and 1.25 mM dNTP. PCR cycling was carried out at 94°C for 5 minutes, followed by 35 cycles of 94°C for 30 seconds, 63°C for 30 seconds, 72°C for 30 seconds and then at 72°C for 10 minutes for elongation. *Inpp4b*<sup>lox/+</sup> PCR assay was used to distinguish between a floxed allele or wild-type allele (250 bp and 150

bp, respectively), *Inpp4b*<sup>Δ</sup> generated a Δ, or deleted, allele (180 bp), *Cre* generated a single *Cre*<sup>+</sup> allele (500 bp) and hGH generated a single transgenic allele (500 bp).

Table 1: Genotyping primers

Primer Name	Sequence
gl FOR 1	5'-CCTCTGGAAGACTAATACTTGCTG-3'
gl REV 1	5'-GCCTGGAACAGAGCAAAGC-3'
gl FOR 2	5'-GCTACATCTGGGTCCTTTTCG-3'
gl REV 2	5'-CGCTTGCTTTTGTCTGTTACCTTTGTGTTC-3'
Cre FOR	5'-AATGCTTCTGTCCGTTTGC-3'
Cre REV	5'-CGGCAACACCATTTTTTCTG-3'
hGH FOR	5'-CAGGAGGTATGCTTTCAACATG-3'
hGH REV	5'-AATGGTTGGGAAGGCACTGCC-3'
KO I4B qFOR	5'-GCTTCTGATAAAACATGGG-3'
KO I4B lox qREV	5'-TCAAAAGGCCCTACTGGTAAAA-3'
KO I4B del qREV	5'-TGTTTAAAAGCCTTGCTAAGTGTG-3'
Inpp4b 132 FOR	5'-AGGATTATGCTCTAGTCCTG-3'
Inpp4b 334 REV	5'-AACATGGCCAGCTATCTGAG-3'
Inpp4b 550 REV	5'-ACACCACATGAAGCTCAGTC-3'

### 3.1.4 Breeding

*Inpp4b* conditional knock-out mice were generated by crossing *Inpp4b*<sup>lox/lox</sup> mice with hOcn-Cre mice to generate F1 double transgenic *Inpp4b*<sup>lox/+;hOcn-Cre</sup> mice. These F1

animals were then intercrossed to obtain the double transgenic  $Inpp4b^{lox/lox};hOcn-Cre$  experimental mice.

$Inpp4b$  transgenic mice ( $Inpp4b^{TR/+}$  or  $hOcn-Inpp4b-hGH$ ) were generated as outlined above by crossing  $Inpp4b^{TR/+}$  mice with  $Inpp4b^{+/+}$ .

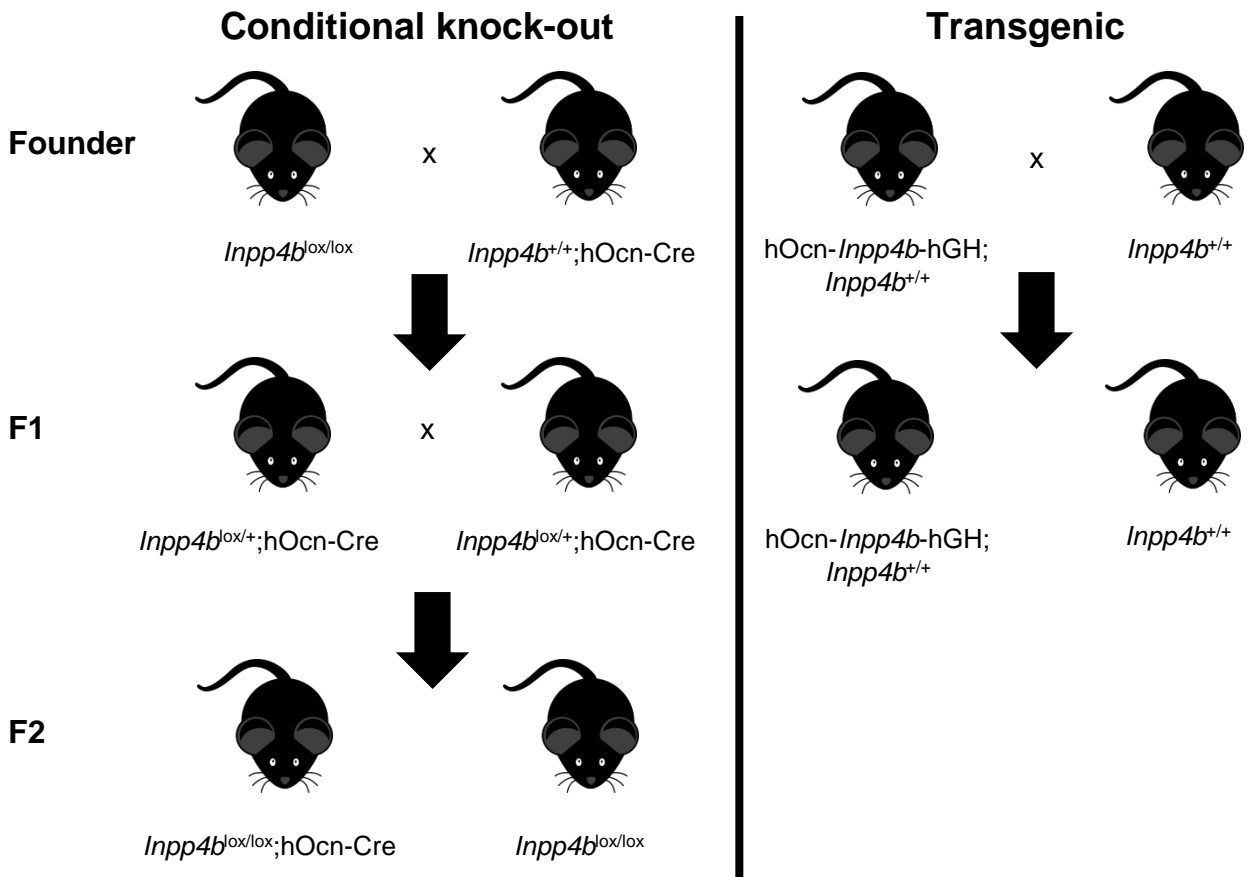


Figure 3.2: Mating scheme to represent generation of mice.

### 3.2 Cell culture

Unless otherwise noted, all cell cultures were maintained in a cell culture medium consisting of alpha-modified minimum essential medium ( $\alpha$ MEM, Sigma-Aldrich, M0644)

supplemented with 10% fetal bovine serum (FBS) and 0.1% penicillin/streptomycin (PS). Before differentiation, cells were counted using 3% acetic acid and trypan blue on a hemocytometer and primary osteoblasts were plated at a concentration of 10,000 cells per cm<sup>2</sup> while primary osteoclasts were plated at a concentration of 12,500 cells per cm<sup>2</sup>. Lastly, cells were grown in a 37°C incubator (5% CO<sub>2</sub>).

### **3.2.1 Primary cell culture (osteoblast)**

Neonate P5 mice were sacrificed by decapitation and the calvaria dissected. Calvaria were then processed with five successive digestions of 4 mg/mL collagenase type II (Worthington, LS004176), supplemented with 5% trypsin/EDTA and un-supplemented  $\alpha$ MEM. Each digestion was incubated and shaken at 37°C. The first three supernatants were discarded, and the last two supernatants were pooled and centrifuged at ~120 g for 5 minutes. The pellet was then re-suspended in culture medium. Cells were grown to ~70% confluency after which they were detached with a trypsin-EDTA solution. The cell suspension was then counted and plated at a concentration of 10,000 cells per cm<sup>2</sup> and once cells were again ~70% confluent, they were grown in differentiation medium containing cell culture medium further supplemented with 0.01 M of  $\beta$ -glycerophosphate (Sigma-Aldrich, G9422-50G) and 0.05 mg/mL of ascorbic acid (Sigma-Aldrich, A4544-25G). Medium was changed every three days for 24 days.

### **3.2.2 Primary cell culture (osteoclast)**

Adult mice (5-week-old) were sacrificed by CO<sub>2</sub> inhalation and long bones dissected. Femurs and tibia were flushed with sterile medium and bone marrow progenitors plated

in a medium containing cell culture medium further supplemented with 15% macrophage colony-stimulating factor (MCSF). Once cells reached ~70% confluency, they were detached with a PBS solution containing 0.25% trypsin and plated at a concentration of 25,000 cells per cm<sup>2</sup> in a differentiation medium containing cell culture medium with 5% MCSF and 100 ng/mL of purified receptor-activated NFκB ligand (RANKL). Medium was changed every three days for six days.

### **3.2.3 Co-culture**

Osteoblast precursors were extracted from calvaria and grown until ~70% confluency (as outlined above), at which point cells were counted and re-plated at a concentration of 50,000 cells per cm<sup>2</sup> in undifferentiated αMEM. The next day, the medium was replaced with co-culture medium (cell culture medium supplemented with 0.01 mM vitamin D<sub>3</sub> and 0.01 mM prostaglandin E<sub>2</sub>). Forty-eight hours later, bone marrow from adult mice were flushed from femurs and tibia, then single-cell suspension was counted and then added at a concentration of 1.7x10<sup>6</sup> cells per cm<sup>2</sup> to the osteoblast cell cultures. Co-culture medium was then changed every two days for 18 days.

## **3.3 Molecular analyses**

### **3.3.1 DNA extraction**

Adult mice (3-week-old) were sacrificed by CO<sub>2</sub> inhalation and tissues collected (brain, bone, calvarium, tail, heart, lungs, liver, spleen, thymus, and kidneys). Portions of each tissue were then processed in 500 μL of digestion buffer (50 mM Tris-HCl pH 8, 100 mM EDTA pH 8, 100 mM NaCl, 1% sodium dodecyl sulfate (SDS), 100-200 μg proteinase K)

at 37°C for 24-48 hours. DNA from digested tissues was extracted following a standard 1:1 phenol/chloroform extraction and then precipitated using a salt/ethanol treatment (5 M NaOH, 100% EtOH). The DNA pellet was washed with 75% EtOH and re-suspended in TE buffer (10 mM Tris-HCl pH8, 1 mM EDTA pH 8) and quantified by UV spectroscopy with absorbance reading at 260 nm.

### **3.3.2 *Inpp4b* deletion**

Extracted DNA was diluted to 0.1 µg/µL for a PCR reaction (outlined above) to confirm the specific deletion of *Inpp4b* in tissues and cell culture (extraction outlined above). Specific forward and reverse exon primers (see Table 1) were designed to identify exon 11 deletion of *Inpp4b*. *Inpp4b* (Intron 10) For, *Inpp4b* (Intron 10) Rev and *Inpp4b* (Intron 11) Rev, which resulted in amplification products of 750 bp, 680 bp and 500 bp for the lox, wild-type and delta alleles, respectively. The resulting amplicons were visualized on a 2% 1X TBE-agarose gel stained with ethidium bromide.

### **3.3.3 RNA isolation**

Total cell lysate and tissue RNA were extracted using a standard Trizol protocol (Gibco), with or without polytron homogenizer, and stored at -80°C until extraction. Once ready, RNA samples were thawed on ice and then extracted using chloroform. The RNA was subsequently precipitated and washed using isopropanol and ethanol, respectively, and re-suspended in diethyl pyrocarbonate (DEPC)-treated water. RNA integrity was assessed using a 1.5% 1X TBE agarose gel stained with ethidium bromide and the concentration was quantified by UV spectroscopy with absorbance reading at 260 nm.

### **3.3.4 Reverse transcription PCR**

RNA was reverse transcribed following DNase treatment. In brief, 0.25-1 µg of RNA was incubated with a reaction mix consisting of RNase-free DNase I (New England BioLabs) at room temperature for 15-20 minutes. The enzyme was then inactivated by addition of 25 mM EDTA for 10 minutes at 65°C. Next, 10 µM oligodT primers and 2.5 mM dNTPs were added to the reaction mixture for 10 minutes at 70°C to allow annealing of primers to polyA tail. Lastly, samples were incubated with reverse transcriptase (New England BioLabs) for one hour at 42°C in a reaction mix containing M-MuLV buffer. The enzyme was then inactivated by incubation at 70°C for 15 minutes. A 1/10-1/5 dilution of cDNA was used to perform either standard PCR or qPCR for the genes of interest with β-actin and S16 were used as internal controls, respectively. For conventional PCR reactions, the reactions were carried out at 94°C for 5 minutes, followed by 25-40 cycles of 94°C for 30 seconds, 65°C for 30 seconds, 72°C for 30 seconds and then at 72°C for 10 minutes for elongation.

### **3.3.5 qPCR**

cDNA was prepared by reverse transcription and a 1/10-1/5 dilution was used for SybrGreen qPCR (Qiagen) with the ViiA7-96 system (Thermo Fisher). 1 µL of diluted cDNA sample was used in the reaction and ribosomal S16 was used as an internal control. The reaction was carried out at 50°C for 2 minutes, followed by 95°C for 2 minutes, then 45 cycles at 95°C for 15 seconds and 60°C for 1 minute (see Table 2 for list of primers).

Table 2: RT-PCR/qPCR primers

<b>Primer Name</b>	<b>Sequence</b>
β-actin FOR	5'-TGACGATATCGCTGCGCTG-3'
β-actin REV	5'-ACATGGCCTGGGGTGTGAAG-3'
S16 FOR	5'-GCTACCAGGGCCTTTGAGATG-3'
S16 REV	5'-AGGACGGATTTGCTGGTGTGG-3'
Ocn FOR	5'-ATAGTGATACCGTAGATGCG-3'
Ocn REV	5'-CTGACAAAGCCTTCATGTCC-3'
Inpp4ba TR FOR	5'-AACATGCTACAGCTGATGGCTTTCCC-3'
hGH TR EX1 REV	5'-ATTGCAGCTAGGTGAGCTGTCCACAGGA-3'
ml4B E11 FOR	5'-GGAATCCTGTGTGTAAGCTGTAT-3'
ml4B E11 REV	5'-GGATGCTTTCTGACATCTGC-3'
qInpp4b E18 FOR	5'-GGAGAAGTGGTGAACCGAGC-3'
qInpp4b E19 REV	5'-TGAAGCTGCTGTAGGAAGCC-3'
qiCre FOR	5'-CCTGGTCTGGACACAGTG-3'
qiCre REV	5'-TTGCCCTGTTTCACTATCC-3'
qRunx2 FOR	5'-CCTCTGACTTCTGCCTCTGG-3'
qRunx2 REV	5'-TAAAGGTGGCTGGGTAGTGC-3'
qAlp FOR	5'-TGTCTGGAACCGCACTGAACT-3'
qAlp REV	5'-CAGTCAGGTTGTTCCGATTCAA-3'
qOcn FOR	5'-CTGACAAAGCCTTCATGTCC-3'
qOcn REV	5'-ATAGTGATACCGTAGATGCG-3'

qOpn FOR	5'-ACAGTCGATGTCCCCAACGG-3'
qOpn REV	5'-TGCCCTTTCCGTTGTTGTCC-3'
mAtg5 FOR	5'-AAGATGGAGAGAAGAGGAGCCA-3'
mAtg5 REV	5'-AATCTGTTGGCTGGGGGAC-3'
mAtg7 FOR	5'-TCGAAAACCCCATGCTCCTC-3'
mAtg7 REV	5'-AGGGCCTGGATCTGTTTTGG-3'
mRANK FOR	5'-CGAGCACTGGTTCTTGGATAA-3'
mRANK REV	5'-GTCTGAGGTGGGTGTTTGAA-3'
mRANKL FOR	5'-CCCATCGGGTCCCATAAA-3'
mRANKL REV	5'-ATGTTGGCGTACAGGTAATAGA-3'
qOPG FOR	5'-GGGCGTTACCTGGAGATCG-3'
qOPG REV	5'-GAGAAGAACCCATCTGGACATTT-3'

### 3.3.6 Recombination efficiency

cDNA from neonatal calvarial osteoblast cultures were prepared as previously described and a 1/10 dilution was used to perform a SybrGreen-based comparative qPCR (procedure outlined above) to determine the level of expression of *Inpp4b* in both control and cKO osteoblasts. Ribosomal *S16* expression was used as an internal control. Results were analyzed using the QuantStudio program and results determined the overall levels of *Inpp4b* gene expression. Recombination efficiency was determined as the ratio of *Inpp4b* expression in cKO osteoblasts to controls.

### **3.3.7 Southern blot for transgene integrity and copy number**

To establish transgene integrity, 10 µg of genomic DNA was prepared by overnight digestion at 37°C with 0.5 µL per mL of either HindIII or BamHI restriction enzyme. The digested DNA was then migrated on a 0.7% 1X TAE agarose gel overnight at 40 mA. After migration, the gel was incubated with a denaturing solution consisting of 1 M NaCl and 0.5 M NaOH to separate the double strands into single strands. Neutralization was carried out next with another solution containing 3 M NaCl and 0.5 M Tris-HCl pH 7.5. Lastly, the DNA was transferred to a nylon membrane by capillarity in 20X SSC solution (3 M NaCl, 0.3 M sodium citrate pH 7) overnight. The next day, the DNA was crosslinked to the membrane for 15 minutes under UV light exposure.

### **3.3.8 Radiolabelling probes and membrane hybridization**

The DNA template for the probes was amplified using a PCR reaction (outline described above), in which a 900 bp amplicon was expected. This amplicon was then run on a 1% 1X TBE gel and the DNA was isolated by electroelution. DNA was precipitated following an ethanol/salt procedure (100% EtOH, 0.2 M NaCl) and stored at -20°C. Before membrane hybridization of the probe, the membrane was incubated with 100 µg/mL of salmon sperm DNA in hybridization buffer (5X SSC: 1.5 M NaCl, 75 mM sodium citrate; 5X Denhardt: 1% ficoll, 1% polyvinylpyrrolidone, 1% bovine serum albumin; and 0.1% SDS) for four hours at 65°C to block any non-specific binding of the probe. Next, the probe was prepared as follows: 100 ng of the isolated probe DNA underwent nick translation by DNA polymerase I (New England BioLabs) in the presence of <sup>32</sup>P dCTP to generate a radiolabelled probe, which was added to the pre-hybridization buffer for

overnight incubation at 65°C. Upon overnight incubation, the radiolabelled membrane was washed approximately twice for 5 minutes each with Southern Solution II (0.3 M NaCl, 15 mM sodium citrate, 0.1% SDS) and then twice for 5 minutes each with Solution III (0.03 M NaCl, 1.5 mM sodium citrate, 0.1% SDS). Finally, the membrane was exposed to film at -80°C for 1-3 days (with possible rewashing in Southern Solution III). The expected genomic fragments for transgene integrity and copy number were 4.2 kb and 7.5 kb, respectively.

### **3.3.9 Osteoblast mineralization activity *ex vivo***

Mineral formation by mature osteoblasts was assessed using several classical staining procedures, including alkaline phosphatase (0.1 M Tris-HCl pH 8.8, 1 M MgCl<sub>2</sub>, Triton-10%, 10 mg/mL Fast Red [Sigma-Aldrich, F3381-1G], naphthol AS-MS), alizarin red (0.02 mg/mL alizarin red [ICN Biochemicals, 100375]) and von Kossa (0.05 g/mL AgNO<sub>3</sub>) and a fluorescent calcein staining. For the classical staining procedures, cell cultures were washed twice with PBS 1X, then fixed in 4% formalin for 15 minutes at room temperature. The cells were then washed again once with PBS 1X before being stored at 4°C in PBS 1X until needed. Once ready, these fixed cells were incubated with the desired stain for approximately one hour at room temperature and shaking to determine mineral formation in these cells. For the calcein staining, mineral formation was observed using a fluorescent Ca<sup>2+</sup>-sensing dye that allowed tracking of mineral formation without fixing cells. In brief, 24 hours prior to imaging, the cells were washed twice with unsupplemented  $\alpha$ MEM before adding a modified differentiation medium containing 30  $\mu$ M of calcein (Sigma-Aldrich, C0875-5G). The next day, the cells, with excitation and emission

wavelengths at 470nm and 509nm, respectively, were imaged using fluorescent light microscopy (Axiovert S100TV microscope system). After imaging, differentiation medium was added once more and cells were returned to the incubator. In both classical and fluorescent staining, the mineral formation ability was quantified using the ImageJ software with specific pixel threshold settings depending on the stain being studied to remove any background or non-specific staining. Each pixel was first converted to grayscale, after which the mean gray value was obtained. The mean gray value represents the sum of the gray values of all the pixels in the selection divided by the number of pixels.

### **3.3.10 Osteoclast staining *ex vivo***

To determine the number and size of osteoclasts in culture, tartrate-resistant acid phosphatase (TRAP) staining was performed. In brief, cell cultures were washed twice with PBS 1X. Next, 4% formalin was added to fix the cells at room temperature for 15 minutes, after which the formalin was removed. Cells were once again washed with PBS 1X, then wrapped in plastic wrap and stored at 4°C (in PBS 1X) until use. Once ready, cells were washed once with PBS 1X and then incubated with TRAP staining solution (0.01% naphthol AS-TR phosphate, 0.1 M sodium acetate pH 5.2, 0.06% Fast Red Violet, 1.15% sodium tartrate and 0.1% Triton X) for 30-45 minutes at 37°C. After staining, cells were rinsed once with distilled water and cell number and size quantified using Volocity software.

### **3.4 Biochemical analyses**

#### **3.4.1 Antibodies and reagents**

Mouse anti- $\beta$ -actin (Sigma-Aldrich) was used in this study. Rabbit polyclonal antibodies for INPP4B were generated in-house. Secondary antibodies included horseradish peroxidase (HRP)-labeled goat anti-mouse and goat anti-rabbit IgG (BioRad).

#### **3.4.2 Protein extraction**

Cell culture medium was aspirated and cells were washed twice with PBS 1X and then homogenized in 1 mL of 1X RIPA buffer (150 mM NaCl, 1% NP40, 0.5% sodium deoxycholate, 0.1% SDS, 50 mM Tris-HCl pH 8) with protease inhibitors (1 mM PMSF, 1 mM  $\beta$ -glycerophosphate, 1mM sodium orthovanadate, 1/1000 of Protease Inhibitor Cocktail [Sigma-Aldrich]). Homogenized samples were stored at -80°C until use. Once ready, samples were thawed and then centrifuged for 15 minutes at 9,000 g at room temperature. Supernatant was transferred to a new tube and quantified using the Bradford assay.

#### **3.4.3 SDS-PAGE**

Resolving gels (6-15%) and 5% stacking gels were prepared depending on the size of protein of interest. In each well, 15-30  $\mu$ g of protein were loaded after 10 minutes of boiling in sample buffer (62.5 mM Tris-HCl pH6.8, 2% SDS, 10% glycerol, 0.002% bromophenol blue, 5%  $\beta$ -mercaptoethanol). Samples were migrated in 1X running buffer (25 mM Tris-HCl, 190 mM glycine, 0.1% SDS) at 100 V until complete migration through stacking gel, at which point voltage was increased to 150 V constant.

#### **3.4.4 Western blot**

Following migration, proteins were transferred to polyvinylidene fluoride (PVDF) membranes at 300 mA for 90 minutes in a 1X transfer buffer (25 mM Tris-HCl and 190 mM glycine). Membranes were next washed once with 1X TBS-T pH7.6 (20 mM Tris-HCl, 137 mM NaCl, 0.1% Tween) for 10 minutes and then blocked for one hour in 5% skim milk in 1X TBS-T, all with shaking at room temperature. The membranes were then washed once more with 1X TBS-T for 10 minutes being incubated overnight at 4°C, with shaking, in primary antibody diluted in 3% BSA in 1X TBS-T. The next day, membranes were washed three times for 10 minutes each at room temperature with 1X TBS-T. A 1:10,000 dilution of secondary antibody in 5% skim milk in 1X TBS-T was then added to the membranes for one hour at room temperature, with shaking. After secondary antibody incubation, membranes were washed three times with 1X TBS-T for 10 minutes each at room temperature. Lastly, membranes were exposed to ECL Western Blotting Detection kit (Amersham GE Healthcare). For membranes that required further blotting, they were washed twice with 1X TBS-T for 15 minutes each at room temperature before re-incubating with another primary antibody overnight at 4°C.

#### **3.4.5 Enzyme-linked immunosorbent assay (ELISA)**

Solid phase sandwich ELISA was performed on both cell culture medium and serum. Co-culture cell-conditioned media were collected and centrifuged at 150 g for 10 minutes at 4°C. Cell-free supernatants were isolated and stored at -80°C until use. Serum levels of RANKL and OPG were extracted from whole blood samples by cardiac puncture. 8-week- and 4-month-old mice were first anesthetized using intraperitoneal injections of

avertin 2.5% solution (0.0165 mL per g of body weight). Next, whole blood was collected via cardiac puncture using a 22 g needle and syringe into a 1.5 mL Eppendorf tube. Blood was left undisturbed at room temperature for approximately 30 minutes to allow clotting. Following this, blood samples were centrifuged for 10 minutes at 1,500 g at 4°C. Supernatant was transferred to a new Eppendorf tube and stored at -80°C until use. ELISA assay was performed as per manufacturer's protocol (BioAim Scientific Inc.) to quantify secretion of RANKL and OPG.

### **3.5 Structural analyses**

#### **3.5.1 Histology**

Eight-week- and four-month-old mice were sacrificed by CO<sub>2</sub> inhalation. Next, skin was removed and then mice were fixed in 4% formalin overnight at 4°C. 24 hours later, mice were dehydrated in 70% EtOH at 4°C. The following day, non-decalcified vertebral sections and femurs and tibia were dissected (muscle removed). Femurs and tibia were kept in 70% EtOH at 4°C until analyzed by micro computed tomography (μCT) at the McGill Centre for Bone and Periodontal Research. Vertebral sections were further dehydrated in a graded ethanol series (70% → 85% → 96% → 100% EtOH) for embedding with methylmethacrylate (MMA). In brief, after dehydration, vertebral sections were infiltrated with two successive solutions consisting of destabilized MMA, n-propyl gallate and benzoyl peroxide both overnight at 4°C in dark. These sections were then embedded in a polymerization embedding solution that included dimethylpropiothetin overnight at 4°C protected from light. These MMA-embedded vertebrae were sectioned at 7μm using a microtome and a tungsten carbide blade and stretched and pressed at

42°C for 48 hours. Then the sections were deplastified with 2-methoxyethyl acetate, rehydrated in a graded ethanol series (100% → 96% → 80% → 70% → 50% → H<sub>2</sub>O) and then stained with toluidine blue, TRAP or von Kossa to assess histomorphometric parameters or mineralization *in vivo*.

### **3.5.2 Histomorphometry**

Mice were injected twice with calcein before sacrifice; once five days prior and then again at two days prior to sacrifice by intraperitoneal injection at 2.5 mg/mL at 10 mL per kg of body weight at each time point. After sacrifice, mice were prepared for embedding (outlined above) and after deplastification and staining, vertebrae were analyzed for calcein incorporation. Analyses were carried out using the Osteomeasure (DM4000B) system to quantify the mineralisation apposition rate (MAR).

### **3.6 Statistical analyses**

Values are expressed as mean  $\pm$  SEM. Unpaired two-sample Student t-test was used for analysis of significance, with p values of  $p < 0.05$  and below considered significant.

# CHAPTER 4: RESULTS

## 4.1 CONDITIONAL KNOCK-OUT (cKO) OF *Inpp4b*

### 4.1.1 Specific deletion of *Inpp4b* in mature osteoblasts

Previous studies have generated the *Inpp4b*-null mouse model, through which further characterization has defined its role as a negative regulator of osteoclastogenesis and as a novel prognostic marker for human osteoporosis (Ferron *et al.*, 2011; Ferron & Vacher, 2006). Interestingly, however, these *Inpp4b*-null mice also demonstrated a dysregulation in mature osteoblasts – specifically in the mineral formation of these cells both *ex vivo* and *in vivo*. This observed uncoupling between the activities of the osteoblasts and osteoclasts, therefore, prompted further studies into the role of this lipid phosphatase specifically in the mature osteoblast. To do so, a conditional knock-out (cKO) mouse model of the *Inpp4b* gene was generated using a Cre-lox system in which exon 11 of the *Inpp4b* gene was floxed and excised following Cre-mediated recombination under the control of the human osteocalcin (hOcn) promoter. These *Inpp4b*<sup>lox/lox</sup>;hOcn-Cre, or *Inpp4b* cKO OB mice were born at expected Mendelian frequencies, with no obvious phenotypic defects compared to littermate controls. To elucidate the osteoblast-specific role of *Inpp4b*, a combination of *ex vivo* and *in vivo* analyses was performed.

Osteocalcin is the most abundant non-collagenous protein found in bone and is expressed exclusively by the mature osteoblast (Hauschka *et al.*, 1989; Stein *et al.*, 2004). As one of the few osteoblast-specific genes, it was considered to exert a role in bone homeostasis through hydroxyapatite binding, cell signaling, and monocytic cell recruitment (Ducy *et al.*, 1996; Hoang *et al.*, 2003). This cell-specific nature of osteocalcin, therefore, was employed to produce an osteoblast-deficient mouse model of *Inpp4b*.

More specifically, Cre recombinase under the control of the human osteocalcin promoter (hOcn-Cre) was used to generate the conditional knock-out of *Inpp4b* in the mature osteoblast (Zhang *et al.*, 2002).

To generate the cKO mice, *Inpp4b* floxed mice previously produced in the laboratory (Ferron *et al.*, 2011) were crossed to hOcn-Cre mice to ensure specific deletion in mature osteoblasts (Kanazawa *et al.*, 2015; Zhang *et al.*, 2002). In brief, loxP sites, as well as a Neomycin (Neo) resistance selection cassette, were inserted via homologous recombination in J1 mouse embryonic stem cells (ES). These sites were inserted to flank exon 11 of *Inpp4b*, in order to create a frameshift mutation that would result in a premature stop codon, similarly to the spontaneous mutation in exon 10 of *Inpp4a* (Nystuen *et al.*, 2001). These ES cells were subsequently selected for and then reimplanted into C57BL/6J blastocysts, after which those that were Neo-resistant were subsequently crossed to knock-in *FLPeR* mice, which express flippase recombinase, to excise the Neo cassette and FRT sites. These *Inpp4b*<sup>lox/+</sup> mice were then intercrossed to obtain *Inpp4b*<sup>lox/lox</sup> mice and then crossed to *Inpp4b*<sup>+/+;hOcn-Cre</sup> mice as indicated (see Materials and Methods) to generate *Inpp4b* cKO OB mice.

The recombination events leading to the mature osteoblast conditional deletion of *Inpp4b* were further analyzed at the DNA, RNA, and protein levels to confirm its specificity and efficiency.

#### 4.1.2 Recombination specificity – DNA analyses

To confirm that the *Inpp4b* deletion occurred only in the mature osteoblast, we first analyzed DNA extracts to ensure that the deletion was present only in Cre-expressing tissues. By PCR analysis, the deletion ( $\Delta$ ) allele was only present in total bone extracts in the presence of the Cre recombinase and not in the brain tissues, which served as controls (Figure 4.1A).

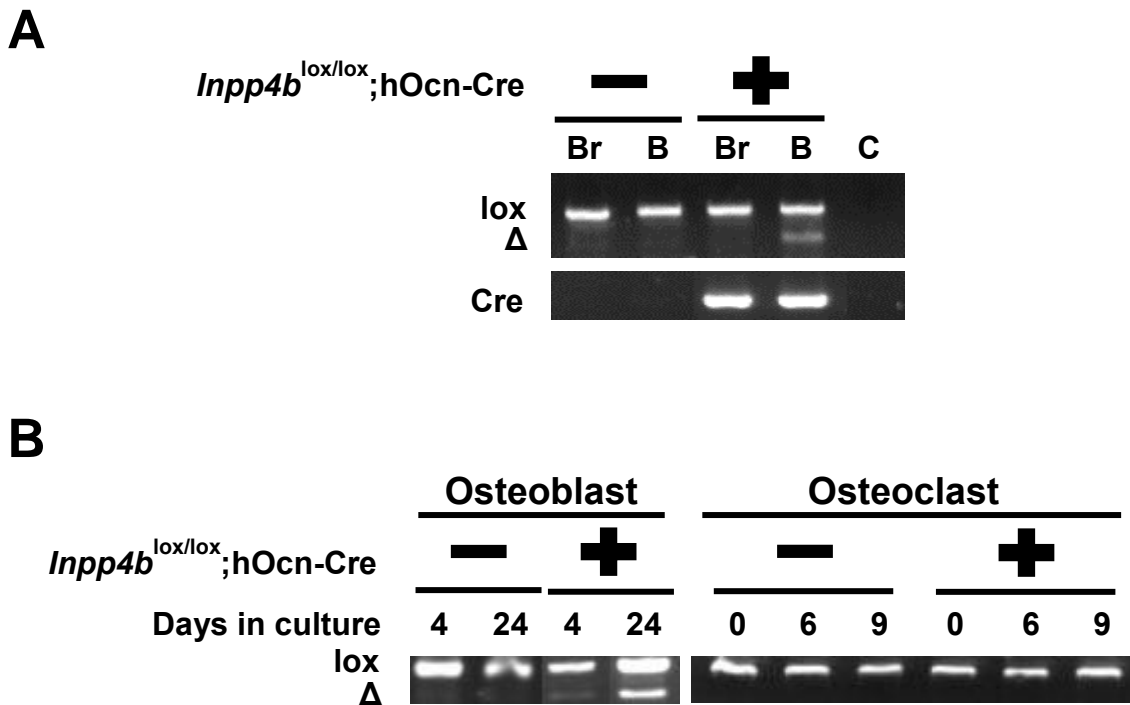


Figure 4.1: PCR assays to determine the specific deletion of *Inpp4b* in the mature osteoblast.

(A) The *Inpp4b*  $\Delta$  allele is present only in total bone extracts expressing the Cre recombinase and not in brain extracts. (Br=brain, B=bone, C=H<sub>2</sub>O). (B) The *Inpp4b*  $\Delta$  allele is present only in the mature osteoblast and not in the osteoclast, confirming the osteoblast-specific deletion of *Inpp4b*.

Due to the cell heterogeneity in total bone tissue, we next sought to confirm that recombination in the presence of hOcn-Cre (i.e. the deletion) was occurring in the mature osteoblast, and not in the osteoclast. To do so, DNA extracts from differentiated cultured primary osteoblasts and osteoclasts of *Inpp4b*<sup>lox/lox</sup>;hOcn-Cre<sup>+</sup> and Cre<sup>-</sup> mice were analyzed. The  $\Delta$  allele was detected in DNA extracts from Cre-expressing mature osteoblasts. Only the *Inpp4b*<sup>lox</sup> allele was detected in osteoclasts and therefore no recombination occurred (Figure 4.1B).

#### 4.1.3 Recombination efficiency – RNA analyses

Having confirmed the cell specificity of the deletion, we next sought to quantify the gene expression of *Inpp4b* following ablation in osteoblasts. More specifically, we were interested in assessing the level of mRNA reduction in these mature *Inpp4b* cKO OB. Firstly, calvarial osteoblasts from neonatal cKO mice were differentiated into mature osteoblasts, after which total mRNA was extracted for RT-PCR analysis to confirm the differentiation and maturation of the primary osteoblasts *ex vivo* (Figure 4.2A). We then quantified the level of gene expression of both *Cre* and *Inpp4b* with qPCR from cultured primary osteoblasts. *Cre* expression increased with time (Figure 4.2B) and after 24 days in culture, these mature osteoblasts expressed approximately 60% less *Inpp4b* than controls (Figure 4.2C). Additionally, there was no *Cre* expression in osteoclasts, further demonstrating the specific loss of *Inpp4b* in the mature osteoblast (Figure 4.2D).

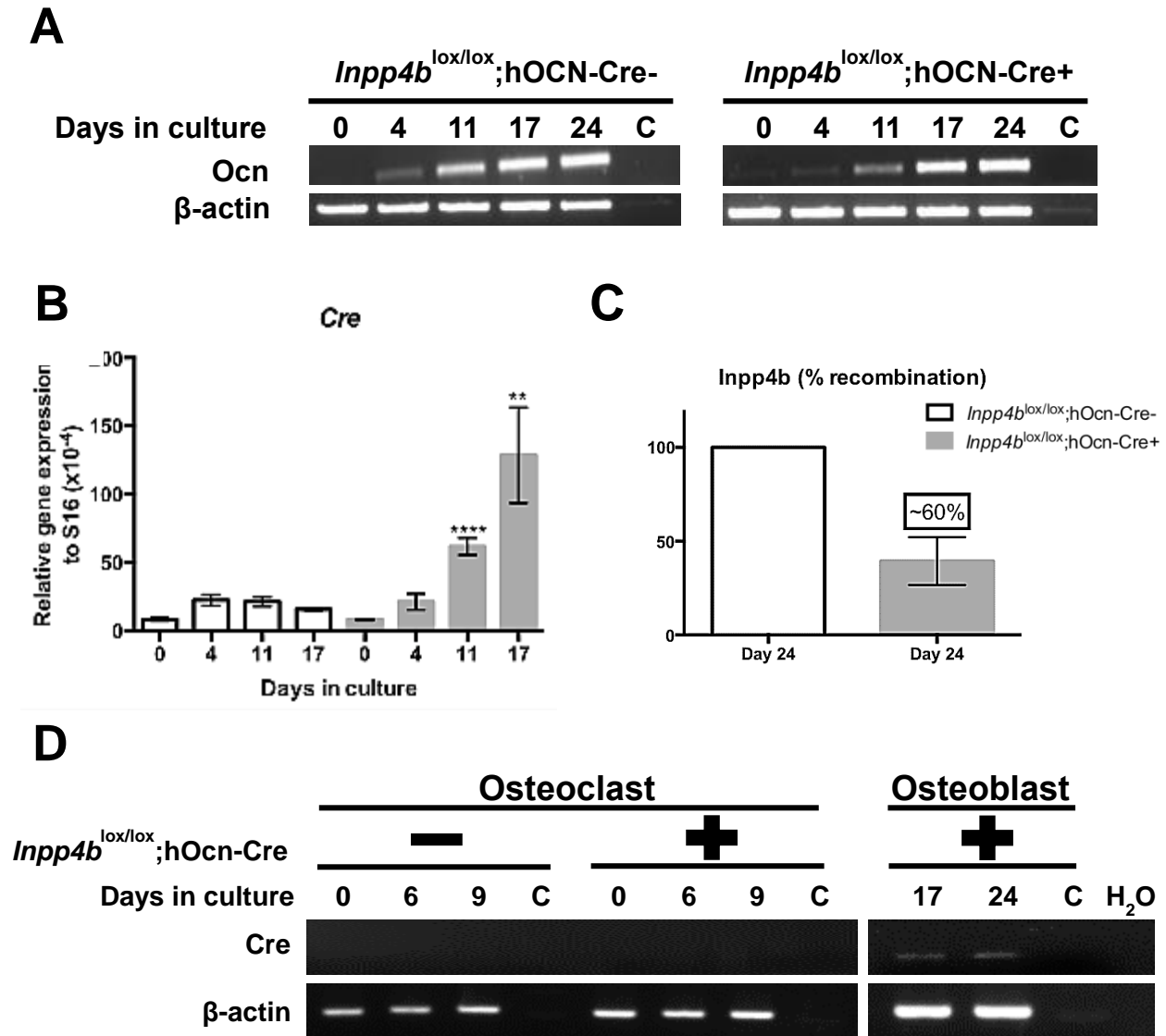


Figure 4.2: Specificity and efficiency of gene expression in *Inpp4b* cKO OB.

(A) Semi-quantitative PCR assay for osteocalcin (*Ocn*) expression in reverse transcribed DNA, demonstrating the uninterrupted differentiation of osteoblasts in cell culture.  $\beta$ -actin served as an internal control. (C=-RT control). (B) qPCR analysis of *Cre* expression, demonstrating increasing expression with OB differentiation. \*\* $p < 0.01$ , \*\*\*\* $p < 0.0001$ . (C) qPCR analysis of *Inpp4b* relative expression in cKO osteoblasts revealed approximately 60% reduction compared to endogenous levels in controls ( $n=3$ ). (D) Semi-quantitative PCR assay for *Cre* expression in reverse transcribed DNA, demonstrating *Cre* expression in mature osteoblasts and not in the osteoclast. (C=-RT control).

#### 4.1.4 Inpp4b protein expression during osteoblast differentiation

The specific deletion and decreased expression level of *Inpp4b* in the mature osteoblast prompted us to assess the reduction of Inpp4b protein in cKO osteoblasts. Total protein extracts were prepared from cultured osteoblasts and expression of Inpp4b was analyzed by Western blot. Quantification revealed that Inpp4b protein expression was reduced approximately by ~70% in cKO osteoblasts compared to endogenous controls (Figure 4.3).

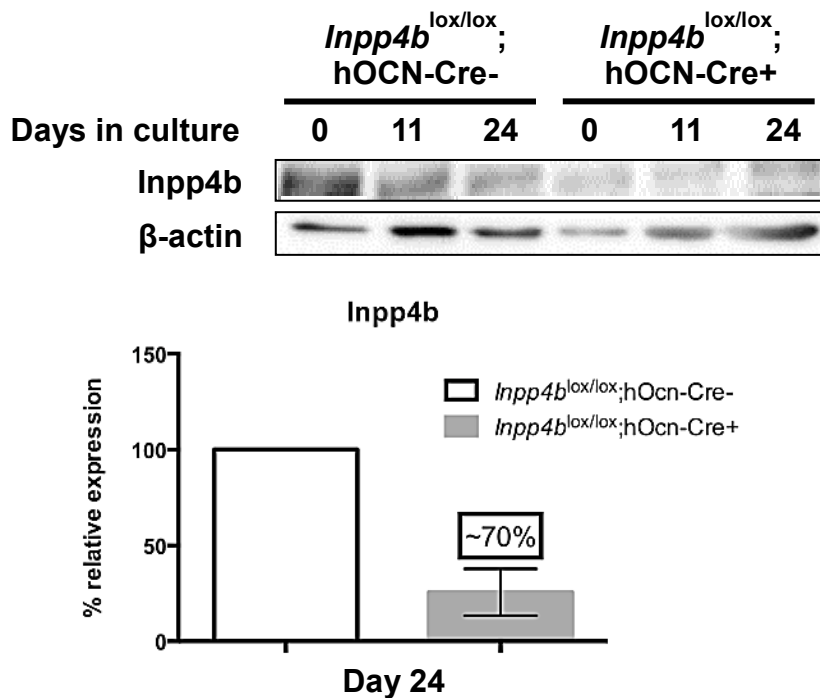


Figure 4.3: Expression of Inpp4b protein in *Inpp4b* cKO OB.

Quantification of Western blot revealed a decrease of approximately 70% of Inpp4b protein expression in cKO osteoblasts relative to controls after 24 days in culture.

Together, these results demonstrate the specific ablation and significant reduction of Inpp4b expression at both RNA and protein levels in the mature osteoblast of *Inpp4b* cKO mice.

Given these findings, we next characterized whether loss of *Inpp4b* may affect the molecular and cellular signalling that occur in the absence of *Inpp4b* in the mature osteoblast.

#### **4.1.5 Osteoblast-specific gene expression in *Inpp4b* cKO OB**

Having determined the deletion of *Inpp4b* in the mature osteoblast, we wanted to characterize the gene expression profile of the cKO osteoblasts during differentiation *ex vivo* to determine whether there were any transcriptional defects in these cells (Hu *et al.*, 2005). Total RNA extractions were performed on cultured primary osteoblast cultures from the calvaria of neonatal mice, after which reverse transcription was conducted to produce cDNA for qPCR analyses. Following qPCR, we found that there was dysregulation of the key osteoblastic gene markers, Runt-related transcription factor 2 (*Runx2*), alkaline phosphatase (*Alp*), osteocalcin (*Ocn*), and osteopontin (*Opn*) (Figure 4.4).

More importantly, these results suggest changes in the differentiation kinetics and/or population of osteoblasts. Specifically, an approximate ~1.5-, ~7-, and ~5-fold decrease in expression of *Runx2*, *Alp*, and *Ocn*, respectively, suggest a reduction in the early and late osteoblast populations, while a ~3-fold increase in expression of *Opn* suggests an increased inhibition of mineral formation by these *Inpp4b* cKO osteoblasts.

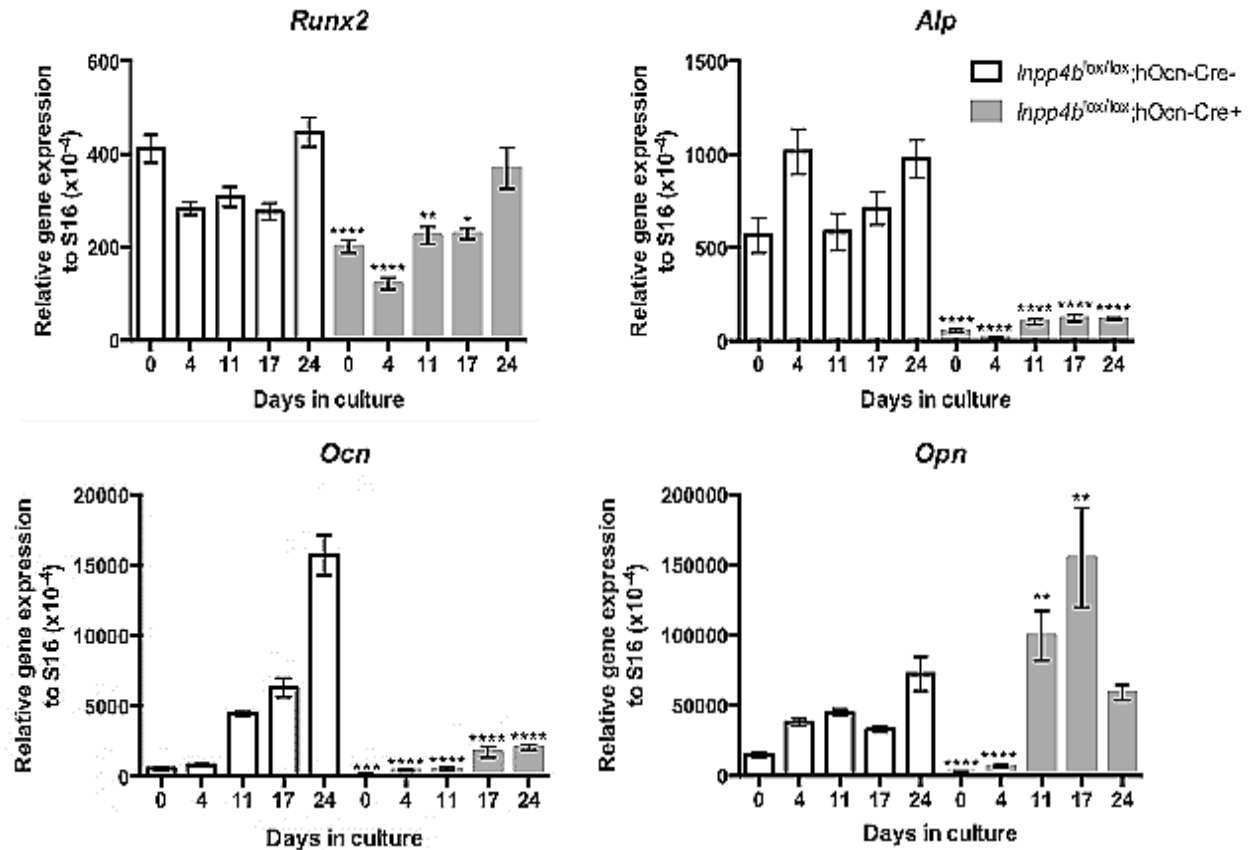


Figure 4.4: qPCR gene expression profiles in *Inpp4b* cKO osteoblasts and controls.

*Runx2* and *Alp* are expressed in early osteoblast differentiation, while *Ocn* and *Opn* are expressed at later stages. There is a significant decrease in *Runx2*, *Alp*, and *Ocn* expression, concomitant with an increase in *Opn* (n=3). \*p<0.05, \*\*p<0.01, \*\*\*p<0.001, \*\*\*\*p<0.0001.

#### 4.1.6 *Ex vivo* mineral nodule formation in *Inpp4b* cKO OB

Mature osteoblasts are responsible for secreting and mineralizing the extracellular bone matrix (Harada & Rodan, 2003). Given the dysregulation in osteoblast-specific gene expression, wherein we observed a decrease in the differentiation kinetics of *Inpp4b* cKO OB and an increase in the inhibition of mineralization, we investigated the ability of these *Inpp4b* cKO OB to produce minerals.

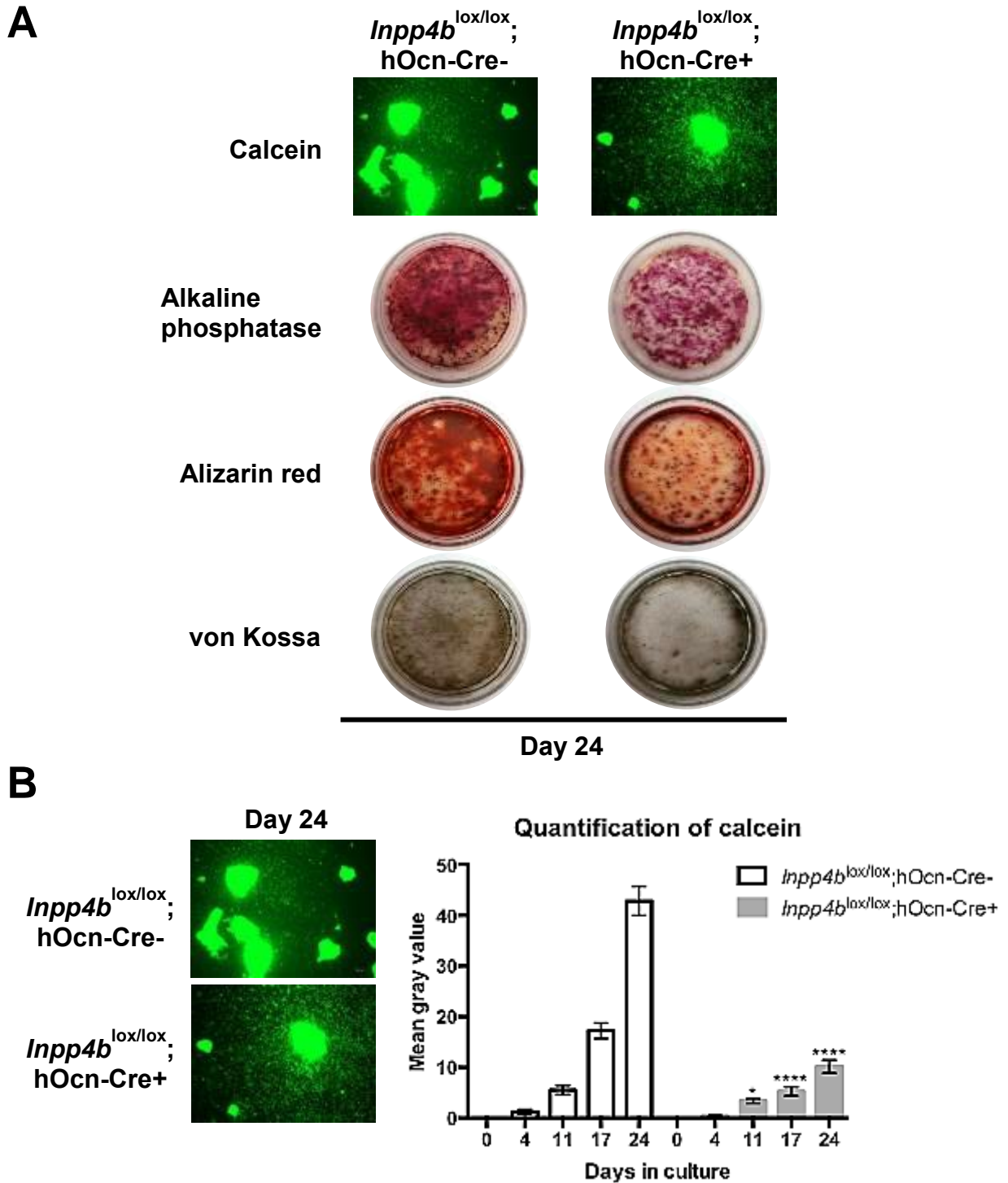


Figure 4.5: Mineralization assay for osteoblasts.

(A) Comparison of different staining procedures of mature osteoblasts. (B) Quantification of calcein stain, wherein there is ~75% reduction in *Inpp4b* cKO OB compared to controls (n=3). \*p<0.05, \*\*\*\*p<0.0001.

As such, we monitored the mineral formation ability of the *Inpp4b* cKO OB *ex vivo* using a combination of classical staining procedures, including alizarin red (AR), von Kossa (VK), and alkaline phosphatase (ALP), along with the fluorescent dye, calcein (Figure 4.5A).

In brief, alizarin red is a colorimetric reaction in which calcium, and thus calcific depositions are stained red. Von Kossa is a precipitation reaction involving silver ions that react with phosphate, after which the silver is deposited and reduced under light. Alkaline phosphatase is an indicator of osteoblast activity. Lastly, calcein is a fluorescent dye with excitation/emission wavelengths at 495/515nm, respectively, and chelates to  $\text{Ca}^{2+}$  ions. Interestingly, *Inpp4b* CKO osteoblasts displayed a significant decrease in mineralization when compared to controls (Figure 4.5B).

#### **4.1.7 Autophagy in *Inpp4b* cKO OB *ex vivo***

The process of autophagy has been previously implicated in the mechanism of bone mineralization (Hocking *et al.*, 2012; Nollet *et al.*, 2014). More specifically, autophagosomes have been shown to act as vehicles for osteoblasts to release minerals. This was particularly evident in studies of *Atg5*-deficient osteoblasts, wherein the OB-specific deletion of *Atg5* resulted in a reduction of mineralization capacity *ex vivo* (Nollet *et al.*, 2014). Thus, we quantified the expression of the autophagy-related genes, *Atg5* and *Atg7*, in cultured *Inpp4b* cKO osteoblasts by qPCR.

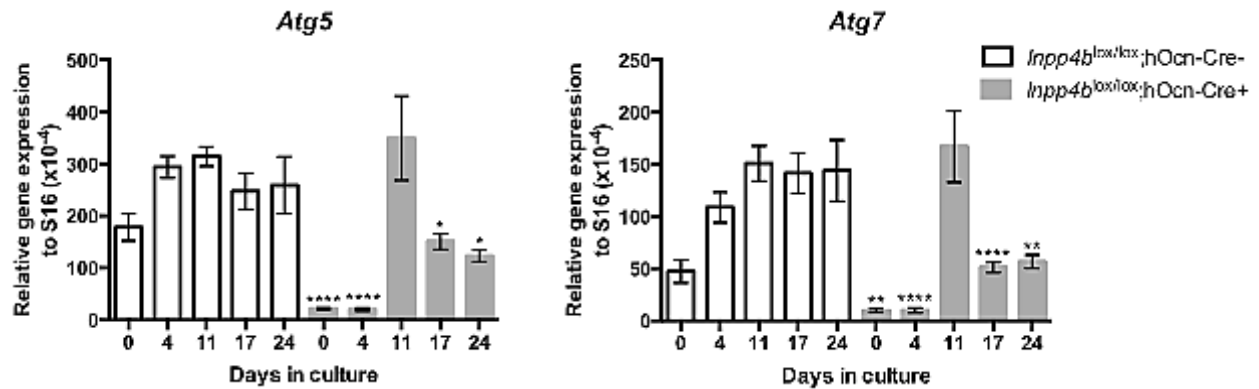


Figure 4.6: qPCR analysis of *Atg5* and *Atg7* gene expression.

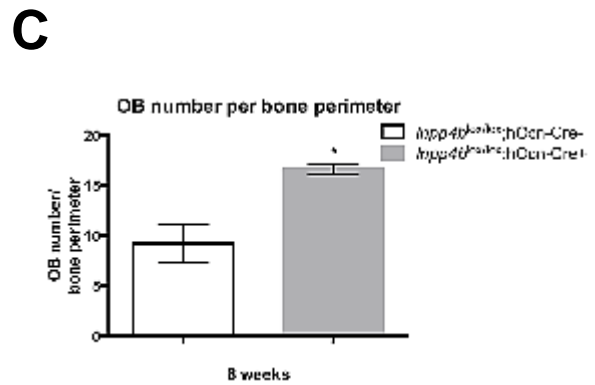
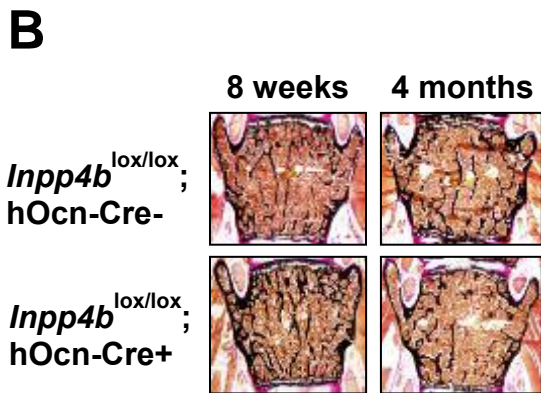
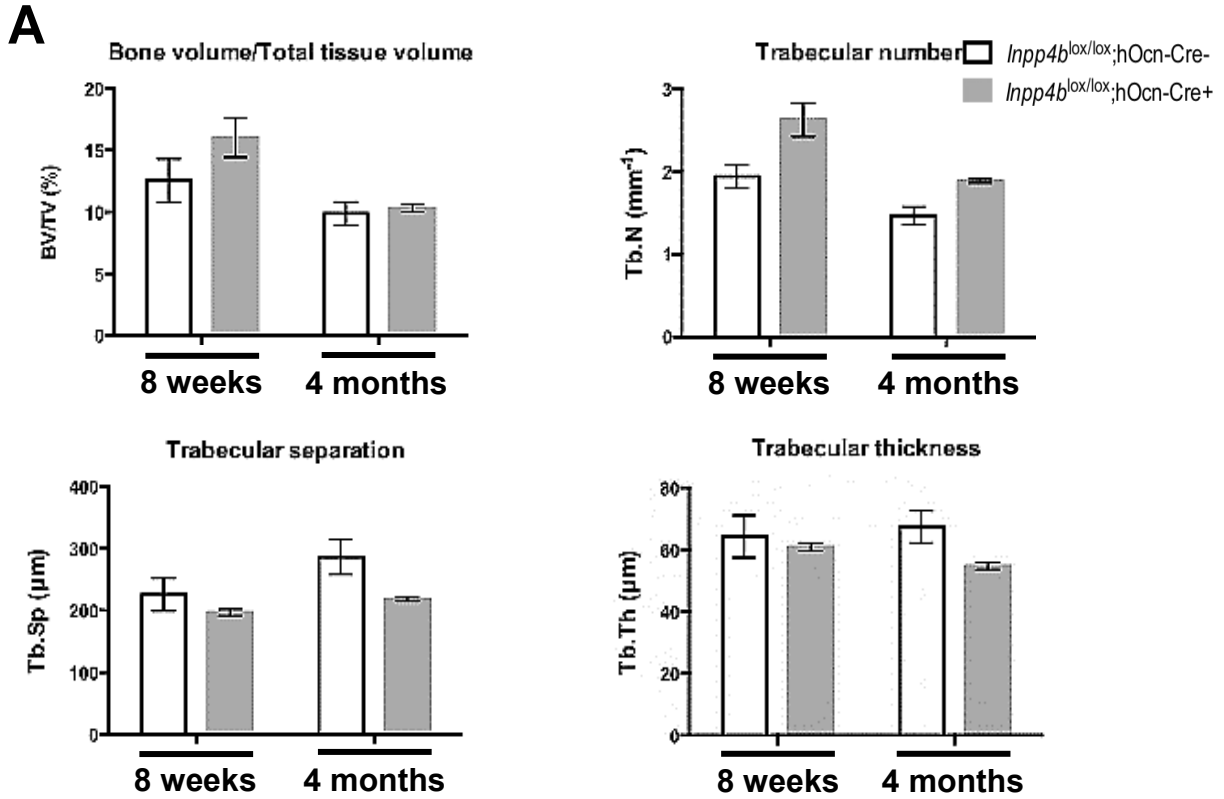
*Inpp4b* cKO OB exhibit ~4.8-fold decrease in *Atg5* expression and ~2.7-fold decrease in *Atg7* expression (n=3). \*p<0.05, \*\*\*\*p<0.0001.

Quantification of qPCR results showed a significant decrease of *Atg5* and *Atg7* genes expression in the absence of *Inpp4b* expression in osteoblasts (Figure 4.6).

#### 4.1.8 *In vivo* mineral apposition rate of *Inpp4b* cKO OB mice

These cellular changes *ex vivo* elicited the need to study *in vivo* the bone phenotype associated with conditional *Inpp4b* ablation in mature osteoblasts. Micro computed tomography (micro CT) analysis provides an overview of the long bone architecture, which was quantified in mice at two time points: 8 weeks of age and 4 months of age, so that we could focus analysis on time points during which bone mass is rapidly increasing and reaching peak mass levels, respectively. Concurrently, we performed von Kossa staining of un-decalcified 7  $\mu$ m vertebral sections that were initially embedded in methyl methacrylate (MMA) and deplastified with 2-methoxyethyl acetate. Analysis revealed that these *Inpp4b* cKO OB mice seemed to have slightly elevated bone mass compared to controls at 8 weeks of age, though overall there was no overt change in bone mass *in*

*in vivo* (Figure 4.7A, B). However, these mice did appear to have a 0.5-fold increase in number of osteoblasts at 8 weeks of age (Figure 4.7C), coupled with a one-fold increase in the mineral apposition rate (MAR) (Figure 4.7D, E).



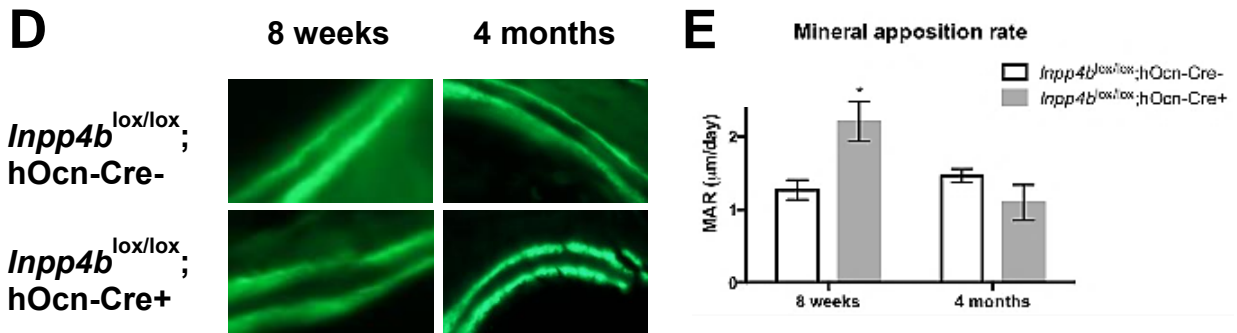


Figure 4.7: *In vivo* bone analyses of *Inpp4b* cKO OB mice at 8 weeks and 4 months of age.

(A) Micro CT quantification of femur trabecular bone parameters (n=3). (B) Representative images of von Kossa stained, van Gieson counterstained, lumbar (L4) vertebral sections from 8-week-old and 4-month-old mice (n=3). (C) Quantification of osteoblast population *in vivo*, revealed by toluidine blue staining of L4 vertebral sections from 8-week-old mice (n=3), revealing an approximate 0.5-fold increase in *Inpp4b* cKO OB mice compared to controls. (D) Representative images of double calcein-labeling in L4 vertebra to measure the mineral apposition rate (MAR). (E) Quantification of MAR from L4 vertebral sections (n=3), revealing an approximate one-fold increase in *Inpp4b* cKO OB mice compared to controls. \*p<0.05.

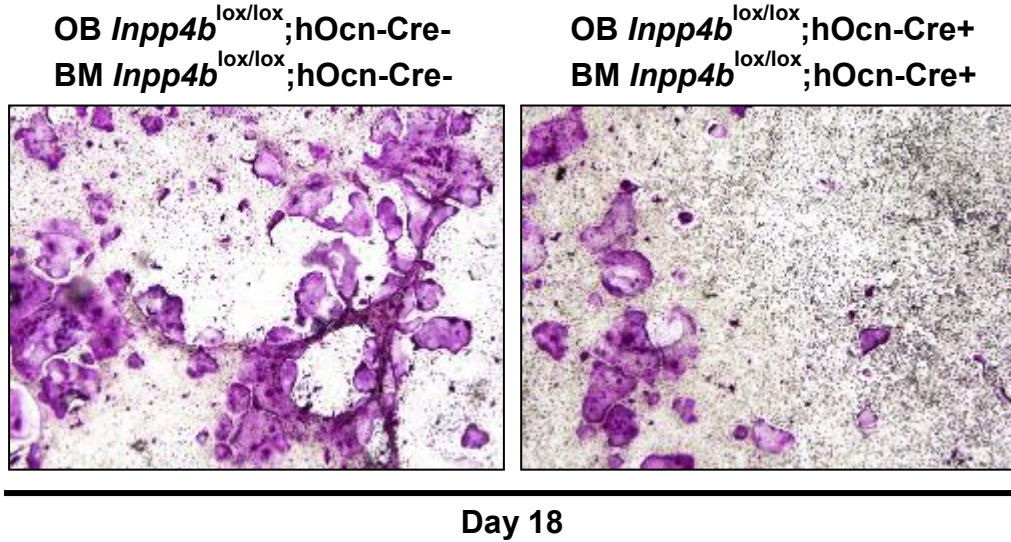
Double calcein-labeling was used to quantify the mineral apposition rate, or mineralizing activity, *in vivo*. Despite this increase in osteoblast cell population and activity, however, bone mass remained unchanged, suggesting a possible compensation mechanism *in vivo*.

#### 4.1.9 Evaluation of *Inpp4b* cKO OB capacity to modulate osteoclastogenesis

Since crosstalk between the osteoblasts and osteoclasts is essential for maintaining bone homeostasis, we investigated the capacity for *Inpp4b* cKO osteoblasts to support

osteoclastogenesis *ex vivo*. Moreover, we were interested in knowing whether the specific loss of *Inpp4b* in mature osteoblasts could modulate osteoclastogenesis.

**A**



**B**

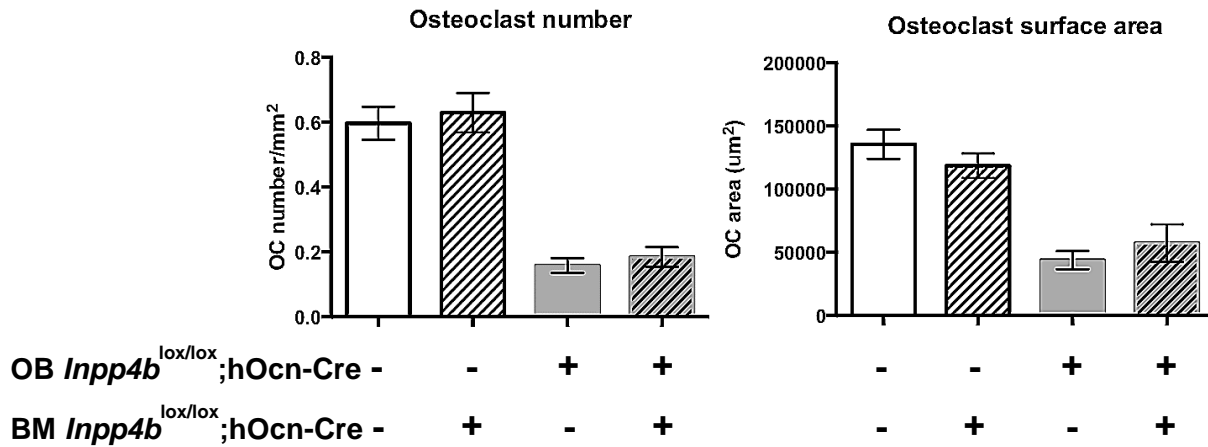


Figure 4.8: Quantification of TRAP-positive osteoclasts in co-culture.

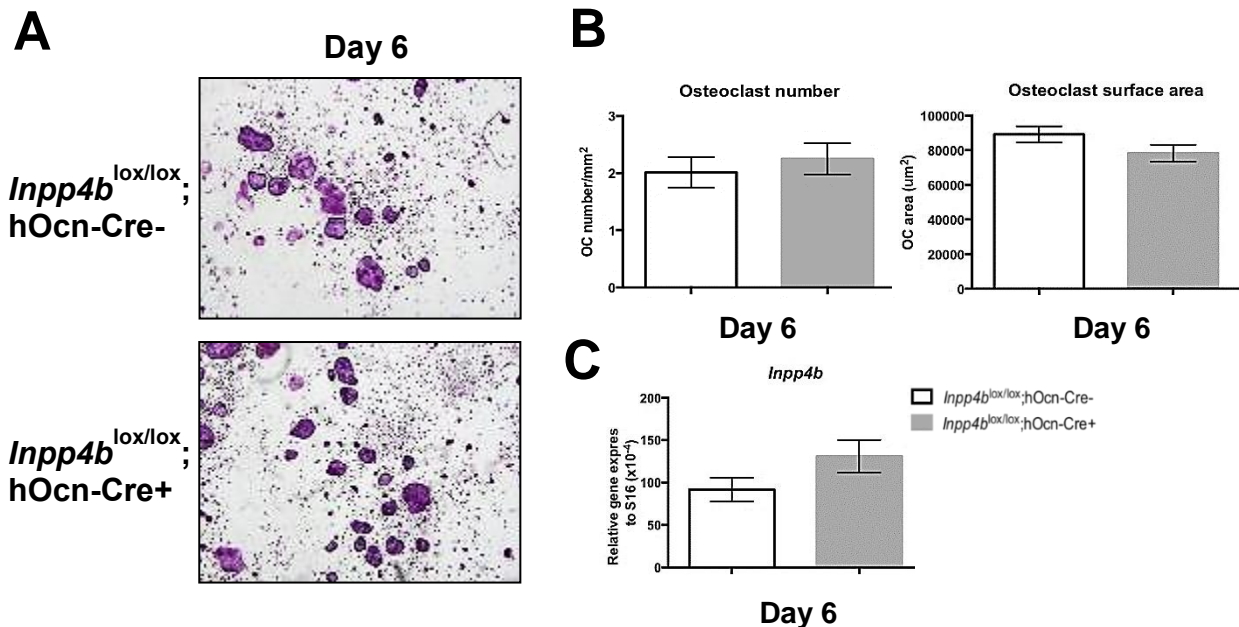
(A) Representative image of TRAP staining in *Inpp4b* cKO OB and controls after 18 days of co-culture. (B) Quantification of mature osteoclast number and size (n=2). (BM=bone marrow).

To this end, we utilized a co-culture system in which bone marrow-derived osteoclast progenitors were cultured in the presence of primary osteoblasts isolated from day 5

neonatal mouse calvaria and stimulated with vitamin D<sub>3</sub> and prostaglandin E<sub>2</sub>. After 18 days in culture, production of multinucleated mature osteoclasts was revealed following TRAP staining (Figure 4.8A). As shown in Figure 4.8B, the number of multinucleated OCLs generated in presence of *Inpp4b* cKO OB is reduced both in number and size compared to controls.

#### 4.1.10 Osteoclast population in mice with *Inpp4b* cKO in OB

Despite no significant phenotypic difference between the *Inpp4b* cKO OB and control mice, we hypothesized that the osteoclast population may be responsible for maintaining comparable bone mass via intercellular communication and crosstalk between osteoblasts and osteoclasts (Teti, 2012).



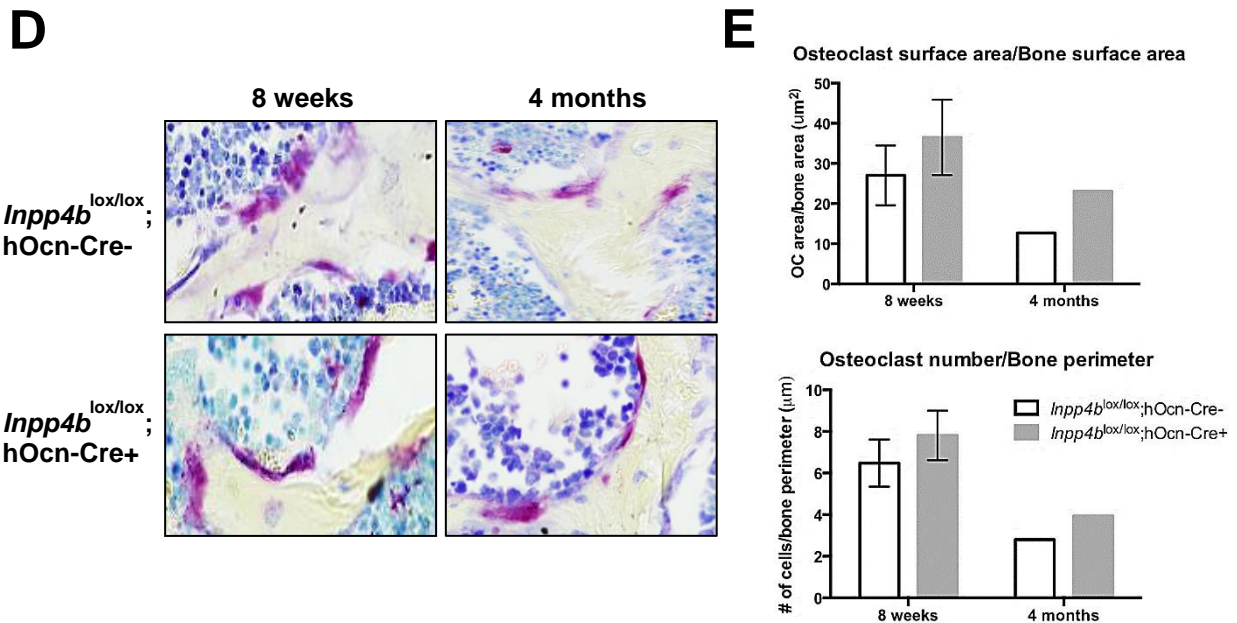


Figure 4.9: Characterization of osteoclast population in *Inpp4b* cKO OB mice.

(A) Representative images of *ex vivo* mature osteoclasts on plastic, revealed by TRAP staining. (B) Quantification of *Inpp4b* cKO TRAP-stained *ex vivo* mature osteoclasts display similar number and size compared to controls (n=3). (C) Comparable *Inpp4b* expression was quantified by qPCR (n=3). (D) Representative images of *in vivo* TRAP staining of L4 vertebral sections from 8-week-old *Inpp4b* cKO OB mice. (E) Quantification of TRAP staining *in vivo* demonstrated comparable quantitative values for osteoclast number and size compared to controls in both 8-week-old and 4-month-old mice.

*Ex vivo* cultures of bone marrow-derived primary osteoclasts from *Inpp4b* cKO OB mice demonstrated no significant change in number, size, or *Inpp4b* osteoclast expression (Figure 4.9A, B, C). *In vivo* analyses also showed no significant differences between the osteoclast population of *Inpp4b* cKO OB mice and controls (Figure 4.9D, E), thereby suggesting that the increased number and activity of the osteoblast is not sufficient to significantly alter bone mass. Alternatively, other mechanisms and pathways may be responsible for keeping bone mass at comparable levels.

#### 4.1.11 Characterization of OPG/RANKL ratio in *Inpp4b* cKO OB mice

Co-culture experiments suggest that osteoblasts with a conditional ablation of *Inpp4b* induce less and smaller osteoclasts compared to control osteoblasts. However, *in vivo*, we found that there is no change in osteoclast population. Given the fact that osteoblasts can alter osteoclastogenesis via secretion of the cytokines, RANKL and OPG, we decided to assess whether these signalling factors were affected. Preliminary results from ELISA assays revealed that in co-culture, there seems to be an increase in OPG/RANKL ratio, favouring the inhibition of osteoclast differentiation (Figure 4.10A). *In vivo*, levels of these proteins were unchanged between *Inpp4b* cKO OB mice and controls (Figure 4.10B).

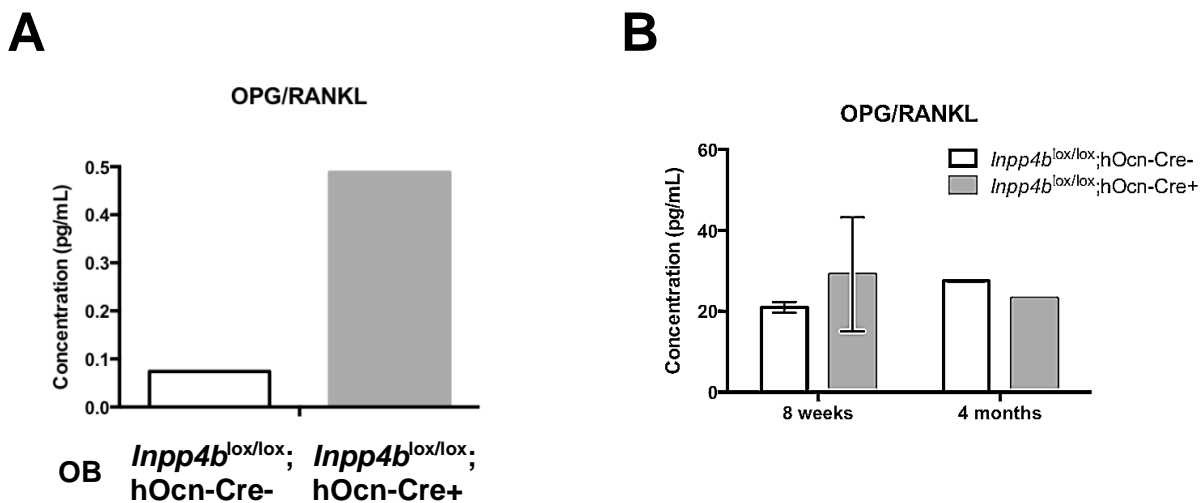


Figure 4.10: OPG/RANKL ratio in osteoblast cell culture media and sera.

(A) Co-culture cell-conditioned media suggests that *Inpp4b* cKO OB favour osteoclastogenesis due to an increased OPG/RANKL ratio. (B) Serum levels from *Inpp4b* cKO OB mice and controls suggest unaffected OPG/RANKL ratio.

These initial findings indicate, therefore, that *Inpp4b* may modulate osteoblastogenesis in culture and thus the ability for these osteoblasts to induce osteoclast differentiation.

## 4.2 OSTEOBLAST-SPECIFIC EXPRESSION OF *Inpp4b* IN TRANSGENIC (TR) MICE

### 4.2.1 Targeted overexpression of *Inpp4b* in mature osteoblasts

To complement studies in the *Inpp4b* cKO OB mice, we also generated an osteoblast-specific *Inpp4b* transgene under the control of the human osteocalcin promoter wherein *Inpp4b* would be overexpressed in the mature osteoblast. Transgenic hOcn-*Inpp4b*-hGH (*Inpp4b* TR OB) founders were identified by PCR and intercrossed to establish four transgenic lines. These mice were born at expected Mendelian frequencies, with no obvious phenotypic defects compared to littermate controls. As in the case of the *Inpp4b* cKO OB, a combination of *ex vivo* and *in vivo* analyses were performed to assess the osteoblast-specific role of *Inpp4b*.

### 4.2.2 Generation of transgenic *Inpp4b* mice

In transgenics, the human osteocalcin promoter has previously been shown to direct bone-specific expression of several transgenes (Clemens *et al.*, 1997). Transgenic founder lines were identified by PCR and four founders were selected for further characterization. A schematic representation of the linearized construct can be found in Figure 4.11 below.

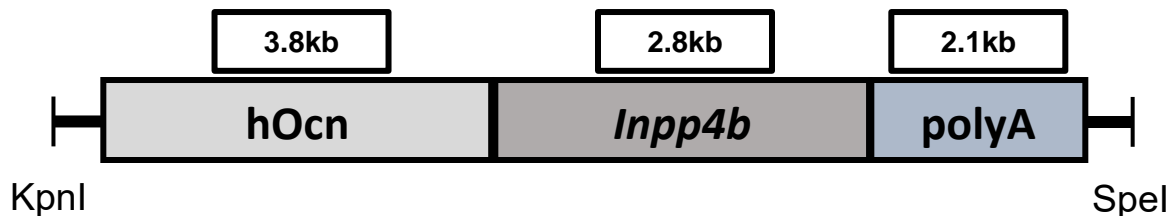


Figure 4.11: Linearized *Inpp4b* transgene construct.

### **4.2.3 Determination of copy number**

Four transgenic founder mouse lines were generated and analyzed for transgene copy number and integrity by Southern blot. To this end, our lab generated four transgenic hOcn-*Inpp4b*-hGH lines: TR95, TR352, TR363, and TR362 with 8, 7, 6, and 5 copies of the transgene, respectively (Figure 4.12A). Subsequent quantitative gene expression analysis was conducted, after which the TR95 and TR362 were studied further *in vivo* as they showed the lowest and highest expression, respectively.

### **4.2.4 Specific transgene expression**

Following confirmation of transgene integrity and quantification of copy number, specific transgene expression in mature osteoblasts was confirmed by RT-PCR of primary osteoblast cultures. Calvarial osteoblasts from neonatal TR mice were cultured and differentiated, after which total RNA was extracted and reverse transcribed for semi-quantitative PCR analysis. As shown in Figure 4.12B, there is specific expression of the *Inpp4b* transgene with maturation time *ex vivo*, after 18 days of culture. Importantly, this increase in expression is in accordance with *Ocn* gene expression, which also increases with maturation time, thereby demonstrating the specificity of the human *Ocn* promoter. Non-transgenic samples were used as controls.

### **4.2.5 Quantitative transgene expression**

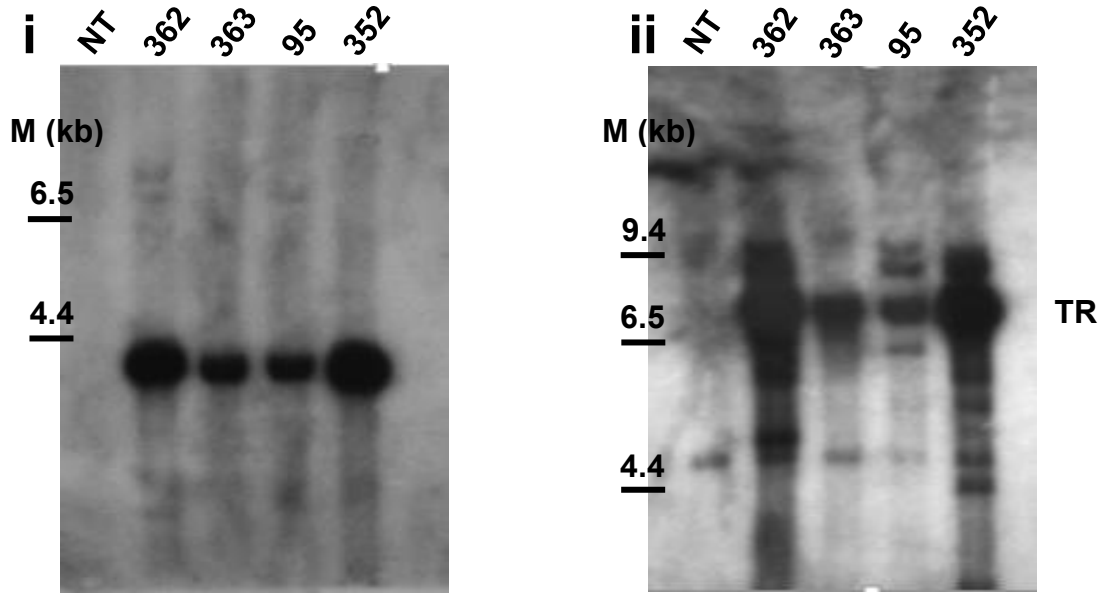
As the transgene is expected to be highly expressed at the mature osteoblast stage, we then moved onto quantitative PCR to determine the level of expression of the transgene in fully differentiated osteoblasts. The level of overexpression was expressed as a fold

change ratio over the non-transgenic control (Figure 4.12C). At the last day of culture (day 24), mature osteoblasts from the TR95 line had an approximate 10-fold increase in *Inpp4b* expression, while the TR362 line had an approximate 40-fold increase in expression. These findings further confirmed that the *Inpp4b* TR is expressed specifically, and highly, at the mature osteoblast stage of osteoblast differentiation and maturation.

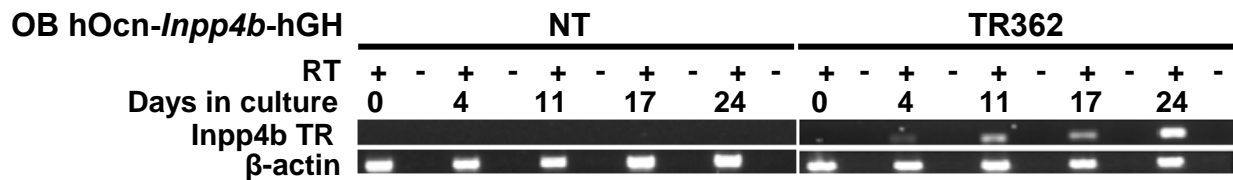
#### **4.2.6 Inpp4b protein expression during osteoblast differentiation**

Having confirmed the specific expression of the transgene and its increased levels of expression with osteoblast differentiation, we next analyzed endogenous protein expression by Western blot analysis to evaluate Inpp4b protein overexpression compared to endogenous protein levels of non-transgenic controls. As shown in Figure 4.12D, increased levels of Inpp4b protein expression were detected in extracts from the TR95 and TR362 lines and reached a peak at day 24 in culture. This increased Inpp4b protein expression correlates with the gene expression pattern for both the TR95 and TR362 lines (Figure 4.12E).

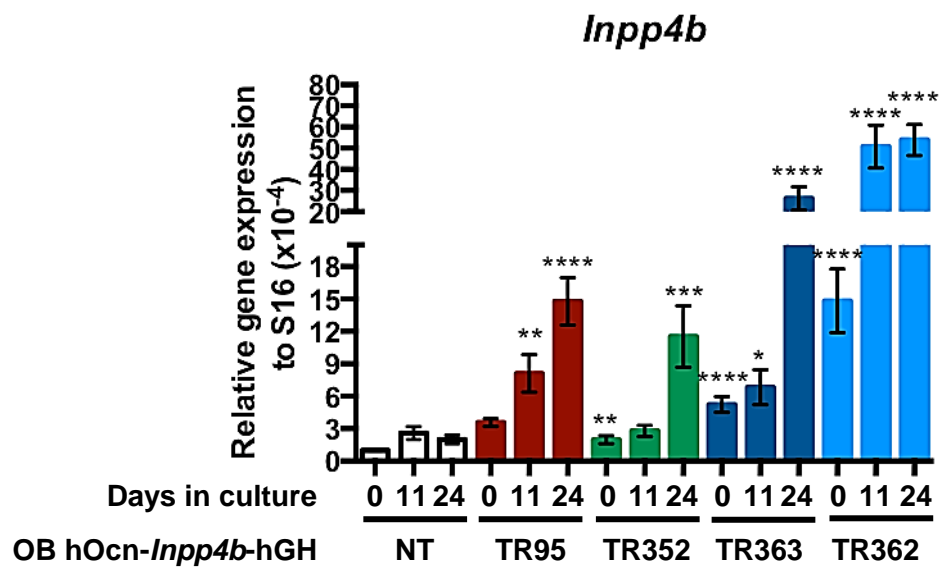
**A**



**B**



**C**



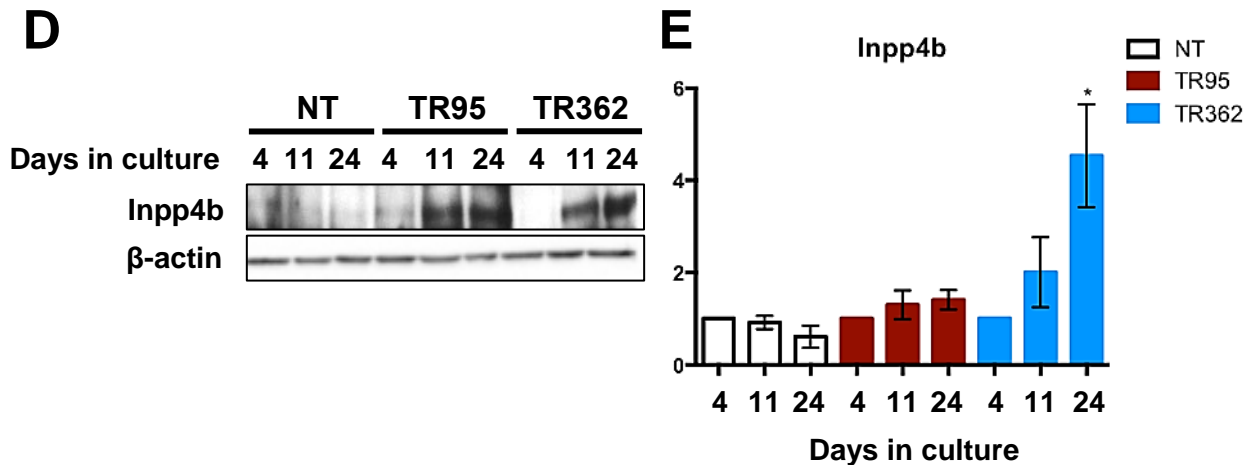


Figure 4.12: Characterization of *Inpp4b* TR OB mice.

(A) Southern blot of transgenic mice using 10 µg of genomic DNA extract from mouse tail tips. (i) Probe designed to assess transgene integrity (HindIII digestion; 4.2 kb band). (ii) Probe designed to quantify transgene copy number (BamHI digestion; 7.5 kb band). (B) Semi-quantitative PCR assay for *Inpp4b* transgene expression in reverse transcribed DNA from osteoblast extracts differentiated in cell culture. β-actin served as an internal control. (C) qPCR analysis of transgene expression, demonstrating increasing expression with osteoblast differentiation (n=3). \*p<0.05, \*\*p<0.01, \*\*\*p<0.001, \*\*\*\*p<0.0001. (D) Western blot analysis of Inpp4b protein expression. (E) Quantification of Western blot suggest increase in Inpp4b protein expression of transgenic mice compared to non-transgenic controls (n=3). \*p<0.05.

#### 4.2.7 Osteoblast-specific gene expression in *Inpp4b* TR OB

Following analyses that confirmed the specific overexpression of *Inpp4b* in the mature osteoblast, we studied the gene expression profile of differentiated osteoblasts *ex vivo*. cDNA was prepared as previously described and analyzed by qPCR. Quantification of these results revealed an increase of gene expression of both *Runx2* and *Ocn* (Figure 4.13). Specifically, these findings suggest that there are alterations of osteoblast differentiation kinetics and/or population as the observed increases demonstrate an upregulation of both early and late osteoblastic gene markers. Moreover, these results suggest that overall, there appears to be no significant change in osteoblast differentiation

kinetics of the TR95 line, as compared to the TR362 line, in which we observe an approximate 3- and 33-fold increase in *Runx2* and *Ocn*, respectively.

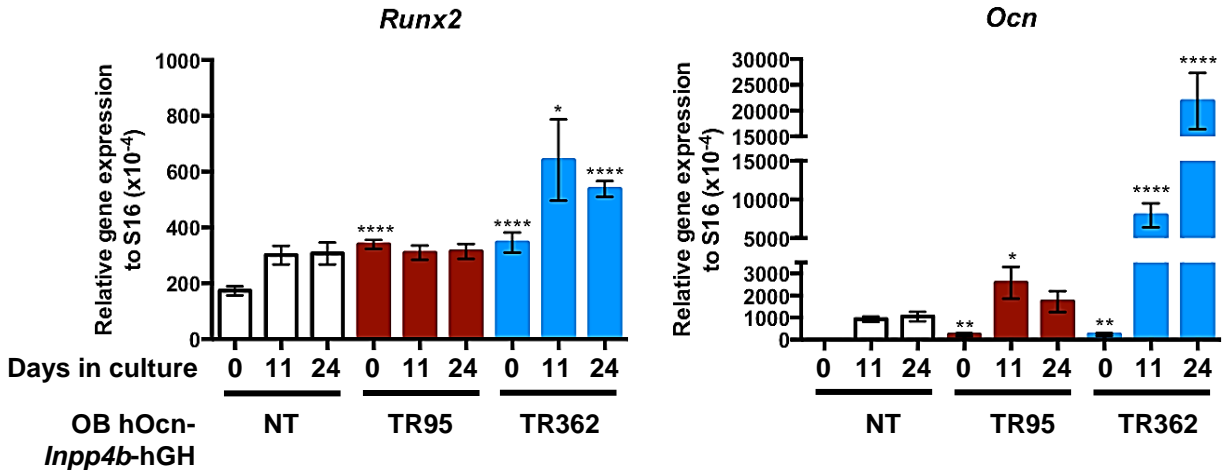


Figure 4.13: qPCR gene expression profiles in *Inpp4b* TR OB and controls.

*Runx2* is expressed in early osteoblast differentiation, while *Ocn* is expressed at later stages. There is a significant increase in *Runx2* and *Ocn* in the TR362 line, which also expresses the most transgene (n=3). \*p<0.05, \*\*p<0.01, \*\*\*\*p<0.0001.

#### 4.2.8 Ex vivo mineral nodule formation in *Inpp4b* TR OB

Given the qPCR findings of *Runx2* and *Ocn* expression in the *Inpp4b* TR OB, wherein we observed an overall increase in the differentiation kinetics of the TR362 line, and not in the TR95 line (Figure 4.13), we next assessed the mineralization potential of these cells. Using a combination of ex vivo staining procedures (ALP, AR, calcein), we found that the TR362 line, and not the TR95 line, displayed an increased ability to form minerals. This was visualized by the increased mineral nodule formation revealed by classical staining procedures (Figure 4.14A). Quantification of calcein staining revealed a similar finding (Figure 4.14B).

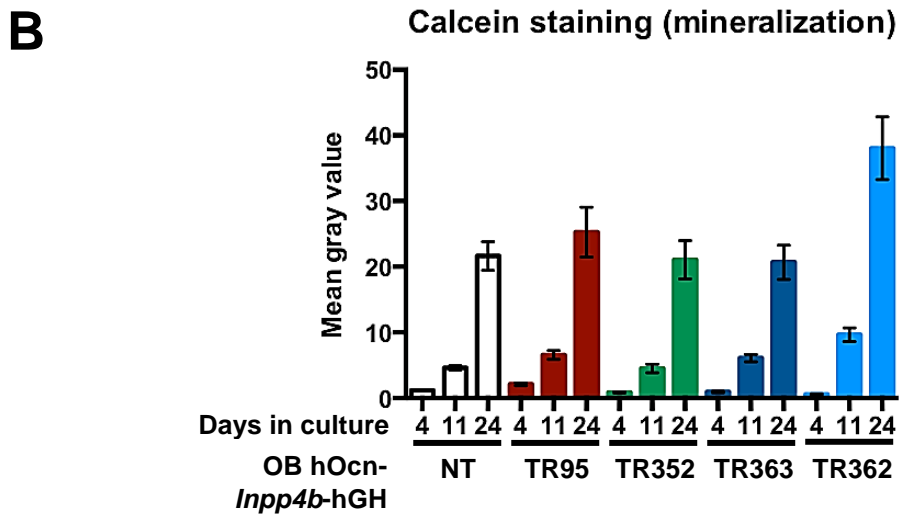
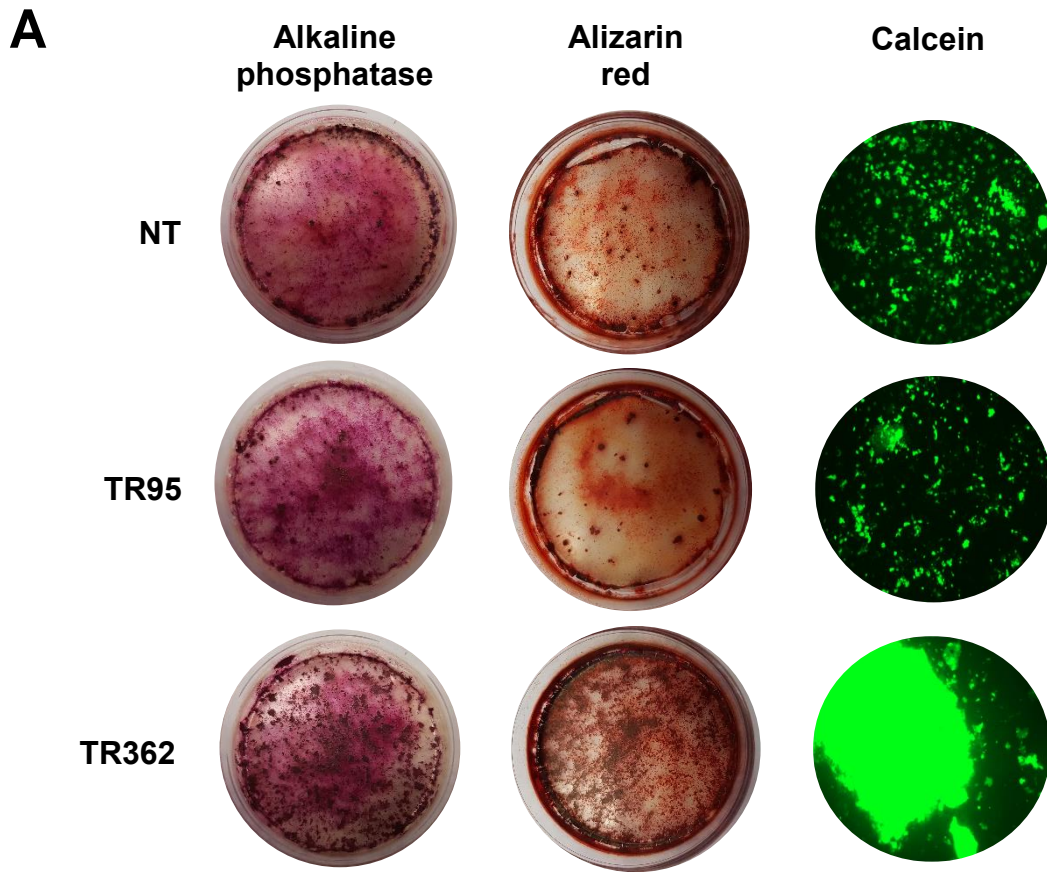
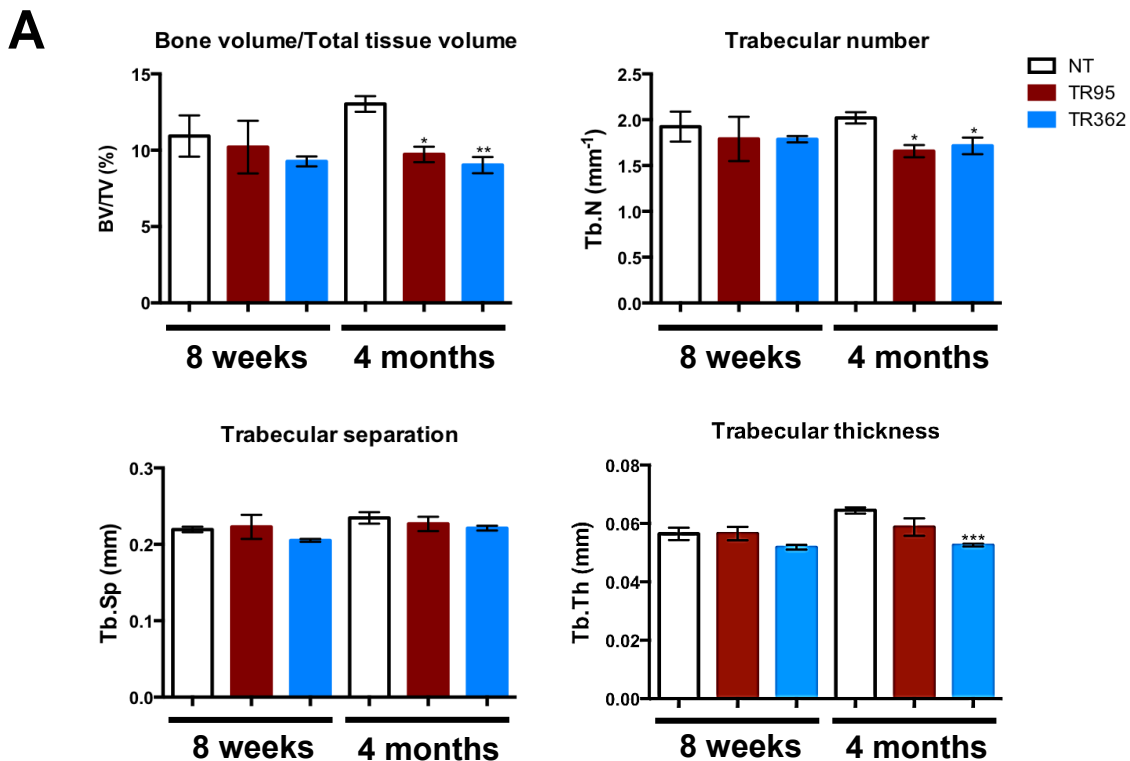


Figure 4.14: Mineralization assay for osteoblasts.

(A) Comparison of different staining procedures of mature osteoblasts after 24 days of culture.  
 (B) Quantification of calcein stain suggests comparable or increased mineralization in transgenic osteoblasts compared to non-transgenic controls.

#### 4.2.9 *In vivo* mineral apposition rate of *Inpp4b* TR OB mice

Given these *ex vivo* findings, we were interested in looking at the *in vivo* phenotype of these *Inpp4b* TR OB mice and whether the specific overexpression of *Inpp4b* in the mature osteoblast can affect bone mass. Firstly, micro CT analysis was performed on dissected femurs to investigate the trabecular bone of these mice at both 8 weeks and 4 months of age, which represent periods of rapid bone remodeling and peak bone mass, respectively. Concurrently, we performed von Kossa staining on un-decalcified 7  $\mu$ m-thick vertebral sections that were initially embedded in MMA and deplastified with 2-methoxyethyl acetate. We observed no initial change in bone mass at 8 weeks of age, as evidenced by these micro CT results and mineral apposition rate (MAR). Interestingly, however, these mice exhibited a reduction in bone mass *in vivo* at 4 months of age (Figure 4.15A, B), which was coupled with a decrease in the MAR of these osteoblasts (Figure 4.15C, D).



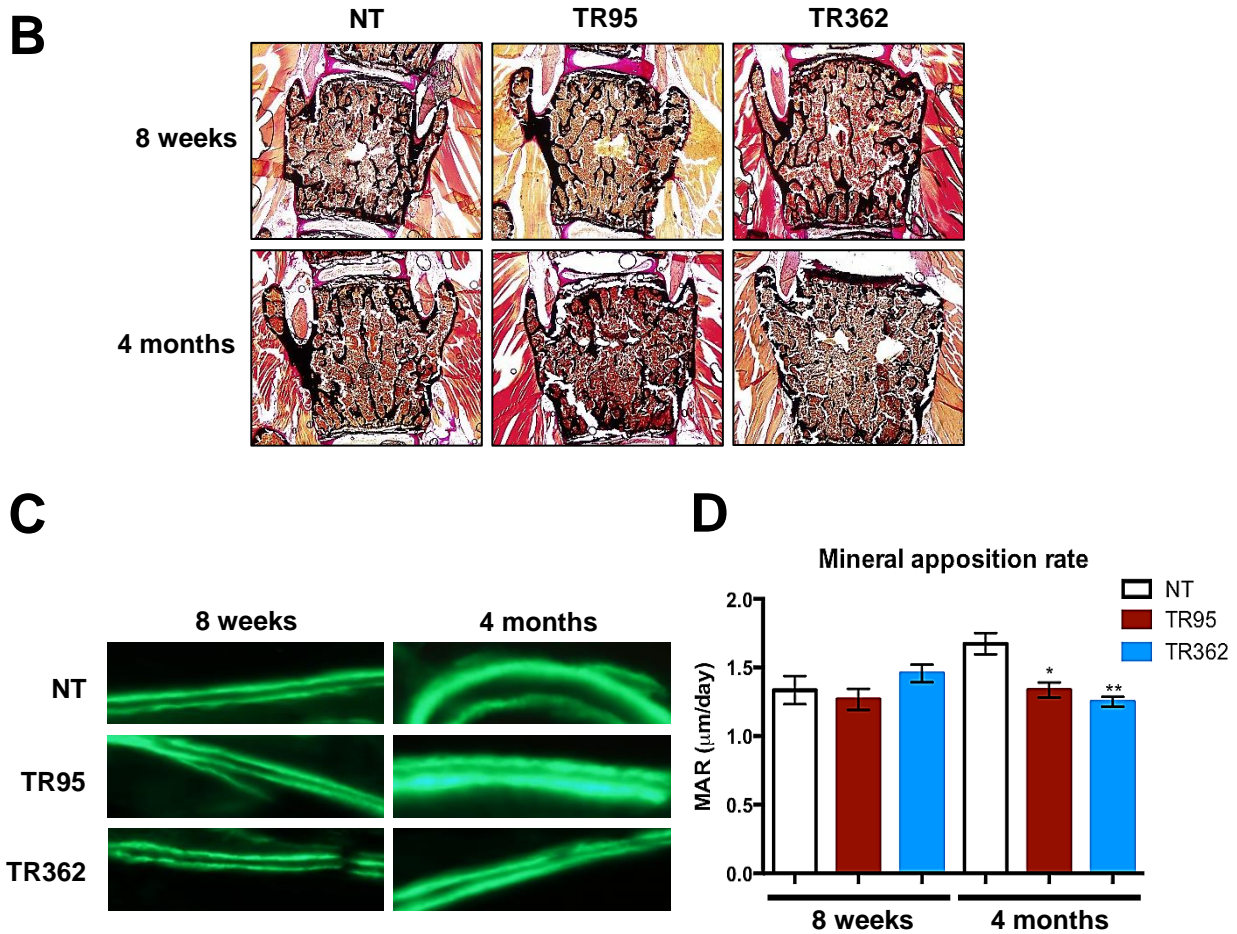


Figure 4.15: *in vivo* bone analyses of *Inpp4b* TR OB mice at 8 weeks and 4 months of age.

(A) Representative images of von Kossa stained, van Gieson counterstained, lumbar (L4) vertebral sections from non-transgenic (NT) and transgenic (TR) mice 8-week- and 4-month-old mice (n=3). (B) micro CT quantification of femur trabecular bone parameters, revealing significant bone loss in 4-month-old mice compared to non-transgenic controls (n=3). \* $p < 0.05$ , \*\* $p < 0.01$ , \*\*\* $p < 0.001$ . (C) Representative images of double calcein-labeling in L4 vertebra of 8-week-old and 4-month-old mice to measure mineral apposition rate (MAR). (D) Quantification of MAR, revealing a significant decrease in mineralizing activity of transgenic osteoblasts compared to non-transgenic controls (n=3). \* $p < 0.05$ , \*\* $p < 0.01$ .

This suggests that the specific overexpression of *Inpp4b* in mature osteoblasts decreases the mineralization activity, thereby decreasing the overall bone mass.

Taken together with the findings from the *ex vivo* analyses of these *Inpp4b* TR OB, we observed opposing results; more specifically, we see that *in vivo*, these mice display decreased bone mass, despite mineralizing at comparable or increased levels compared to non-transgenic controls *ex vivo*.

#### **4.2.10 Evaluation of *Inpp4b* TR OB capacity to modulate osteoclastogenesis**

With the observation that *Inpp4b* TR OB mice display a reduced bone mass *in vivo*, we next sought to determine whether there was a dysregulation in the crosstalk between the osteoblasts and osteoclasts. Herein, osteoclast progenitors were isolated from bone marrow and seeded on confluent primary osteoblast cultures isolated from neonatal mice calvaria. Fully differentiated osteoclasts were subsequently TRAP stained on day 18. This staining on co-cultures between controls and transgenic mice from the TR362 line revealed an apparent increase in the number of osteoclasts, without any change in size (Figure 4.16A, B), which could be explained by a decrease in the OPG/RANK ratio (Figure 4.16C). These results suggest, therefore, that the low bone mass observed in the *Inpp4b* TR OB mice could be explained, in part, by the increased stimulation of osteoclastogenesis by the osteoblasts specifically expressing higher levels of *Inpp4b*.

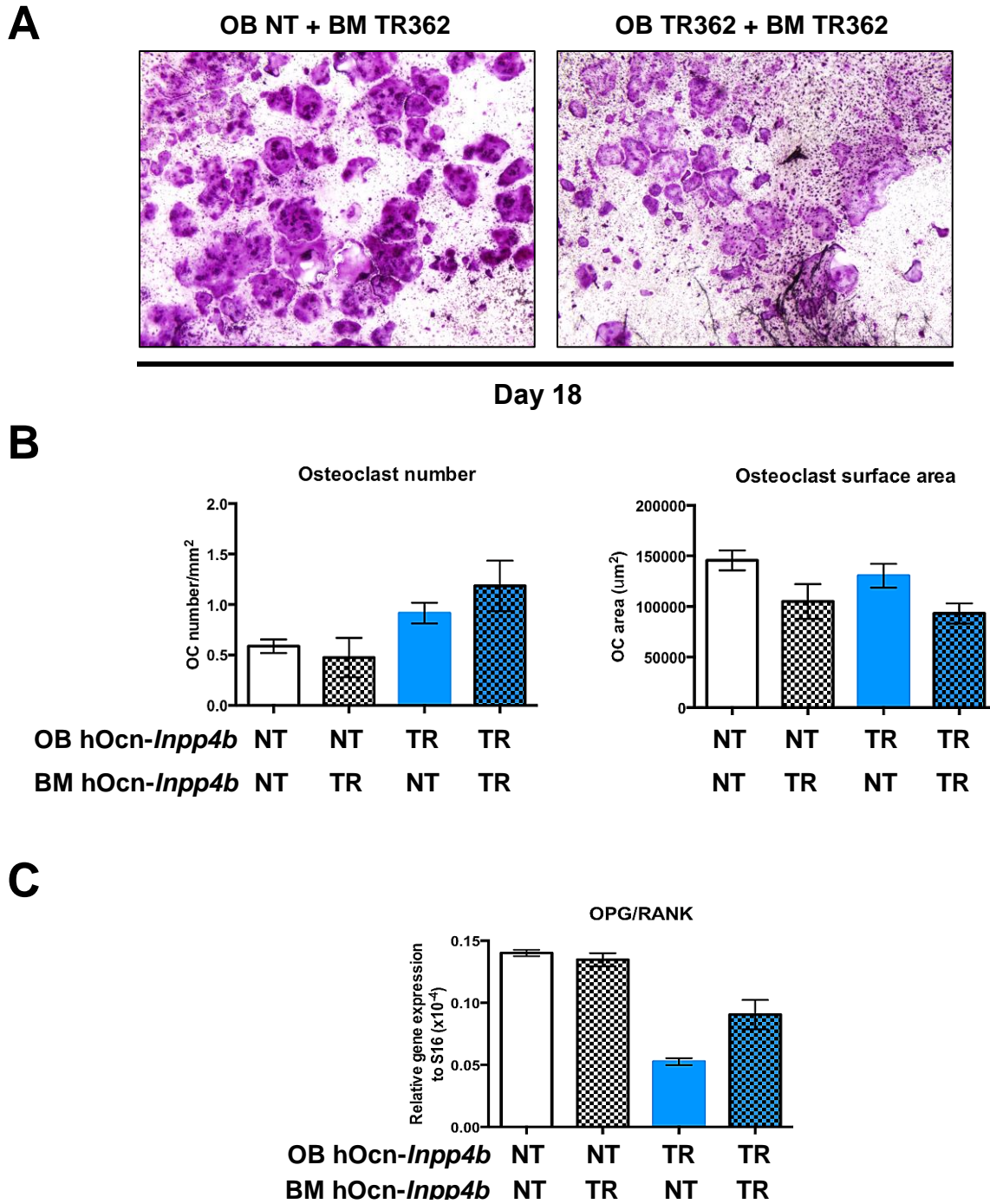
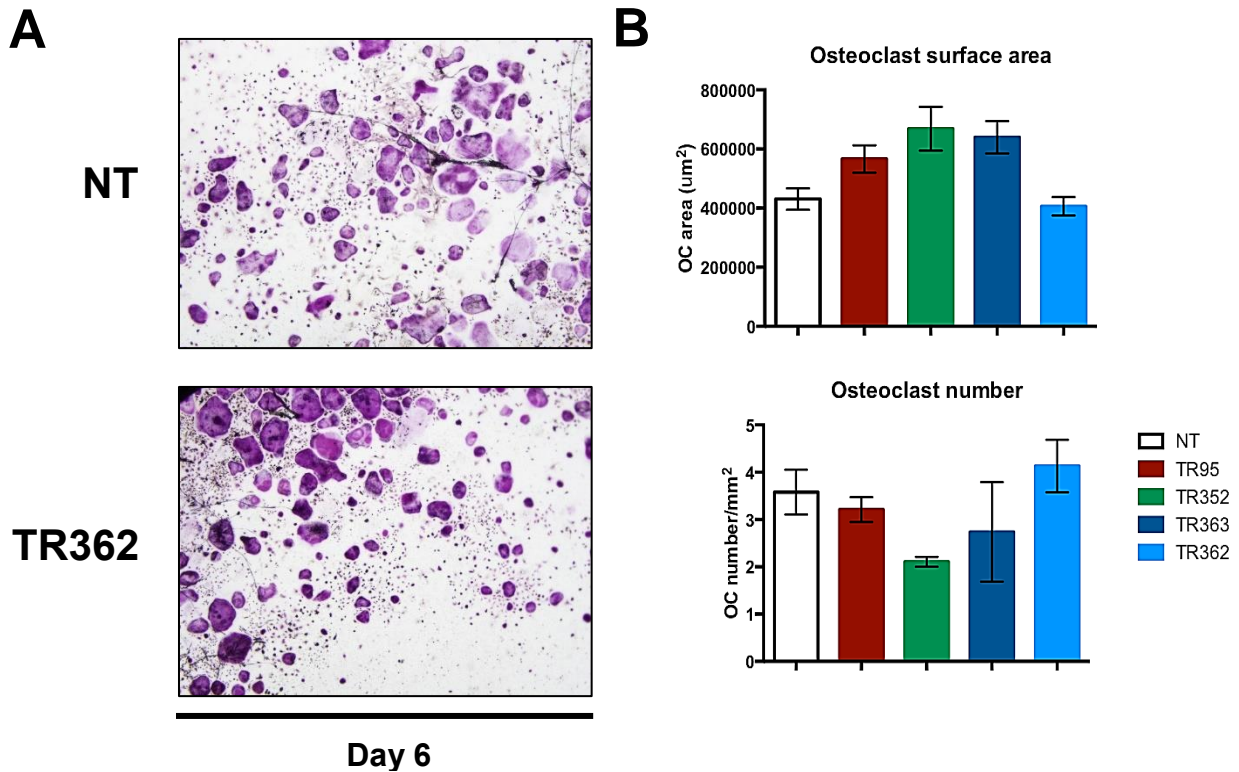


Figure 4.16: Quantification of TRAP-positive osteoclasts in co-culture.

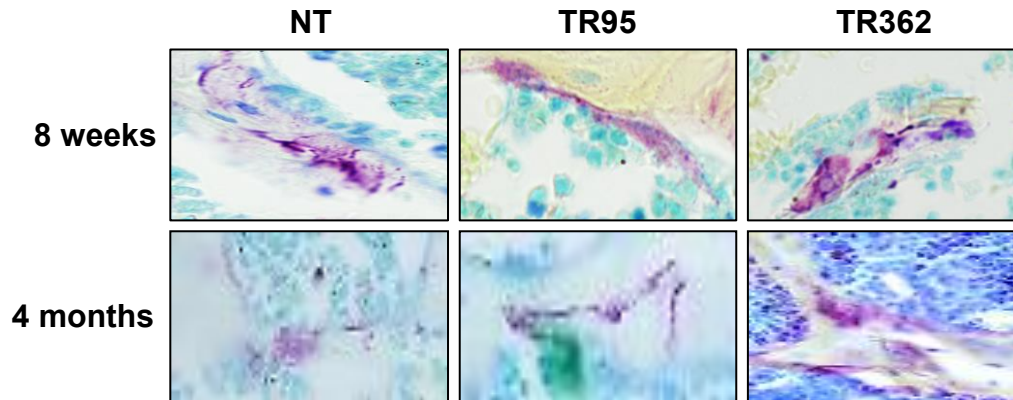
(A) Representative image of TRAP staining in *Inpp4b* TR OB and controls. (B) Quantification of mature osteoclast number and size (n=2). BM=bone marrow. (C) Ratio of OPG and RANK gene expression evaluated by qPCR suggests enhanced osteoclastogenesis by transgenic osteoblasts compared to non-transgenic controls. BM=bone marrow.

#### 4.2.11 Osteoclast population in *Inpp4b* TR OB mice

Since these *Inpp4b* TR OB mice displayed a reduction in bone mass compared to non-transgenic controls, we were interested in characterizing the osteoclast population both *ex vivo* and *in vivo* to see whether the specific overexpression of *Inpp4b* could modulate the cellular crosstalk between osteoblasts and osteoclasts. To this end, we observed no significant difference in bone marrow-derived osteoclasts from transgenic mice cultured *ex vivo* (Figure 4.17A, B). However, *in vivo* analysis revealed that *Inpp4b* TR OB mice produced more osteoclasts than control mice (Figure 4.17C, D). Therefore, this prompted us to study more in-depth the crosstalk between osteoblasts and osteoclasts by co-culture and ELISA analyses.



C



D

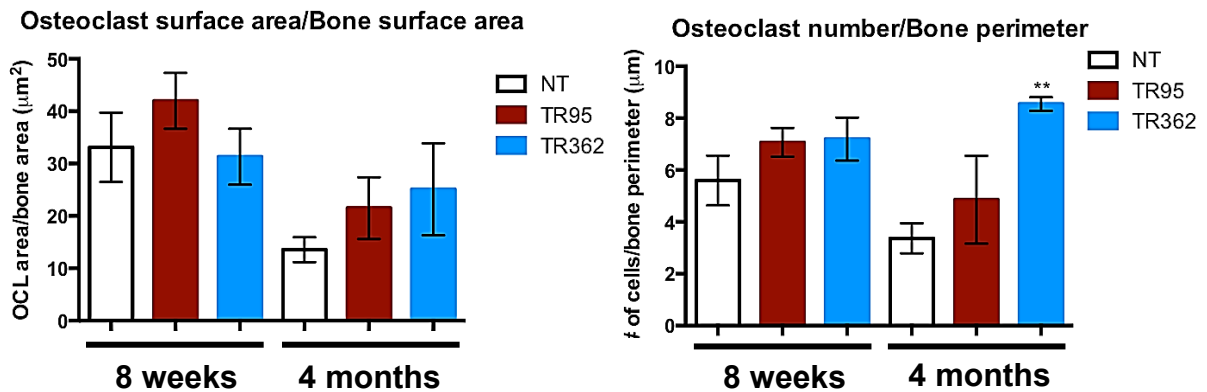


Figure 4.17: Characterization of osteoclast population in *Inpp4b* TR OB mice.

(A) Representative images of *ex vivo* mature osteoclast population on plastic, with TRAP staining. (B) Quantification of *Inpp4b* TR TRAP-stained *ex vivo* mature osteoclasts demonstrate similar numbers and size compared to controls (n=2). (C) Representative images of *in vivo* TRAP staining of L4 vertebral sections from 8-week-old and 4-month-old *Inpp4b* TR OB mice. (D) Quantification of TRAP staining *in vivo* demonstrated an increase in osteoclast number, but not size (n=2). \*\*p<0.01.

#### 4.2.12 Characterization of OPG/RANKL ratio in *Inpp4b* TR OB mice

Co-culture experiments suggest that osteoblasts overexpressing *Inpp4b* induce more osteoclasts compared to control osteoblasts, which was found to be concomitant with

decreased OPG/RANK gene expression. Moreover *in vivo* data demonstrated an increased osteoclast population of 4-month-old *Inpp4b* TR OB mice. These findings could be explained by a decreased ratio of OPG/RANKL protein levels, thereby favouring osteoclastogenesis and the subsequent bone loss seen at 4 months by micro CT. Preliminary results from ELISA revealed that in co-culture, there seems to be a decrease in OPG/RANKL ratio, favouring the stimulation of osteoclast differentiation (Figure 4.18A). *In vivo*, the ratio of these proteins was also decreased between *Inpp4b* cKO OB mice and controls (Figure 4.18B).

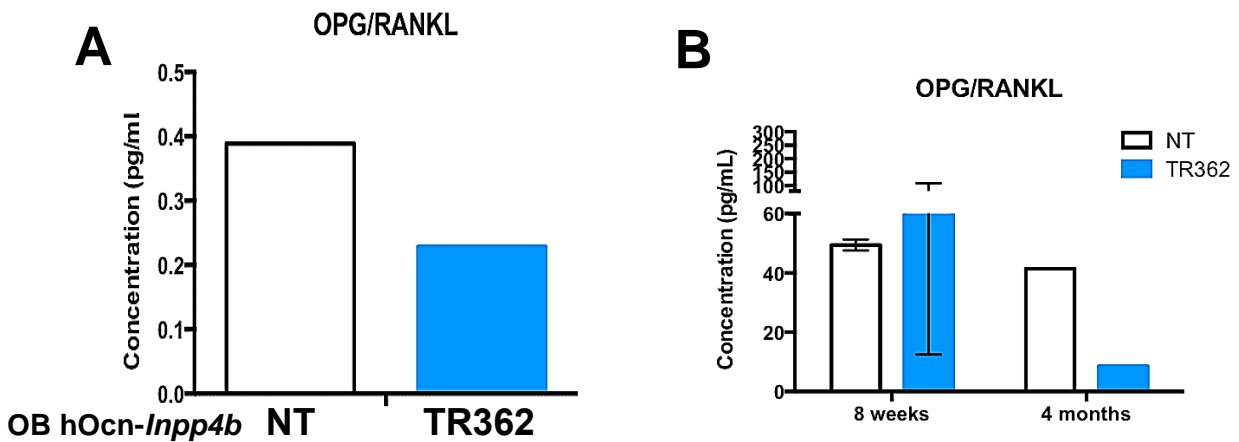


Figure 4.18: Quantification of OPG/RANKL ratio in cell culture media and sera of the TR362 line.

(A) Co-culture cell-conditioned media suggests that *Inpp4b* TR OB inhibit osteoclastogenesis due to a decreased OPG/RANKL ratio. (B) Serum levels from TR362 mice suggest unaffected OPG/RANKL ratio in 8-week-old mice, but decreased ratio in 4-month-old mice.

# CHAPTER 5: DISCUSSION

Bone is a dynamic organ that serves many important functions, namely, it provides mechanical support for various tissues and organs, acts as “levers” for muscle action, protects the central nervous system, maintains homeostatic ion concentrations, and supports hematopoiesis, to name a few (Rodan, 1998). To achieve this diverse set of roles, bone itself must constantly undergo a process of remodelling, during which old bone is destroyed and new bone is formed. Bone destruction, otherwise known as resorption, and formation are processes that are mediated by two bone cell types, called osteoclasts and osteoblasts, respectively (Hadjidakis & Androulakis, 2006; Rodan, 1998). Therefore, a balance in bone resorption and bone formation must be maintained from early development and throughout life; without it, metabolic bone diseases such as osteoporosis and osteopetrosis can arise. The continued understanding of these disruptions may provide further insight into potential therapeutic targets.

In many cases, metabolic bone diseases like osteoporosis and osteopetrosis result from an imbalance of cellular activities of either, or both, osteoclasts and osteoblasts. Osteoporosis is a metabolic bone disease wherein an impairment in these functions can result in an overall reduction in bone mass. In turn, osteoporotic individuals are at an even higher risk of developing bone fractures relative to the progressive bone loss associated with increasing age (Bernabei *et al.*, 2014). Conversely, osteopetrosis can arise from either non-functional or absent/non-differentiated osteoclasts, thereby leading to dense, but brittle bones (Sobacchi *et al.*, 2013). The symptoms of osteopetrosis can range from relatively benign (adult onset) to severe/lethal (malignant infantile).

Our lab is primarily interested in the murine model of autosomal recessive osteopetrosis (ARO), which is the result of a mutation in the *Ostm1* gene. ARO patients with mutations in *OSTM1* present non-functional osteoclasts, resulting in an increased bone mineral density (BMD) and absent bone marrow space. Moreover, ARO patients also present with impaired hematopoiesis and severe neurological defects. For these reasons, *OSTM1*-associated ARO is severe and lethal, which results in premature death.

To elucidate the molecular mechanism and pathology of the *Ostm1* mutation, our lab characterized the murine model of ARO, otherwise known as the grey-lethal (*gl*) mouse. The diseased phenotype of these mice closely resembles that of humans and therefore provides the opportunity to identify novel effectors of bone homeostasis. A differential display expression screen was therefore conducted on *gl/gl* mice, which revealed a significant down-regulation of the Inositol-polyphosphate-4-phosphatase type II (*Inpp4b*) gene transcript in these *Ostm1*-deficient mice (Ferron *et al.*, 2011). Little was known about the role of *Inpp4b*, a member of the PI3K signalling pathway, in bone physiology at the time, thus prompting further studies into this lipid phosphatase.

The lipid phosphatase, *Inpp4b*, is a member of the PI3K signalling pathway and therefore regulates phosphoinositide lipid metabolism. Modulation of intracellular lipids by members of the PI3K signalling pathway can affect a variety of biological functions, including cell growth and trafficking (Vanhaesebroeck *et al.*, 2012). Other phosphatases implicated in the PI3K signalling pathway have previously been shown to exert bone-specific effects *in vivo*. More specifically, *Pten*-deficient osteoblasts displayed enhanced

and prolonged bone accumulation compared to controls via FGF stimulation (Guntur *et al.*, 2011; Liu *et al.*, 2007). Conversely, *Ship*-deficient mice display an osteoporotic phenotype due to the hyperactivation of osteoclasts (Takeshita *et al.*, 2002). Given these previously reported findings, we became interested in studying *Inpp4b* as, at the time, very little was known about the role of this lipid phosphatase in bone homeostasis. Using a combination of *in vitro*, *ex vivo*, and *in vivo* studies of full knock-out mice, we identified *Inpp4b* as a novel prognostic locus for osteoporosis (Ferron *et al.*, 2011; Ferron & Vacher, 2006).

A systemic deletion of *Inpp4b* in mice revealed its role as a negative regulator of osteoclastogenesis. Importantly, these mice displayed an increase in the number and size of mature osteoclasts, as well as an increase in their resorptive activity. Furthermore, micro-computed tomography (micro CT) revealed that these *Inpp4b*-null mice exhibited decreased bone mass compared to wild-type controls. To explain these findings, *in vitro* studies on RAW clones overexpressing either phosphatase-inactive or wild-type *Inpp4b* were conducted (Ferron *et al.*, 2011). Importantly, our lab determined that the increased osteoclastogenesis was due to NFATc1 auto-amplification in osteoclasts. Interestingly, *Inpp4b*<sup>-/-</sup> mice also exhibited an increased osteoblast population, which was coupled with an increased mineral apposition rate *in vivo* and mineralization potential *ex vivo*. As mineralization is a function of the mature osteoblast (Dallas & Bonewald, 2010; Wang *et al.*, 2006), we hypothesized that *Inpp4b* could exert a cell-autonomous function in the mature osteoblast, which in turn could contribute to our understanding of bone homeostasis.

Considering these previously reported findings, the goal of this thesis was to determine the role of *Inpp4b* in osteoblast physiology. To accomplish this, we used complementary conditional knock-out and transgenic mice to specifically delete or overexpress *Inpp4b* in the mature osteoblast, respectively. To do so, we used the human osteocalcin promoter (hOcn), which is expressed only at the mature stage of osteoblast differentiation.

### **5.1 *Inpp4b* modulates osteoblast mineral formation *ex vivo***

The hOcn promoter is a previously reported promoter that directs bone-specific expression at the mature osteoblast stage (Clemens *et al.*, 1997; Frenkel *et al.*, 1997; Zhang *et al.*, 2002). Knowing this, we generated a conditional knock-out mouse model wherein exon 11 of *Inpp4b* was specifically deleted by crossing the previously generated *Inpp4b*<sup>lox/lox</sup> mice with mice expressing Cre recombinase under the control of the human osteocalcin promoter (hOcn-Cre) to produce *Inpp4b*<sup>lox/lox</sup>;hOcn-Cre mice (Ferron *et al.*, 2011). Additionally, we used a complementary transgenic approach wherein the *Inpp4b* transgene was under the control of the hOcn promoter, and thus specifically expressed at the most mature stage of osteoblast differentiation.

For the osteoblast-specific conditional knock-out of *Inpp4b* (*Inpp4b* cKO OB), we utilized calvarial osteoblast cultures to confirm that this deletion was specific to cells of the osteoblast lineage and, more specifically, that the deletion was highest for mature osteoblasts. Quantitative PCR analysis determined that there was approximately 60% reduction in *Inpp4b* gene expression at the last day of cell culture. We also observed a concomitant increase in *Cre* gene expression that increased with maturation time of these

osteoblasts. Endogenous *Ocn* expression increased with time as well. *Ocn* is a mature osteoblast gene that is highly expressed in the most mature osteoblasts. Therefore, this endogenous expression provides support that the specific deletion of *Inpp4b* was highest at the most mature stages of differentiation. More specifically, it demonstrates that the specific loss of *Inpp4b* was highest when *Ocn* was also elevated (and thus occurring in the mature osteoblast). Western blot analyses revealed an overall 70% decrease of *Inpp4b* protein level in the knock-out osteoblasts compared to controls. Importantly, bone marrow-derived osteoclasts appeared unchanged in both number and size when cultured *ex vivo*. *Inpp4b* expression was also unaffected in these osteoclasts. Thus, any observed defects resulted from the *Inpp4b*-deficient osteoblasts.

For the osteoblast-specific overexpression of *Inpp4b* (*Inpp4b* TR OB), we first identified transgenic founder lines, which were analyzed by Southern blot for copy number integration. We also cultured calvarial osteoblasts and analyzed *Inpp4b* gene expression throughout osteoblast differentiation. The transgene displayed increasing expression with time, reaching peak values at day 24 of culture. This overexpression resulted in an approximate 10- to 40-fold increase relative to controls. Despite its low expression, endogenous *Inpp4b* also increased with time, concomitant with the transgene. Furthermore, this expression pattern correlated with endogenous *Ocn* expression as well, demonstrating that overall, *Inpp4b* is expressed in mature osteoblasts. This observed overexpression of the transgene correlated with increasing *Inpp4b* protein expression. As was the case for the *Inpp4b* cKO OB, there was no significant change in osteoclast number or size.

Having confirmed the specificity of both the deletion and overexpression, we next sought to determine whether there were any defects in mineralization, as was observed in the full knock-out (Ferron *et al.*, 2011). To do so, we used a number of classical staining procedures (i.e. alkaline phosphatase, alizarin red, von Kossa, calcein) to quantify the mineralization potential of these osteoblasts *ex vivo*. In the case of the *Inpp4b*-deficient osteoblasts, we observed a significant decrease in mineral formation compared to controls. Conversely, we found comparable or increased mineralization in culture, which was dependent on the level of transgene expression. Interestingly, these results appear to contradict findings from the *Inpp4b* full knock-out. In the case of the *Inpp4b*<sup>-/-</sup>, MAR and von Kossa revealed an increase in the mineralization of these osteoblasts both *in vivo* and *ex vivo*, respectively. These findings, however, may be explained by the fact that in the case of the full knock-out, where *Inpp4b* is expressed at a higher level in osteoclasts than osteoblasts, there is a hyperactivation of osteoclastogenesis via NFATc1 nuclear translocation. Therefore, there are increased numbers and size of osteoclasts, as well as activity; thus, osteoblasts would be required to mineralize more in response. Additionally, *Inpp4b* is absent throughout development in the full knock-out, therefore it may exert its effect at the earlier, proliferative stage of osteoblast differentiation, whereas in the case of this present study, the deletion of *Inpp4b* is specific to the mature osteoblast.

To further explain this mineralization change *ex vivo*, we examined and characterized the gene expression of several osteoblastic marker genes. Quantitative PCR analysis revealed a significant down-regulation of marker genes, including *Runx2* and *Ocn* in the *Inpp4b* cKO OB, suggesting a decrease in the early and late osteoblast populations. In

comparison, the *Inpp4b* TR OB exhibited an increase in these genes, thereby suggesting an increase in these cellular populations. As such, the modulation of mineral formation in culture can be explained by the fact that the specific deletion of *Inpp4b* results in cellular changes of the osteoblast population. Further supporting this, a study on Menin (*Men1*) displayed similar *ex vivo* findings as our present study (Kanazawa *et al.*, 2015). Since *Men1* was known to modulate the TGF- $\beta$ /BMP2 signalling pathway *in vitro*, which is important for osteoblastogenesis, the human osteocalcin promoter was used to specifically delete or overexpress the *Men1* gene and characterize the *in vivo* phenotype. *Men1*-deficient osteoblasts were found to produce less mineralized nodules compared to controls, while the transgenic osteoblasts produced more. This alteration of mineralization was concomitant with changes in key osteoblastic genes. Given the limited data demonstrating a role for lipid phosphatases in osteoblastogenesis, the dephosphorylation of effectors of pathways such as TGF- $\beta$ /BMP2 by phosphatases may modulate intracellular signalling.

## **5.2 Overexpression of *Inpp4b* results in bone mass reduction *in vivo***

*Inpp4b*<sup>-/-</sup> full knock-out mice are osteoporotic, owing to increased osteoclast differentiation and activity. Herein, *in vivo* analyses were performed to assess and determine an osteoblast-specific role for *Inpp4b* on bone physiology. To this end, we analyzed femurs from male *Inpp4b* cKO OB and TR OB mice at two time points: 8 weeks and 4 months. These time points were important as they represent the period during which there is enhanced bone growth (8 weeks) and peak bone mass (4 months).

Femurs from the *Inpp4b* cKO OB mice demonstrated no significant change in bone mass, as assessed by micro CT analysis. Despite no significant difference, there was, however, an increase in the mineral apposition rate (MAR) in these mice at 8 weeks of age, which was coupled with an increase in the number of osteoblasts. For this reason, it's possible that although there are more osteoblasts that are mineralizing faster, each cell is mineralizing less than control cells, in which case this could explain the decreased nodule formation *ex vivo* as well as lack of significant change in overall bone *in vivo*. Indeed, von Kossa staining of vertebral sections reveals no significant change in mineralization, along with no change in osteoclast number or size. We did not assess activity of these osteoclasts, therefore the lack of a bone phenotype may be due, at least in part, to an increased activity of these osteoclasts to balance the increased MAR of the osteoblasts. Alternatively, the osteoclasts may be unaffected, and instead there is insufficient deletion of *Inpp4b* in the mature osteoblast (recall, there is ~60% and ~70% reduction in gene and protein expression, respectively) to cause any defects.

Unlike the *Inpp4b* cKO OB mice, micro CT analysis using femurs of *Inpp4b* TR OB mice demonstrated that the specific overexpression of *Inpp4b* in the mature osteoblast results in reduced bone mass at 4 months of age *in vivo*. Compared to 4-month-old non-transgenic controls, *Inpp4b* TR OB mice exhibited an overall decrease in bone volume-to-tissue volume ratio, trabecular number, and trabecular thickness, which correlates with the level of overexpression (i.e. the highest-expressing line exhibits more dramatic defects than the lowest-expressing line). There was no change in cortical bone volume of the transgenic mice. Moreover, *Inpp4b* TR OB mice also displayed decreased mineral

apposition rate. Considering that the *ex vivo* cultures revealed comparable or increased mineral formation from transgenic osteoblasts, it may be possible that *in vivo*, mineralization is occurring at a slower rate, but with a higher amount of mineralization per osteoblast compared to non-transgenic controls. Again, we did not assess the activity of osteoclasts, but given the higher numbers in the transgenic mice, it is likely that with more mature osteoclasts, more bone resorption is occurring and therefore contributing to the shift towards osteoporosis. The observation of enhanced osteoclast population prompted further studies into the intercellular communication between osteoblasts and osteoclasts.

Although we find opposing effects *ex vivo* and *in vivo*, there are many explanations that can explain these differences. *Ex vivo* studies are powerful tools that can closely mimic physiological *in vivo* processes, however, they are limited in that they are still controlled environments in which we supplement with exogenous factors. Moreover, bone development is a process that involves more than just osteoblasts and osteoclasts. There are, for example, osteocytes which have been found to be the main source of the osteoclast-stimulating factor, RANKL (O'Brien *et al.*, 2013). They have also been shown to inhibit bone formation (Schaffler & Kennedy, 2012) and therefore serve as an important cell in the context of bone homeostasis.

### **5.3 *Inpp4b* modulates osteoblast-osteoclast crosstalk**

Although the osteoblast is mainly involved in the process of mineralization, it has another important role in osteoclastogenesis. This intercellular communication, or crosstalk, between the two bone cell types has been well-characterized and is known to involve

receptor activator of nuclear factor kappa-B ligand (RANKL), receptor activator of nuclear factor kappa-B (RANK), and osteoprotegerin (OPG) (Boyce & Xing, 2007, 2008; Teti, 2012). In short, osteoclasts rely on the interaction of RANKL and RANK, which is the receptor found on osteoclast precursors, to activate osteoclastogenesis. Once committed to the RANKL/RANK signalling pathway, intracellular signalling cascades are activated, which ultimately result in the nuclear translocation of the master regulator of osteoclastogenesis, NFATc1 (Koga *et al.*, 2004). Osteoblast stromal cells are a source of RANKL production, despite also producing the decoy receptor, OPG, which competes with membrane-bound RANK for RANKL. It is therefore the ratio of RANKL and OPG secretion that either favours or inhibits osteoclast differentiation.

Seeing that *Inpp4b* TR OB mice have increased osteoclast numbers, we assessed the capacity for these osteoblasts to induce osteoclastogenesis. Firstly, we utilized a co-culture system wherein bone marrow-derived cells were grown in the presence of calvarial osteoblasts. Our results demonstrate that those cells that overexpress *Inpp4b* appear to enhance osteoclastogenesis, when compared to non-transgenic controls. Gene expression analysis also revealed that this stimulation of osteoclastogenesis was likely due to decreased expression of OPG relative to RANK gene expression. Interestingly, *Inpp4b* cKO OB seemed to stimulate osteoclast differentiation more than controls, despite no significant change in the bone mass nor size or number of osteoclasts *in vivo*. This finding was further supported by observation of increased OPG expression in the conditional knock-out osteoblasts, suggesting therefore that the deletion of *Inpp4b* can stimulate osteoclastogenesis via decreased inhibition.

To further corroborate these findings, we performed ELISA to detect RANKL and OPG secretion in both cell culture media and sera. Although we observed no significant difference in bone mass between *Inpp4b* cKO OB mice and controls, preliminary results suggest that *Inpp4b*-deficient osteoblasts have a reduced capacity to support osteoclastogenesis due to an increased ratio of OPG/RANKL. It is possible that the partial deletion in cKO mice is not enough to elicit a physiological response. Therefore, increased ablation of *Inpp4b* may result in a more dramatic effect on bone mass through changes in the OPG/RANKL ratio.

Interestingly, *Inpp4b* TR OB appeared to stimulate osteoclastogenesis, due to observed decreases in the OPG/RANKL ratio. Furthermore, 4-month-old transgenic mice also expressed decreased OPG/RANKL in serum, supporting findings of the increased TRAP-positive cells observed *in vivo* and overall reduction in bone mass. Taken together, these results suggest that the disrupted communication observed in osteoblasts may affect bone mass in these mice. Increased sample sizes should be performed to confirm these results. Importantly, however, we have provided preliminary evidence to demonstrate a role for *Inpp4b* in modulating the intercellular communication between osteoblasts and osteoclasts.

# CHAPTER 6: CONCLUSIONS

Bone metabolic disorders arise in response to an imbalance of bone formation or bone resorption. Understanding these processes, and the subsequent modulation of either or both activities, is therefore critical for the development of novel therapeutic targets for conditions like osteoporosis. As such, mouse models such as the *Ostm1*-related ARO provide the opportunity to explore novel regulators of bone homeostasis and proper maintenance, as was the case for the lipid phosphatase, *Inpp4b*. The goal of this present study was to determine the effect(s) of *Inpp4b*, in osteoblast physiology.

Although our lab has utilized the full knock-out of *Inpp4b* to demonstrate that it acts as a negative regulator of osteoclastogenesis, it was important to determine whether this phosphatase may also play a role in osteoblastogenesis. The complementary approaches of the specific knock-out and overexpression used in this thesis revealed an osteoblast-specific role for *Inpp4b* in bone homeostasis.

In this study, we demonstrated that the human osteocalcin promoter is efficient in selectively deleting or overexpressing *Inpp4b* in mature osteoblasts. Furthermore, we could show that this alteration of *Inpp4b* expression can affect osteoblasts and their ability to mineralize *ex vivo*. This, however, was not limited solely to mineralization; in fact, we observed significant dysregulation of osteoblast marker genes that demonstrate the capacity for this lipid phosphatase to influence the osteoblast population and differentiation kinetics.

We also demonstrated that the specific overexpression of *Inpp4b* results in mice with reduced bone mass, similar to the *Inpp4b* full knock-out. This osteoporotic phenotype resulted from a decreased rate of mineralization, coupled with enhanced osteoclastogenesis *in vivo*.

Lastly, we observed that this enhanced osteoporosis is a result of the reduced OPG/RANKL ratio, which favours osteoclastogenesis.

Taken together, our present study demonstrates that *Inpp4b* plays a critical role in bone homeostasis through modulation of the mature osteoblast. More specifically, our results show that *Inpp4b* exerts a negative effect *in vivo* on the function of mature osteoblasts. This new insight further demonstrates that members of the PI3K signalling pathway not only modulate osteoclastogenesis, but may also exert effects on other bone cells. Further characterization and understanding of these, and other pathways, can provide opportunities to explore novel therapeutic targets in the treatment of bone diseases.

# CHAPTER 7: PERSPECTIVES

Results from this work demonstrate that lipid phosphatases, and potentially other members of the PI3K signalling pathway, can modulate bone through the osteoblast. There are, however, many future experiments that should be undertaken to determine exactly the mechanism through which these novel bone effectors can alter skeletal development.

Firstly, *Inpp4b* appears to exert a function both on the population of the osteoblasts, as well as the activity of these cells. This, therefore, prompts the need to further characterize these molecular pathways in order to determine which mechanism(s) are responsible.

With regards to the OB population, it would be important to quantify the level of cell proliferation occurring in the osteoblast lineage, in both the cKO and TR models. For example, qPCR analysis of cell cycle genes such as p15, p21, CDK2, and more, could be used to infer the proliferation profile. As such, any dysregulation of the cell cycle and proliferation may support the *in vivo* findings. BrdU incorporation could also be performed to determine the level of cellular proliferation *in vitro*. Furthermore, if changes are detected in the proliferation status of these osteoblasts, it would then be important to also characterize the osteocytes. Osteocytes are terminally-differentiated osteoblasts, which are responsible for controlling bone formation via secretion of proteins such as sclerostin, PHEX, and others (Winkler *et al.*, 2003). As such, their relative abundance may account for the bone mass phenotype (or lack thereof) and provide further evidence to suggest that *Inpp4b* is regulating the proliferation and/or differentiation from osteoblast to osteocyte. The characterization of the osteocyte population can be accomplished via

toluidine blue staining and the evaluation of osteocytic proteins can be conducted via qPCR and Western blotting. Importantly, assessment of the level of apoptosis occurring should also be conducted. As the *Inpp4b* transgenic mice exhibit decreased bone mass, it would be important to determine whether this is due to increased cell death of the osteoblast, or increased differentiation from osteoblast to osteocyte. This could be accomplished through either TUNEL staining on vertebral sections or by cleaved caspase 3 protein levels. These findings could provide evidence for a role of the lipid phosphatase *Inpp4b* in the regulation of cell death and/or survival, as is the case for other PI3K members, like *Pten* (Figure 5.1A) wherein a knock-out of this phosphatase resulted in accumulation of the pro-survival signal, *Akt* (Figure 5.1B, C).

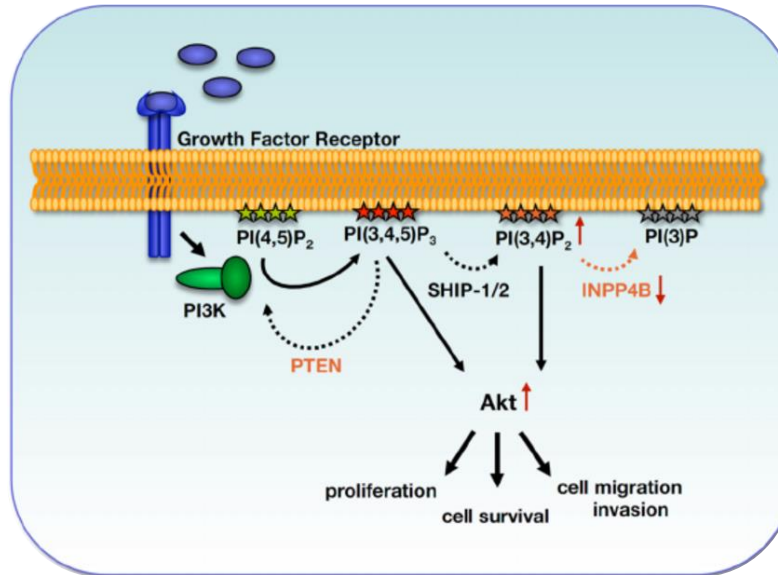
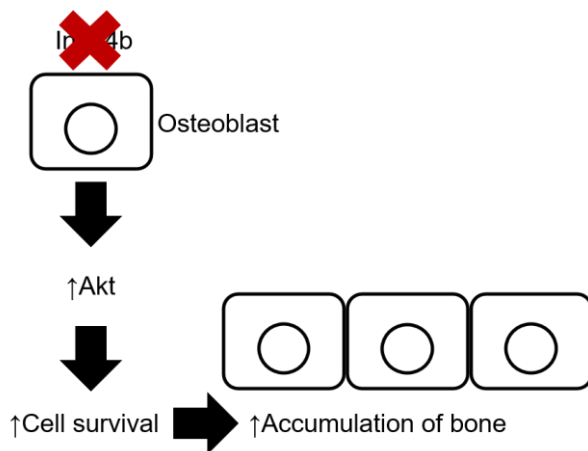
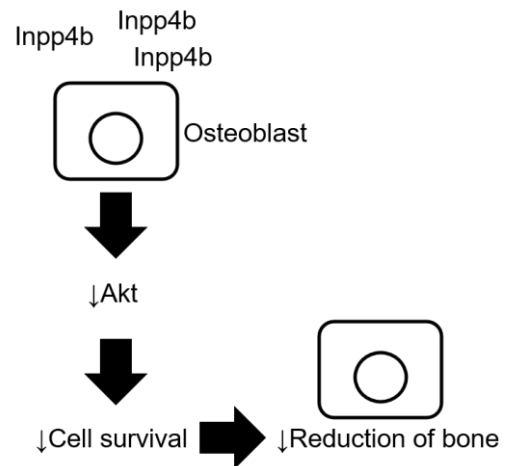
**A****B****C**

Figure 5.1: Potential mechanism of *Inpp4b* in Akt-mediated cell survival.

(A) INPP4B acts as a tumour suppressor to inhibit PI3K signalling. (Reprinted from Cancer Cell, Volume 16, Gewinner *et al.*, Evidence that Inositol Polyphosphate 4-Phosphatase Type II Is a Tumor Suppressor that Inhibits PI3K Signaling, Page 14, Copyright (2009), with permission from Elsevier) (B) In the absence of INPP4B, there is an accumulation of AKT, leading to an increase in cell survival signals in osteoblasts. (C) In the presence of excess INPP4B, there is a decrease in AKT, leading to a reduction in cell survival signals in osteoblasts.

To further elucidate the role of *Inpp4b*, it would be important to examine the pathways through which it can modulate osteoblastogenesis. Previous studies in our lab have revealed that *Inpp4b* can modulate osteoclastogenesis via the NFATc1 signalling pathway (Ferron *et al.*, 2011). Interestingly, this pathway has also been implicated in osteoblastogenesis, as well as the coupling of bone formation and bone resorption (Winslow *et al.*, 2006). It would therefore be interesting to determine whether the conditional ablation or overexpression of *Inpp4b* controls NFATc1 nuclear translocation in the osteoblast. To do so, nuclear and cytosolic protein extracts can be isolated and analyzed by Western blot.

Given the fact that the defect seen in the full knock-out was related to the mineralization potential of the osteoblasts, which is a function of the mature osteoblast, it would be worthwhile to use earlier conditional knock-out and transgenic mouse models to determine whether this change in mineralization resulted from impaired osteoblast function or decreased proliferation. For this reason, use of the previously characterized *Prx1*-Cre (for mesenchymal stem cells) and *Osx*-Cre (for pre-osteoblasts) mouse models could be used to accomplish this aim.

In summary, this thesis presents a novel role for *Inpp4b* in regulating osteoblastogenesis. Herein, we have utilized a conditional knock-out and a transgenic mouse model to demonstrate that this gene can exert a cell-autonomous role *in vivo*. Although there is future work to be done on the exact mechanism and/or pathway through which *Inpp4b* is

acting, this work may yield promising avenues in the development of pharmacological intervention.

# APPENDIX 1



La formation et la recherche *la vie*

Comité de protection des animaux  
Animal Care Committee

February 16<sup>th</sup> 2015

Dr. Jean Vacher  
Cellular Interactions and development

**Subject: Protocol 2015-04 entitled "Characterization of the role of Inpp4 in Bone Physiology"**

Dear Colleague,

I'm pleased to inform you that the above mentioned protocol submitted to the Animal Care Committee has been formally approved. Please take note that this protocol is valid from February 16<sup>th</sup> 2015 to September 30<sup>th</sup> 2017.

I would like to remind you to label animal cages with the appropriate approved protocol number related to your project and to clearly indicate the protocol number in your purchase order of animals.

Best regards,

A handwritten signature in blue ink, appearing to read 'J. Di Noia', is written over a horizontal line.

Dr. Javier Di Noia  
Chair

Affilié à l'Université de Montréal

110 avenue des Pins Ouest, Montréal (Québec) Canada H2W 1R7

<http://intranet.ircmq.ca>

# BIBLIOGRAPHY

- Addison, W. N., Azari, F., Sørensen, E. S., Kaartinen, M. T., & McKee, M. D. (2007). Pyrophosphate Inhibits Mineralization of Osteoblast Cultures by Binding to Mineral, Up-regulating Osteopontin, and Inhibiting Alkaline Phosphatase Activity. *Journal of Biological Chemistry*, 282(21), 15872-15883.
- Agoulnik, I. U., Hodgson, M. C., Bowden, W. A., & Ittmann, M. M. (2011). INPP4B: the New Kid on the PI3K Block. *Oncotarget*, 2(4), 321-328.
- Arnett, T. (2007). Regulation of bone cell function by acid–base balance. *Proceedings of the Nutrition Society*, 62(2), 511-520. doi:10.1079/PNS2003268
- Banerjee, C., Stein, J. L., Van Wijnen, A. J., Frenkel, B., Lian, J. B., & Stein, G. S. (1996). Transforming growth factor-beta 1 responsiveness of the rat osteocalcin gene is mediated by an activator protein-1 binding site. *Endocrinology*, 137(5), 1991-2000. doi:10.1210/endo.137.5.8612540
- Bernabei, R., Martone, A. M., Ortolani, E., Landi, F., & Marzetti, E. (2014). Screening, diagnosis and treatment of osteoporosis: a brief review. *Clinical Cases in Mineral and Bone Metabolism*, 11(3), 201-207.
- Bestebroer, J., V'Kovski, P., Mauthe, M., & Reggiori, F. (2013). Hidden Behind Autophagy: The Unconventional Roles of ATG Proteins. *Traffic*, 14(10), 1029-1041. doi:10.1111/tra.12091
- Bollerslev, J., & Andersen, P. E. (1988). Radiological, biochemical and hereditary evidence of two types of autosomal dominant osteopetrosis. *Bone*, 9. doi:10.1016/8756-3282(88)90021-x
- Boskey, A. L. (2013). Bone composition: relationship to bone fragility and antiosteoporotic drug effects. *BoneKEy Rep*, 2. doi:10.1038/bonekey.2013.181
- Bougeard, G., Renaux-Petel, M., Flaman, J.-M., Charbonnier, C., Fermey, P., Belotti, M., . . . Frebourg, T. (2015). Revisiting Li-Fraumeni Syndrome From TP53 Mutation Carriers. *Journal of Clinical Oncology*, 33(21), 2345-2352. doi:10.1200/JCO.2014.59.5728
- Boyce, B. F., & Xing, L. (2007). Biology of RANK, RANKL, and osteoprotegerin. *Arthritis Research & Therapy*, 9(Suppl 1), S1-S1. doi:10.1186/ar2165
- Boyce, B. F., & Xing, L. (2008). Functions of RANKL/RANK/OPG in bone modeling and remodeling. *Archives of biochemistry and biophysics*, 473(2), 139-146. doi:10.1016/j.abb.2008.03.018
- Boyle, W. J., Simonet, W. S., & Lacey, D. L. (2003). Osteoclast differentiation and activation. *Nature*, 423(6937), 337-342.
- Cantley, L. C. (2002). The phosphoinositide 3-kinase pathway. *Science*, 296(5573), 1655-1657. doi:10.1126/science.296.5573.1655
- Chalhoub, N., Benachenhou, N., Rajapurohitam, V., Pata, M., Ferron, M., Frattini, A., . . . Vacher, J. (2003). Grey-lethal mutation induces severe malignant autosomal recessive osteopetrosis in mouse and human. *Nat Med*, 9(4), 399-406.
- Chen, G., Deng, C., & Li, Y.-P. (2012). TGF- $\beta$  and BMP Signaling in Osteoblast Differentiation and Bone Formation. *International Journal of Biological Sciences*, 8(2), 272-288. doi:10.7150/ijbs.2929
- Choi, Y., Arron, J. R., & Townsend, M. J. (2009). Promising bone-related therapeutic targets for rheumatoid arthritis. *Nat Rev Rheumatol*, 5(10), 543-548.
- Chung, K.-Y., Agarwal, A., Uitto, J., & Mauviel, A. (1996). An AP-1 Binding Sequence Is Essential for Regulation of the Human 2(I) Collagen (COL1A2) Promoter Activity by Transforming Growth Factor. *Journal of Biological Chemistry*, 271(6), 3272-3278.

- Clarke, B. (2008). Normal Bone Anatomy and Physiology. *Clinical Journal of the American Society of Nephrology : CJASN*, 3(Suppl 3), S131-S139. doi:10.2215/CJN.04151206
- Clemens, T. L., Tang, H., Maeda, S., Kesterson, R. A., Demayo, F., Pike, J. W., & Gundberg, C. M. (1997). Analysis of Osteocalcin Expression in Transgenic Mice Reveals a Species Difference in Vitamin D Regulation of Mouse and Human Osteocalcin Genes. *Journal of Bone and Mineral Research*, 12(10), 1570-1576. doi:10.1359/jbmr.1997.12.10.1570
- Cuetara, B. L. V., Crotti, T. N., O'Donoghue, A. J., & McHugh, K. P. (2006). CLONING AND CHARACTERIZATION OF OSTEOCLAST PRECURSORS FROM THE RAW264.7 CELL LINE. *In vitro cellular & developmental biology. Animal*, 42(7), 182-188. doi:10.1290/0510075.1
- Dallas, S. L., & Bonewald, L. F. (2010). Dynamics of the Transition from Osteoblast to Osteocyte. *Annals of the New York Academy of Sciences*, 1192, 437-443. doi:10.1111/j.1749-6632.2009.05246.x
- Datta, S. R., Dudek, H., Tao, X., Masters, S., Fu, H., Gotoh, Y., & Greenberg, M. E. (1997). Akt Phosphorylation of BAD Couples Survival Signals to the Cell-Intrinsic Death Machinery. *Cell*, 91(2), 231-241. doi:[http://dx.doi.org/10.1016/S0092-8674\(00\)80405-5](http://dx.doi.org/10.1016/S0092-8674(00)80405-5)
- Day, T. F., Guo, X., Garrett-Beal, L., & Yang, Y. (2005). Wnt/ $\beta$ -Catenin Signaling in Mesenchymal Progenitors Controls Osteoblast and Chondrocyte Differentiation during Vertebrate Skeletogenesis. *Developmental Cell*, 8(5), 739-750. doi:<https://doi.org/10.1016/j.devcel.2005.03.016>
- Denhardt, D. T., & Noda, M. (1998). Osteopontin expression and function: Role in bone remodeling. *Journal of Cellular Biochemistry*, 72(S30-31), 92-102. doi:10.1002/(SICI)1097-4644(1998)72:30/31+<92::AID-JCB13>3.0.CO;2-A
- Dougall, W. C., Glaccum, M., Charrier, K., Rohrbach, K., Brasel, K., De Smedt, T., . . . Schuh, J. (1999). RANK is essential for osteoclast and lymph node development. *Genes & Development*, 13(18), 2412-2424.
- Ducy, P., Desbois, C., Boyce, B., Pinero, G., Story, B., Dunstan, C., . . . Karsenty, G. (1996). Increased bone formation in osteocalcin-deficient mice. *Nature*, 382(6590), 448-452.
- Ducy, P., Zhang, R., Geoffroy, V., Ridall, A. L., & Karsenty, G. (1997). Osf2/Cbfa1: A Transcriptional Activator of Osteoblast Differentiation. *Cell*, 89(5), 747-754. doi:[https://doi.org/10.1016/S0092-8674\(00\)80257-3](https://doi.org/10.1016/S0092-8674(00)80257-3)
- Dünker, N., & Krieglstein, K. (2002). Tgf $\beta$ 2  $-/-$  Tgf $\beta$ 3  $-/-$  double knockout mice display severe midline fusion defects and early embryonic lethality. *Anatomy and Embryology*, 206(1), 73-83. doi:10.1007/s00429-002-0273-6
- Durfee, R. A., Mohammed, M., & Luu, H. H. (2016). Review of Osteosarcoma and Current Management. *Rheumatology and Therapy*, 3(2), 221-243. doi:10.1007/s40744-016-0046-y
- Ferron, M., Boudiffa, M., Arsenault, M., Rached, M., Pata, M., Giroux, S., . . . Vacher, J. (2011). Inositol Polyphosphate 4-Phosphatase B as A Regulator of Bone Mass in Mice and Human. *Cell metabolism*, 14(4), 466-477. doi:10.1016/j.cmet.2011.08.013
- Ferron, M., & Lacombe, J. (2014). Regulation of energy metabolism by the skeleton: Osteocalcin and beyond. *Archives of biochemistry and biophysics*, 561, 137-146. doi:<http://dx.doi.org/10.1016/j.abb.2014.05.022>
- Ferron, M., & Vacher, J. (2006). Characterization of the murine Inpp4b gene and identification of a novel isoform. *Gene*, 376(1), 152-161. doi:<http://dx.doi.org/10.1016/j.gene.2006.02.022>
- Florencio-Silva, R., Sasso, G. R. d. S., Sasso-Cerri, E., Simões, M. J., & Cerri, P. S. (2015). Biology of Bone Tissue: Structure, Function, and Factors That Influence Bone Cells. *BioMed Research International*, 2015, 421746. doi:10.1155/2015/421746
- Frenkel, B., Capparelli, C., van Auken, M., Baran, D., Bryan, J., Stein, J. L., . . . Lian, J. B. (1997). Activity of the Osteocalcin Promoter in Skeletal Sites of Transgenic Mice and

- during Osteoblast Differentiation in Bone Marrow-Derived Stromal Cell Cultures: Effects of Age and Sex\*. *Endocrinology*, 138(5), 2109-2116. doi:10.1210/endo.138.5.5105
- Gambacciani, M., & Levancini, M. (2014). Hormone replacement therapy and the prevention of postmenopausal osteoporosis. *Przegląd Menopauzalny = Menopause Review*, 13(4), 213-220. doi:10.5114/pm.2014.44996
- Gewinner, C., C Wang, Z., Richardson, A., Teruya-Feldstein, J., Etemadmoghadam, D., Bowtell, D., . . . Cantley, L. (2009). Evidence that Inositol Polyphosphate 4-Phosphatase Type II Is a Tumor Suppressor that Inhibits PI3K Signaling (Vol. 16)
- Gilbert, S. F. (2000). Osteogenesis: The Development of Bones. *Developmental biology*. doi:<https://www.ncbi.nlm.nih.gov/books/NBK10056/>
- Glass li, D. A., Bialek, P., Ahn, J. D., Starbuck, M., Patel, M. S., Clevers, H., . . . Karsenty, G. (2005). Canonical Wnt Signaling in Differentiated Osteoblasts Controls Osteoclast Differentiation. *Developmental Cell*, 8(5), 751-764. doi:<https://doi.org/10.1016/j.devcel.2005.02.017>
- Golub, E. E. (2009). Role of Matrix Vesicles in Biomineralization. *Biochimica et biophysica acta*, 1790(12), 1592-1598. doi:10.1016/j.bbagen.2009.09.006
- Gordon, K. J., & Blobe, G. C. (2008). Role of transforming growth factor- $\beta$  superfamily signaling pathways in human disease. *Biochimica et Biophysica Acta (BBA) - Molecular Basis of Disease*, 1782(4), 197-228. doi:<https://doi.org/10.1016/j.bbadis.2008.01.006>
- Guntur, A. R., Reinhold, M. I., Cuellar, J., & Naski, M. C. (2011). Conditional ablation of Pten in osteoprogenitors stimulates FGF signaling. *Development (Cambridge, England)*, 138(7), 1433-1444. doi:10.1242/dev.058016
- Hadjidakis, D. J., & Androulakis, I. I. (2006). Bone Remodeling. *Annals of the New York Academy of Sciences*, 1092(1), 385-396. doi:10.1196/annals.1365.035
- Harada, S.-i., & Rodan, G. A. (2003). Control of osteoblast function and regulation of bone mass. *Nature*, 423(6937), 349-355.
- Hauschka, P. V., Lian, J. B., Cole, D. E., & Gundberg, C. M. (1989). Osteocalcin and matrix Gla protein: vitamin K-dependent proteins in bone. *Physiological Reviews*, 69(3), 990-1047.
- Hazen, A. L., Smith, M. J., Desponts, C., Winter, O., Moser, K., & Kerr, W. G. (2009). SHIP is required for a functional hematopoietic stem cell niche. *Blood*, 113(13), 2924-2933. doi:10.1182/blood-2008-02-138008
- Hoang, Q. Q., Sicheri, F., Howard, A. J., & Yang, D. S. C. (2003). Bone recognition mechanism of porcine osteocalcin from crystal structure. *Nature*, 425(6961), 977-980. doi:[http://www.nature.com/nature/journal/v425/n6961/supinfo/nature02079\\_S1.html](http://www.nature.com/nature/journal/v425/n6961/supinfo/nature02079_S1.html)
- Hocking, L. J., Whitehouse, C., & Helfrich, M. H. (2012). Autophagy: A new player in skeletal maintenance? *Journal of Bone and Mineral Research*, 27(7), 1439-1447. doi:10.1002/jbmr.1668
- Hodgson, M. C., Shao, L.-j., Frolov, A., Li, R., Peterson, L. E., Ayala, G., . . . Agoulnik, I. U. (2011). Decreased Expression and Androgen Regulation of the Tumor Suppressor Gene INPP4B in Prostate Cancer. *Cancer research*, 71(2), 572-582. doi:10.1158/0008-5472.CAN-10-2314
- Hu, H., Hilton, M. J., Tu, X., Yu, K., Ornitz, D. M., & Long, F. (2005). Sequential roles of Hedgehog and Wnt signaling in osteoblast development. *Development*, 132(1), 49-60. doi:10.1242/dev.01564
- Huang, Z., Ren, P.-G., Ma, T., Smith, R. L., & Goodman, S. B. (2010). Modulating osteogenesis of mesenchymal stem cells by modifying growth factor availability. *Cytokine*, 51(3), 305-310. doi:<https://doi.org/10.1016/j.cyto.2010.06.002>
- Iwata, J.-i., Hosokawa, R., Sanchez-Lara, P. A., Urata, M., Slavkin, H., & Chai, Y. (2010). Transforming Growth Factor- $\beta$  Regulates Basal Transcriptional Regulatory Machinery to Control Cell Proliferation and Differentiation in Cranial Neural Crest-derived Osteoprogenitor Cells. *Journal of Biological Chemistry*, 285(7), 4975-4982.

- Kanazawa, I., Canaff, L., Abi Rafeh, J., Angrula, A., Li, J., Riddle, R. C., . . . Hendy, G. N. (2015). Osteoblast Menin Regulates Bone Mass in Vivo. *The Journal of Biological Chemistry*, 290(7), 3910-3924. doi:10.1074/jbc.M114.629899
- Kapinas, K., & Delany, A. M. (2011). MicroRNA biogenesis and regulation of bone remodeling. *Arthritis Research & Therapy*, 13(3), 220-220. doi:10.1186/ar3325
- Kappel, C. C., Velez-Yanguas, M. C., Hirschfeld, S., & Helman, L. J. (1994). Human Osteosarcoma Cell Lines Are Dependent on Insulin-like Growth Factor I for &em&gt;in Vitro&em&gt; Growth. *Cancer research*, 54(10), 2803.
- Kavsak, P., Rasmussen, R. K., Causing, C. G., Bonni, S., Zhu, H., Thomsen, G. H., & Wrana, J. L. (2000). Smad7 Binds to Smurf2 to Form an E3 Ubiquitin Ligase that Targets the TGF $\beta$  Receptor for Degradation. *Molecular Cell*, 6(6), 1365-1375. doi:[https://doi.org/10.1016/S1097-2765\(00\)00134-9](https://doi.org/10.1016/S1097-2765(00)00134-9)
- Kawamura, N., Kugimiya, F., Oshima, Y., Ohba, S., Ikeda, T., Saito, T., . . . Kawaguchi, H. (2007). Akt1 in Osteoblasts and Osteoclasts Controls Bone Remodeling. *PLoS ONE*, 2(10), e1058. doi:10.1371/journal.pone.0001058
- Kennel, K. A., & Drake, M. T. (2009). Adverse Effects of Bisphosphonates: Implications for Osteoporosis Management. *Mayo Clinic Proceedings*, 84(7), 632-638.
- Kesterson, R. A., Stanley, L., DeMayo, F., Finegold, M., & Pike, J. W. (1993). The human osteocalcin promoter directs bone-specific vitamin D-regulatable gene expression in transgenic mice. *Molecular Endocrinology*, 7(3), 462-467. doi:10.1210/mend.7.3.8483481
- Koga, T., Inui, M., Inoue, K., Kim, S., Suematsu, A., Kobayashi, E., . . . Takai, T. (2004). Costimulatory signals mediated by the ITAM motif cooperate with RANKL for bone homeostasis. *Nature*, 428(6984), 758-763. doi:[http://www.nature.com/nature/journal/v428/n6984/supinfo/nature02444\\_S1.html](http://www.nature.com/nature/journal/v428/n6984/supinfo/nature02444_S1.html)
- Komori, T. (2006). Regulation of osteoblast differentiation by transcription factors. *Journal of Cellular Biochemistry*, 99(5), 1233-1239. doi:10.1002/jcb.20958
- Komori, T., Yagi, H., Nomura, S., Yamaguchi, A., Sasaki, K., Deguchi, K., . . . Kishimoto, T. (1997). Targeted Disruption of Cbfa1 Results in a Complete Lack of Bone Formation owing to Maturational Arrest of Osteoblasts. *Cell*, 89(5), 755-764. doi:[https://doi.org/10.1016/S0092-8674\(00\)80258-5](https://doi.org/10.1016/S0092-8674(00)80258-5)
- Lacombe, J., & Ferron, M. (2015). Gamma-carboxylation regulates osteocalcin function. *Oncotarget*, 6(24), 19924-19925.
- Lacombe, J., Karsenty, G., & Ferron, M. (2013). In vivo analysis of the contribution of bone resorption to the control of glucose metabolism in mice(). *Molecular Metabolism*, 2(4), 498-504. doi:10.1016/j.molmet.2013.08.004
- Lamplot, J. D., Denduluri, S., Qin, J., Li, R., Liu, X., Zhang, H., . . . Luu, H. H. (2013). The Current and Future Therapies for Human Osteosarcoma. *Current cancer therapy reviews*, 9(1), 55-77. doi:10.2174/1573394711309010006
- Langdahl, B., Ferrari, S., & Dempster, D. W. (2016). Bone modeling and remodeling: potential as therapeutic targets for the treatment of osteoporosis. *Therapeutic Advances in Musculoskeletal Disease*, 8(6), 225-235. doi:10.1177/1759720X16670154
- Laurin, N., Brown, J. P., Morissette, J., & Raymond, V. (2002). Recurrent Mutation of the Gene Encoding sequestosome 1 (SQSTM1/p62) in Paget Disease of Bone. *American Journal of Human Genetics*, 70(6), 1582-1588.
- Lee, N. K., Sowa, H., Hinoi, E., Ferron, M., Ahn, J. D., Confavreux, C., . . . Karsenty, G. (2007). Endocrine regulation of energy metabolism by the skeleton. *Cell*, 130(3), 456-469. doi:10.1016/j.cell.2007.05.047
- Liang, J., Zubovitz, J., Petrocelli, T., Kotchetkov, R., Connor, M. K., Han, K., . . . Slingerland, J. M. (2002). PKB/Akt phosphorylates p27, impairs nuclear import of p27 and opposes

- p27-mediated G1 arrest. *Nat Med*, 8(10), 1153-1160.  
doi:[http://www.nature.com/nm/journal/v8/n10/suppinfo/nm761\\_S1.html](http://www.nature.com/nm/journal/v8/n10/suppinfo/nm761_S1.html)
- Liu, W., Toyosawa, S., Furuichi, T., Kanatani, N., Yoshida, C., Liu, Y., . . . Komori, T. (2001). Overexpression of Cbfa1 in osteoblasts inhibits osteoblast maturation and causes osteopenia with multiple fractures. *The Journal of Cell Biology*, 155(1), 157.
- Liu, X., Bruxvoort, K. J., Zylstra, C. R., Liu, J., Cichowski, R., Faugere, M.-C., . . . Clemens, T. L. (2007). Lifelong accumulation of bone in mice lacking Pten in osteoblasts. *Proceedings of the National Academy of Sciences of the United States of America*, 104(7), 2259-2264. doi:10.1073/pnas.0604153104
- Liu, Y., Cheney, M. D., Gaudet, J. J., Chruszcz, M., Lukasik, S. M., Sugiyama, D., . . . Bushweller, J. H. (2006). The tetramer structure of the Nervy homology two domain, NHR2, is critical for AML1/ETO's activity. *Cancer Cell*, 9(4), 249-260.  
doi:<https://doi.org/10.1016/j.ccr.2006.03.012>
- Lo Iacono, N., Blair, H. C., Poliani, P. L., Marrella, V., Ficara, F., Cassani, B., . . . Sobacchi, C. (2012). Osteopetrosis rescue upon RANKL administration to Rankl<sup>-/-</sup> mice: A new therapy for human RANKL-dependent ARO. *Journal of Bone and Mineral Research*, 27(12), 2501-2510. doi:10.1002/jbmr.1712
- Loots, G. G., Kneissel, M., Keller, H., Baptist, M., Chang, J., Collette, N. M., . . . Rubin, E. M. (2005). Genomic deletion of a long-range bone enhancer misregulates sclerostin in Van Buchem disease. *Genome Research*, 15(7), 928-935. doi:10.1101/gr.3437105
- Ma, K., Cheung, S. M., Marshall, A. J., & Duronio, V. (2008). PI(3,4,5)P3 and PI(3,4)P2 levels correlate with PKB/akt phosphorylation at Thr308 and Ser473, respectively; PI(3,4)P2 levels determine PKB activity. *Cellular Signalling*, 20(4), 684-694.  
doi:<http://dx.doi.org/10.1016/j.cellsig.2007.12.004>
- Mackie, E. J., Ahmed, Y. A., Tatarczuch, L., Chen, K. S., & Mirams, M. (2008). Endochondral ossification: How cartilage is converted into bone in the developing skeleton. *The International Journal of Biochemistry & Cell Biology*, 40(1), 46-62.  
doi:<https://doi.org/10.1016/j.biocel.2007.06.009>
- Maranda, B., Chabot, G., Decarie, J. C., Pata, M., Azeddine, B., Moreau, A., & Vacher, J. (2008). Clinical and cellular manifestations of OSTM1-related infantile osteopetrosis. *J Bone Miner Res*, 23. doi:10.1359/jbmr.071015
- Mason, D. J., Suva, L. J., Genever, P. G., Patton, A. J., Steuckle, S., Hillam, R. A., & Skerry, T. M. (1997). Mechanically regulated expression of a neural glutamate transporter in bone: A role for excitatory amino acids as osteotropic agents? *Bone*, 20(3), 199-205.  
doi:[http://dx.doi.org/10.1016/S8756-3282\(96\)00386-9](http://dx.doi.org/10.1016/S8756-3282(96)00386-9)
- Matsunobu, T., Torigoe, K., Ishikawa, M., de Vega, S., Kulkarni, A. B., Iwamoto, Y., & Yamada, Y. (2009). Critical roles of the TGF- $\beta$  type I receptor ALK5 in perichondrial formation and function, cartilage integrity, and osteoblast differentiation during growth plate development. *Developmental biology*, 332(2), 325-338. doi:10.1016/j.ydbio.2009.06.002
- McAllister, T. N., & Frangos, J. A. (1999). Steady and Transient Fluid Shear Stress Stimulate NO Release in Osteoblasts Through Distinct Biochemical Pathways. *Journal of Bone and Mineral Research*, 14(6), 930-936. doi:10.1359/jbmr.1999.14.6.930
- McGonnell, I., Grigoriadis, A., Lam, E., Price, J., & Sunter, A. (2012). A specific role for phosphoinositide 3-kinase and AKT in osteoblasts? *Frontiers in Endocrinology*, 3, 88.
- McKercher, S. R., Torbett, B. E., Anderson, K. L., Henkel, G. W., Vestal, D. J., Baribault, H., . . . Maki, R. A. (1996). Targeted disruption of the PU.1 gene results in multiple hematopoietic abnormalities. *The EMBO Journal*, 15(20), 5647-5658.
- Mirabello, L., Troisi, R. J., & Savage, S. A. (2009). Osteosarcoma incidence and survival rates from 1973 to 2004: Data from the Surveillance, Epidemiology, and End Results Program. *Cancer*, 115(7), 1531-1543. doi:10.1002/cncr.24121

- Miron, R., & Zhang, Y. (2012). *Osteoinduction: A Review of Old Concepts with New Standards* (Vol. 91).
- Miyamoto, T., & Suda, T. (2003). Differentiation and function of osteoclasts. *The Keio Journal of Medicine*, 52(1), 1-7. doi:10.2302/kjm.52.1
- Miyazaki, T., Sanjay, A., Neff, L., Tanaka, S., Horne, W. C., & Baron, R. (2004). Src Kinase Activity Is Essential for Osteoclast Function. *Journal of Biological Chemistry*, 279(17), 17660-17666.
- Murshed, M., Schinke, T., McKee, M. D., & Karsenty, G. (2004). Extracellular matrix mineralization is regulated locally; different roles of two gla-containing proteins. *The Journal of Cell Biology*, 165(5), 625.
- Nakashima, K., Zhou, X., Kunkel, G., Zhang, Z., Deng, J. M., Behringer, R. R., & de Crombrughe, B. (2002). The Novel Zinc Finger-Containing Transcription Factor Osterix Is Required for Osteoblast Differentiation and Bone Formation. *Cell*, 108(1), 17-29. doi:[https://doi.org/10.1016/S0092-8674\(01\)00622-5](https://doi.org/10.1016/S0092-8674(01)00622-5)
- Neale, S. D., Smith, R., Wass, J. A. H., & Athanasou, N. A. (2000). Osteoclast differentiation from circulating mononuclear precursors in Paget's disease is hypersensitive to 1,25-dihydroxyvitamin D3 and RANKL. *Bone*, 27(3), 409-416. doi:[http://dx.doi.org/10.1016/S8756-3282\(00\)00345-8](http://dx.doi.org/10.1016/S8756-3282(00)00345-8)
- Nollet, M., Santucci-Darmanin, S., Breuil, V., Al-Sahlane, R., Cros, C., Topi, M., . . . Pierrefite-Carle, V. (2014). Autophagy in osteoblasts is involved in mineralization and bone homeostasis. *Autophagy*, 10(11), 1965-1977. doi:10.4161/auto.36182
- Noël, D., Gazit, D., Bouquet, C., Apparailly, F., Bony, C., Ponce, P., . . . Jorgensen, C. (2004). Short-Term BMP-2 Expression Is Sufficient for In Vivo Osteochondral Differentiation of Mesenchymal Stem Cells. *STEM CELLS*, 22(1), 74-85. doi:10.1634/stemcells.22-1-74
- Norris, F. A., Atkins, R. C., & Majerus, P. W. (1997). The cDNA Cloning and Characterization of Inositol Polyphosphate 4-Phosphatase Type II: EVIDENCE FOR CONSERVED ALTERNATIVE SPLICING IN THE 4-PHOSPHATASE FAMILY. *Journal of Biological Chemistry*, 272(38), 23859-23864.
- Norris, F. A., Auethavekiat, V., & Majerus, P. W. (1995). The Isolation and Characterization of cDNA Encoding Human and Rat Brain Inositol Polyphosphate 4-Phosphatase. *Journal of Biological Chemistry*, 270(27), 16128-16133.
- Nystuen, A., Legare, M. E., Shultz, L. D., & Frankel, W. N. (2001). A Null Mutation in Inositol Polyphosphate 4-Phosphatase Type I Causes Selective Neuronal Loss in Weeble Mutant Mice. *Neuron*, 32(2), 203-212. doi:[http://dx.doi.org/10.1016/S0896-6273\(01\)00468-8](http://dx.doi.org/10.1016/S0896-6273(01)00468-8)
- O'Brien, C. A., Nakashima, T., & Takayanagi, H. (2013). Osteocyte Control of Osteoclastogenesis. *Bone*, 54(2), 258-263. doi:10.1016/j.bone.2012.08.121
- Otto, F., Thornell, A. P., Crompton, T., Denzel, A., Gilmour, K. C., Rosewell, I. R., . . . Owen, M. J. (1997). Cbfa1, a Candidate Gene for Cleidocranial Dysplasia Syndrome, Is Essential for Osteoblast Differentiation and Bone Development. *Cell*, 89(5), 765-771. doi:[https://doi.org/10.1016/S0092-8674\(00\)80259-7](https://doi.org/10.1016/S0092-8674(00)80259-7)
- Pajevic, P. D. (2009). Regulation of bone resorption and mineral homeostasis by osteocytes. *IBMS BoneKEy*, 6(2), 63-70.
- Palumbo, C., Palazzini, S., & Marotti, G. (1990). Morphological study of intercellular junctions during osteocyte differentiation. *Bone*, 11(6), 401-406. doi:[http://dx.doi.org/10.1016/8756-3282\(90\)90134-K](http://dx.doi.org/10.1016/8756-3282(90)90134-K)
- Pfeilschifter, J., Wolf, O., Naumann, A., Minne, H. W., Mundy, G. R., & Ziegler, R. (1990). Chemotactic response of osteoblastlike cells to transforming growth factor $\beta$ . *Journal of Bone and Mineral Research*, 5(8), 825-830. doi:10.1002/jbmr.5650050805

- Rajapurohitam, V., Chalhoub, N., Benachenhou, N., Neff, L., Baron, R., & Vacher, J. (2001). The mouse osteopetrotic grey-lethal mutation induces a defect in osteoclast maturation/function. *Bone*, 28(5), 513-523. doi:10.1016/S8756-3282(01)00416-1
- Raubenheimer, E., Miniggiio, H., Lemmer, L., & van Heerden, W. (2017). The Role of Bone Remodelling in Maintaining and Restoring Bone Health: an Overview. *Clinical Reviews in Bone and Mineral Metabolism*, 15(2), 90-97. doi:10.1007/s12018-017-9230-z
- Rawlinson, S. C. F., Mosley, J. R., Suswillo, R. F. L., Pitsillides, A. A., & Lanyon, L. E. (1995). Calvarial and limb bone cells in organ and monolayer culture do not show the same early responses to dynamic mechanical strain. *Journal of Bone and Mineral Research*, 10(8), 1225-1232. doi:10.1002/jbmr.5650100813
- Riddle, R. C., Diegel, C. R., Leslie, J. M., Van Koeveering, K. K., Faugere, M.-C., Clemens, T. L., & Williams, B. O. (2013). Lrp5 and Lrp6 Exert Overlapping Functions in Osteoblasts during Postnatal Bone Acquisition. *PLoS ONE*, 8(5), e63323. doi:10.1371/journal.pone.0063323
- Rodan, G. A. (1998). Bone homeostasis. *Proceedings of the National Academy of Sciences*, 95(23), 13361-13362. doi:10.1073/pnas.95.23.13361
- Roodman, G. D., & Windle, J. J. (2005). Paget disease of bone. *Journal of Clinical Investigation*, 115(2), 200-208. doi:10.1172/JCI200524281
- Rutkovskiy, A., Stensl kken, K.-O., & Vaage, I. J. (2016). Osteoblast Differentiation at a Glance. *Medical Science Monitor Basic Research*, 22, 95-106. doi:10.12659/MSMBR.901142
- Saltel, F., Destaing, O., Bard, F., Eichert, D., & Jurdic, P. (2004). Apatite-mediated Actin Dynamics in Resorbing Osteoclasts. *Molecular Biology of the Cell*, 15(12), 5231-5241. doi:10.1091/mbc.E04-06-0522
- Sapkota, G., Knockaert, M., Alarc n, C., Montalvo, E., Brivanlou, A. H., & Massagu , J. (2006). Dephosphorylation of the Linker Regions of Smad1 and Smad2/3 by Small C-terminal Domain Phosphatases Has Distinct Outcomes for Bone Morphogenetic Protein and Transforming Growth Factor-  Pathways. *Journal of Biological Chemistry*, 281(52), 40412-40419.
- Schaffler, M. B., & Kennedy, O. D. (2012). Osteocyte Signaling in Bone. *Current Osteoporosis Reports*, 10(2), 118-125. doi:10.1007/s11914-012-0105-4
- Scheid, M. P., Huber, M., Damen, J. E., Hughes, M., Kang, V., Neilsen, P., . . . Duronio, V. (2002). Phosphatidylinositol (3,4,5)P3 Is Essential but Not Sufficient for Protein Kinase B (PKB) Activation; Phosphatidylinositol (3,4)P2 Is Required for PKB Phosphorylation at Ser-473: STUDIES USING CELLS FROM SH2-CONTAINING INOSITOL-5-PHOSPHATASE KNOCKOUT MICE. *Journal of Biological Chemistry*, 277(11), 9027-9035.
- Sch nlaug, F., Schlesiger, C., Ehrehen, J., Grabbe, S., Sorg, C., & Sunderk tter, C. (2003). Monocyte and macrophage functions in M-CSF-deficient op/op mice during experimental leishmaniasis. *Journal of Leukocyte Biology*, 73(5), 564-573.
- Scott, P. H., Brunn, G. J., Kohn, A. D., Roth, R. A., & Lawrence, J. C. (1998). Evidence of insulin-stimulated phosphorylation and activation of the mammalian target of rapamycin mediated by a protein kinase B signaling pathway. *Proceedings of the National Academy of Sciences of the United States of America*, 95(13), 7772-7777.
- SEER Training Modules, *Anatomy and Physiology*. U. S. National Institutes of Health, National Cancer Institute. 1 Sept 2017  
<https://training.seer.cancer.gov/anatomy/skeletal/classification.html/>.
- Sem nov, M., Tamai, K., & He, X. (2005). SOST Is a Ligand for LRP5/LRP6 and a Wnt Signaling Inhibitor. *Journal of Biological Chemistry*, 280(29), 26770-26775.
- Sobacchi, C., Schulz, A., Coxon, F. P., Villa, A., & Helfrich, M. H. (2013). Osteopetrosis: genetics, treatment and new insights into osteoclast function. *Nat Rev Endocrinol*, 9(9), 522-536. doi:10.1038/nrendo.2013.137

- Sophia Fox, A. J., Bedi, A., & Rodeo, S. A. (2009). The Basic Science of Articular Cartilage: Structure, Composition, and Function. *Sports Health*, 1(6), 461-468. doi:10.1177/1941738109350438
- Sprague, S. M. (2000). Mechanism of transplantation-associated bone loss. *Pediatric Nephrology*, 14(7), 650-653. doi:10.1007/s004670000359
- Stein, G. S., Lian, J. B., Wijnen, A. J. v., Stein, J. L., Montecino, M., Javed, A., . . . Pockwinse, S. M. (2004). Runx2 control of organization, assembly and activity of the regulatory machinery for skeletal gene expression. *Oncogene*, 23(24), 4315-4329.
- Takeshita, S., Namba, N., Zhao, J. J., Jiang, Y., Genant, H. K., Silva, M. J., . . . Ross, F. P. (2002). SHIP-deficient mice are severely osteoporotic due to increased numbers of hyper-resorptive osteoclasts. *Nat Med*, 8(9), 943-949.
- Tatsumi, S., Ishii, K., Amizuka, N., Li, M., Kobayashi, T., Kohno, K., . . . Ikeda, K. (2007). Targeted Ablation of Osteocytes Induces Osteoporosis with Defective Mechanotransduction. *Cell metabolism*, 5(6), 464-475. doi:<https://doi.org/10.1016/j.cmet.2007.05.001>
- Teitelbaum, S. L. (2000). Bone Resorption by Osteoclasts. *Science*, 289(5484), 1504.
- Teitelbaum, S. L., & Ross, F. P. (2003). Genetic regulation of osteoclast development and function. *Nat Rev Genet*, 4(8), 638-649.
- Teti, A. (2011). Bone Development: Overview of Bone Cells and Signaling. *Current Osteoporosis Reports*, 9(4), 264. doi:10.1007/s11914-011-0078-8
- Teti, A. (2012). The fine tuning regulation of osteoblast-osteoclast cross-talk. *Bone*, 51(6), S15. doi:10.1016/j.bone.2012.08.047
- Tolar, J., Teitelbaum, S. L., & Orchard, P. J. (2004). Osteopetrosis. *New England Journal of Medicine*, 351(27), 2839-2849. doi:10.1056/NEJMra040952
- Tu, X., Joeng, K. S., Nakayama, K. I., Nakayama, K., Rajagopal, J., Carroll, T. J., . . . Long, F. (2007). Noncanonical Wnt Signaling through G Protein-Linked PKC $\delta$  Activation Promotes Bone Formation. *Developmental Cell*, 12(1), 113-127. doi:10.1016/j.devcel.2006.11.00
- Udagawa, N., Takahashi, N., Jimi, E., Matsuzaki, K., Tsurukai, T., Itoh, K., . . . Suda, T. (1999). Osteoblasts/stromal cells stimulate osteoclast activation through expression of osteoclast differentiation factor/RANKL but not macrophage colony-stimulating factor. *Bone*, 25(5), 517-523. doi:[https://doi.org/10.1016/S8756-3282\(99\)00210-0](https://doi.org/10.1016/S8756-3282(99)00210-0)
- Vanhaesebroeck, B., Stephens, L., & Hawkins, P. (2012). PI3K signalling: the path to discovery and understanding. *Nat Rev Mol Cell Biol*, 13(3), 195-203.
- Wang, Y.-H., Liu, Y., Maye, P., & Rowe, D. W. (2006). Examination of Mineralized Nodule Formation in Living Osteoblastic Cultures Using Fluorescent Dyes. *Biotechnology progress*, 22(6), 1697-1701. doi:10.1021/bp060274b
- Wei, J., Hanna, T., Suda, N., Karsenty, G., & Ducy, P. (2014). Osteocalcin Promotes  $\beta$ -Cell Proliferation During Development and Adulthood Through Gprc6a. *Diabetes*, 63(3), 1021-1031. doi:10.2337/db13-0887
- Weinstein, R. S., & Manolagas, S. C. (2000). Apoptosis and osteoporosis. *The American Journal of Medicine*, 108(2), 153-164. doi:[https://doi.org/10.1016/S0002-9343\(99\)00420-9](https://doi.org/10.1016/S0002-9343(99)00420-9)
- Wilson, C. J., & Vellodi, A. (2000). Autosomal recessive osteopetrosis: diagnosis, management, and outcome. *Archives of Disease in Childhood*, 83(5), 449.
- Winkler, D. G., Sutherland, M. K., Geoghegan, J. C., Yu, C., Hayes, T., Skonier, J. E., . . . Latham, J. A. (2003). Osteocyte control of bone formation via sclerostin, a novel BMP antagonist. *The EMBO Journal*, 22(23), 6267-6276. doi:10.1093/emboj/cdg599
- Winslow, M. M., Pan, M., Starbuck, M., Gallo, E. M., Deng, L., Karsenty, G., & Crabtree, G. R. (2006). Calcineurin/NFAT Signaling in Osteoblasts Regulates Bone Mass. *Developmental Cell*, 10(6), 771-782. doi:<http://dx.doi.org/10.1016/j.devcel.2006.04.006>

- Wolf, G. (1996). Function of the Bone Protein Osteocalcin: Definitive Evidence. *Nutrition Reviews*, 54(10), 332-333. doi:10.1111/j.1753-4887.1996.tb03798.x
- Wong, F., Boice, J. D., Jr, Abramson, D. H., & et al. (1997). Cancer incidence after retinoblastoma: Radiation dose and sarcoma risk. *Jama*, 278(15), 1262-1267. doi:10.1001/jama.1997.03550150066037
- Yoshiko, Y., Candelieri, G. A., Maeda, N., & Aubin, J. E. (2007). Osteoblast Autonomous P(i) Regulation via Pit1 Plays a Role in Bone Mineralization. *Molecular and Cellular Biology*, 27(12), 4465-4474. doi:10.1128/MCB.00104-07
- Zaman, G., Pitsillides, A. A., Rawlinson, S. C. F., Suswillo, R. F. L., Mosley, J. R., Cheng, M. Z., . . . Lanyon, L. E. (1999). Mechanical Strain Stimulates Nitric Oxide Production by Rapid Activation of Endothelial Nitric Oxide Synthase in Osteocytes. *Journal of Bone and Mineral Research*, 14(7), 1123-1131. doi:10.1359/jbmr.1999.14.7.1123
- Zhang, M., Xuan, S., Bouxsein, M. L., von Stechow, D., Akeno, N., Faugere, M. C., . . . Clemens, T. L. (2002). Osteoblast-specific Knockout of the Insulin-like Growth Factor (IGF) Receptor Gene Reveals an Essential Role of IGF Signaling in Bone Matrix Mineralization. *Journal of Biological Chemistry*, 277(46), 44005-44012.
- Zhang, M., Yan, Y., Lim, Y.-b., Tang, D., Xie, R., Chen, A., . . . Chen, D. (2009). BMP-2 Modulates  $\beta$ -Catenin Signaling Through Stimulation of Lrp5 Expression and Inhibition of  $\beta$ -TrCP Expression in Osteoblasts. *Journal of Cellular Biochemistry*, 108(4), 896-905. doi:10.1002/jcb.22319
- Zhou, S. (2011). TGF- $\beta$  regulates  $\beta$ -catenin signaling and osteoblast differentiation in human mesenchymal stem cells. *Journal of Cellular Biochemistry*, 112(6), 1651-1660. doi:10.1002/jcb.23079
- Zornitza, S., & Savarirayan, R. (2007). Nosology and Classification of Genetic Skeletal Disorders: 2006 Revision. *American Journal of Medical Genetics Part A*, 143A. doi:10.1002/ajmg.a.31483